Worcester Polytechnic Institute

A Dynamic Elbow Flexion Simulator for Cadaveric Testing of UCL Injury and Reconstruction

MAJOR QUALIFYING PROJECT REPORT
SUBMITTED TO THE FACULTY OF
WORCESTER POLYTECHNIC INSTITUTE
IN PARTIAL FULFILLMENT OF THE REQUIREMENTS FOR THE
DEGREE OF BACHELOR OF SCIENCE

Report Submitted To:

Faculty Advisor, Professor Karen Troy

Submitted by:

Alexandrea Dustin

Emily Geer

Tessa Hulburt

April 30, 2015

Acknowledgements

We would like to thank the following individuals and organizations that helped make this project successful:

- Professor Karen Troy for her continued support and guidance throughout this project
- Dr. Joshua Johnson for his technical support in the lab
- Dr. David Magit for performing the reconstruction for the biomechanical study
- Nathan Smith for his help and insight with OpenSim
- Abby White for her support during our project
- Tom Partington for performing the machining necessary to build our device
- Paula Moravek and David Messier for providing the team with training to work in the lab safely
- Professor Page, Professor Reidinger, and Amanda Clement for their time, effort, and guidance

Authorship

Section	Primary Author(s)	Primary Editor(s)	Secondary Editor(s)
Glossary	Emily Geer	All	
Chapter 1: Introduction			
Significance	Tessa Hulburt	Tessa Hulburt, Alexandrea Dustin	Emily Geer
Project Goals	Alexandrea Dustin	Alexandrea Dustin	Emily Geer, Tessa Hulburt
Project Approach	Emily Geer	All	
Chapter 2: Literature Review			
Youth Sports Injuries	Tessa Hulburt	All	
Ulnar Collateral Ligament Injury	Tessa Hulburt	All	
Ulnar Collateral Ligament Epidemiology			
Anatomy	Emily Geer	All	
UCL Injury Epidemiology	Emily Geer	All	
Treatment Options	Emily Geer	All	
Chronic Conditions			
Osteoarthritis	Emily Geer	All	
Risk	Emily Geer	All	
Treatment Options	Emily Geer	All	
Cadaver Testing	Alexandrea Dustin	Alexandrea Dustin	Emily Geer, Tessa Hulburt
Previous Cadaver UCL Testing	Alexandrea Dustin	Alexandrea Dustin	Emily Geer, Tessa Hulburt
Technology			
Material Testers	Emily Geer	Alexandrea Dustin	Tessa Hulburt
Pressure Sensor	Emily Geer	Alexandrea Dustin	Tessa Hulburt
Sensor Implantation	Emily Geer	Alexandrea Dustin	Tessa Hulburt
Summary	Alexandrea Dustin	All	
Chapter 3: Project Strategy			
Initial Client Statement	Emily Geer	All	
Objectives	Tessa Hulburt	All	
Constraints			
Design Constraints	Alexandrea Dustin	Alexandrea Dustin	All
Experimental Constraints	Alexandrea Dustin	Alexandrea Dustin	All
Revised Client Statement	Emily Geer	All	
Project Approach			
A-term	Tessa Hulburt	Alexandrea Dustin	Emily Geer
B-term	Tessa Hulburt	Alexandrea Dustin	Emily Geer
C-term	Tessa Hulburt	Alexandrea Dustin	Emily Geer
D-term	Tessa Hulburt	Alexandrea Dustin	Emily Geer

Financial Strategy	Tessa Hulburt	Alexandrea Dustin	Emily Geer
Chapter 4: Design Alternatives			
Needs Analysis	Alexandrea Dustin	Alexandrea Dustin	Emily Geer, Tessa Hulburt
Functions and Specifications	Alexandrea Dustin	Alexandrea Dustin	Emily Geer, Tessa Hulburt
Conceptual Designs			
Humerus Fixation	Emily Geer	Alexandrea Dustin	Emily Geer, Tessa Hulburt
Forearm Fixation	Emily Geer	Alexandrea Dustin	Emily Geer, Tessa Hulburt
Actuation	Alexandrea Dustin	Alexandrea Dustin	Emily Geer, Tessa Hulburt
Building Prototypes			
Prototype I	Alexandrea Dustin, Emily Geer	Alexandrea Dustin	Emily Geer, Tessa Hulburt
Prototype II	Alexandrea Dustin, Emily Geer	Alexandrea Dustin	Emily Geer, Tessa Hulburt
Prototype III	Alexandrea Dustin, Emily Geer	Alexandrea Dustin	Emily Geer, Tessa Hulburt
Data Analysis	Alexandrea Dustin	Alexandrea Dustin	Emily Geer, Tessa Hulburt
Feasibility Study	Alexandrea Dustin	Alexandrea Dustin	Emily Geer, Tessa Hulburt
Conclusion	Alexandrea Dustin	All	
Chapter 5: Results			
Design Validation			
Pulley Locations	Tessa Hulburt	All	
Polhemus Motion Capture	Tessa Hulburt	All	
Theoretical Calculations	Tessa Hulburt	All	
Setup Validation			
Cardboard Prototype	Emily Geer	Alexandrea Dustin	Emily Geer, Tessa Hulburt
Final Prototype	Emily Geer	Alexandrea Dustin	Emily Geer, Tessa Hulburt
Final Design	Emily Geer	Alexandrea Dustin	Emily Geer, Tessa Hulburt
Design Implementation			
Specimen Preparation	Alexandrea Dustin	Alexandrea Dustin	Emily Geer, Tessa Hulburt

Experimental Protocol	Alexandrea Dustin	Alexandrea Dustin	Emily Geer, Tessa Hulburt
Data Acquisition and Analysis	Alexandrea Dustin	Alexandrea Dustin	Emily Geer, Tessa Hulburt
Results	Emily Geer	Tessa Hulburt	Alexandrea Dustin
Chapter 6: Discussion			
Design Validation			
Pulley Locations	Tessa Hulburt	Alexandrea Dustin	Emily Geer, Tessa Hulburt
Polhemus Motion Capture	Tessa Hulburt	Alexandrea Dustin	Emily Geer, Tessa Hulburt
Setup Validation			
Cardboard Prototype	Emily Geer	Alexandrea Dustin	Emily Geer, Tessa Hulburt
Final Prototype	Emily Geer	Alexandrea Dustin	Emily Geer, Tessa Hulburt
Final Design	Emily Geer	Alexandrea Dustin	Emily Geer, Tessa Hulburt
Design Implementation	Alexandrea Dustin	Alexandrea Dustin	Emily Geer
Limitations			
OpenSim Limitations	Tessa Hulburt	Alexandrea Dustin	Emily Geer, Tessa Hulburt
Polhemus Limitations	Alexandrea Dustin	Alexandrea Dustin	Emily Geer, Tessa Hulburt
Design Limitations	Emily Geer	Alexandrea Dustin	Emily Geer, Tessa Hulburt
Experimental Limitations	Alexandrea Dustin, Emily Geer	Alexandrea Dustin	Emily Geer, Tessa Hulburt
Impact of Design			
Ethics	Emily Geer	All	
Economy	Emily Geer	All	
Health and Safety	Emily Geer	All	
Environmental	Emily Geer	All	
Social Influence	Emily Geer	All	
Political	Emily Geer	All	
Manufacturability	Emily Geer	All	
Sustainability	Emily Geer	All	
Chapter 7: Final Design and Validation			
Objective 1	Tessa Hulburt	Alexandrea Dustin	Emily Geer
Objective 2	Alexandrea Dustin	All	
Chapter 8: Conclusions	Alexandrea Dustin	Alexandrea Dustin	Emily Geer, Tessa Hulburt

Appendix A: Polhemus Motion Capture Analysis	Tessa Hulburt	Emily Geer	
Appendix B: Theoretical Calculations	Tessa Hulburt	Emily Geer	
Appendix C: Experimental Protocol	Emily Geer	All	

Table of Contents

List of Figures

List of Tables

Glossary

Anterior: towards the front of the body

Kinematics: the study of motion without considering forces causing the motion

Lateral: situated away from the middle of the body

Medial: situated near the middle of the body

OA: osteoarthritis

Posterior: towards the back of the body

Pronation: rotation of the hand and forearm so that the palm faces downwards

PTOA: post-traumatic osteoarthritis

Radial: referring to the radius or the lateral side of the arm

Supination: rotation of the forearm and hand so that the palm faces forward or upward

UCL: ulnar collateral ligament

Ulnar: referring to the ulna or the medial side of the arm

Valgus: characterized by an abnormal outward turning of a bone

Varus: characterized by an abnormal inward turning of a bone

WPI: Worcester Polytechnic Institute

Abstract

Ulnar Collateral Ligament (UCL) injuries among overhead throwing athletes are an increasing epidemic. The most common and successful treatment for this injury is reconstruction surgery. Success of UCL reconstruction is only measured in the short-term and little is known about the long-term consequences. No research has been conducted to analyze the effectiveness of reconstruction while accounting for the forces of relevant muscles during dynamic testing. The goal of this project was to design and fabricate a dynamic elbow flexion simulator for cadaveric testing. In the future, a biomechanical study will be conducted using the custom apparatus to investigate potential long-term effects of UCL reconstruction.

1 Introduction

Ulnar Collateral Ligament (UCL) injuries among overhead throwing athletes are an increasing epidemic. Players who participate in sports involving vigorous and repetitive overhead throwing motions, such as football, tennis and baseball, often experience injury to the elbow. The UCL is most commonly injured in these circumstances as it provides primary stability to the elbow joint. If left untreated, UCL injuries are career-ending.

1.1. Significance

In the 1960's, approximately 50% of baseball players reported feeling elbow tenderness and 67% of pitchers showed evidence of degenerative elbow pain (Patel et al., 2014). In today's society, people are becoming involved in competitive athletics at a much younger age. In fact, approximately 55% of high school students participate in sports and in a survey conducted in 2013, baseball was found to be the third most popular sport played among these high school athletes (Patel et al., 2014). There are several benefits for high school students to take part in athletics, however, increases in youth sports participation results in higher occurrences of injury. It has been reported that over two million high school athletes are examined on an annual basis for sports-related injuries and approximately 5% of youth pitchers experience injury to the UCL (Patel et al., 2014; Zellner & May, 2013)**.** A surgical technique to reconstruct UCL tears was developed in the 1970's, commonly referred to as the Tommy John surgery (Langer, Fadale, & Hulstyn, 2006). This surgical technique, along with various modifications, has a success rate of 63-97% depending on the procedure, making this the most common and successful treatment for UCL injury. The success of these surgeries is defined as allowing patients to return to their pre-injury level of play for as little as one year (George A. Paletta et al., 2006). Unfortunately,

short-term effects are not sufficient to judge the success rates of UCL reconstruction since many patients are young and will have to live with the repercussions of this procedure far beyond an athletic career (D. J. Caine & Golightly, 2011). In fact, studies have shown the average elbow undergoes approximately 1,400 cycles of flexion and extension per day and about 500,000 cycles per year for nominal activities of daily living (ADL). The frequency of cycles under strenuous activity is about 7,500 per year (Johnson, Rath, Dunning, Roth, & King, 2000). Given the high level of activity in which the elbow joint endures on a daily basis, it is important to take care to maintain the longevity of its function. Understanding both the short and long term effects of a UCL reconstruction is crucial in determining and improving the best methods of treatment.

Currently, there are no data to determine if UCL reconstruction will cause chronic conditions for patients later in their lifetimes. However, in a 2006 study conducted on cadaver ankle joints, it was determined that any changes to the mechanical profile of the joints caused concentrated contact stress along the articular tissue. Concentrated contact stress in this area are known to lead to cartilage degeneration and eventually to osteoarthritis (OA) (Tochigi, Rudert, Saltzman, Amendola, & Brown, 2006). The objective of our biomechanical study is to explore whether or not elbow UCL reconstruction results in concentrated pressure within the joint space. This will allow us to determine if patients will develop chronic conditions as a result of UCL reconstruction.

1.2. Project Goals

The primary goal of the project was to design and fabricate a dynamic elbow flexion simulator that maintains physiological relevance while testing various UCL efficiencies using cadaveric specimens. The fixture we designed works as a system to simulate elbow flexion and extension while representing relevant physiological activity of flexor and extensor muscles as accurately as

possible. The device interfaces with an Instron actuator to create flexion by applying controlled loads to sutured tendons of the biceps brachii and brachialis of the specimen. A free-hanging weight was attached to the tendons of the triceps brachii to simulate both extension and co-contraction. A system of pulleys was carefully placed on the device to maintain the muscle lines of action of the three aforementioned muscle groups. The locations of these pulleys were calculated using the Arm26 model of the biomechanical program, OpenSim. The overall system simulates dynamic flexion and extension of the elbow in a physiologically accurate manner and the final prototype was used to conduct cadaveric testing in a biomechanical study.

The overall goal of the biomechanical study was to understand the change in biomechanics of the elbow due to UCL injury and reconstruction. With this information, we performed an analysis to assess possible risks for developing chronic conditions as a result of reconstructive surgeries. Many studies have been conducted to compare surgical methods by analyzing the biomechanical changes of the elbow before and after reconstruction, but none have taken into account the effect of the muscles on the elbow while performing dynamic testing. This study is unique because it focuses on the role of joint contact mechanics during dynamic testing while simulating forces of major muscle groups. We designed and created a device that was used to test cadaver specimens dynamically in cycles of flexion and extension at two rates. During this dynamic motion, the contact pressure within the elbow joint space was mapped out using Tekscan pressure sensors. Contact pressure within the joint space was collected at various levels of UCL efficiency: before and after UCL injury as well as after UCL reconstruction. Pressure data collected from the sensors was then converted to contact force. The data obtained from testing, along with

information found in the literature review, was used to understand how changes in elbow biomechanics affect the long-term longevity of the joint.

Due to the time frame, scope and client statement given for this project, there were a number of constraints considered before beginning the design process. We only had one academic year (2014-2015) to complete the project objectives and therefore time was a major limitation. The scope of this project was limited to available technology and the team budget. Additionally, there were design constraints given in the client statement that were taken into account regarding the UCL testing fixture. We primarily avoided causing damage to the wrist or forearm of the cadaver specimens since the client used these regions of the cadaver arm for other experiments. Other experimental constraints were related to the limitations associated with the use of cadaver specimens. Standard information regarding the limitations of working with cadavers will be described in **section 2.5**.

1.3. Project Approach

To accomplish all project objectives, a detailed project approach was developed. There were four phases throughout the entirety of the project, which included: research, design, testing, and analysis. The researching phase extended through the duration of the project so we could continue to gain relevant knowledge as the project progressed. In the design phase, we created a series of prototypes of the dynamic elbow flexion simulator. These prototypes were used for mock testing in order to verify the design. After several stages of refining, the final prototype was eventually developed for cadaveric testing. During the testing phase, we used the final design to test cadaveric specimens in order to better understand if/how the biomechanics of the elbow

are affected by UCL reconstruction. Lastly, in the fourth phase, we used the data found in the biomechanical study, along with background research, to determine future implications of the changes observed in joint contact mechanics resulting from UCL reconstruction.

Sufficient background research and literature review was a crucial aspect for developing an adequate understanding of the concepts involved in this project. Initial research was conducted on elbow anatomy and biomechanics as well as UCL injuries and current treatments. This information was extremely helpful for later phases of the project when identifying desired metrics for our biomechanical study. We also conducted research on previous cadaveric testing along with causes and risk factors of chronic, such as OA. This information was used in the design phase to create the prototype, in the testing phase to create a protocol, and in the analysis phase when understanding how changes in biomechanics of the elbow could increase the risk of chronic conditions.

When an adequate literature review was achieved, we moved on to the design phase. Using the background knowledge and the client statement, we determined essential design requirements for the device and created an initial prototype to use in mock testing with a synthetic elbow model. This was done to ensure the validity of the design and testing protocol before conducting tests on the expensive cadavers. Problems were discovered and rectified several times during the design validation phase.

Once the final design was successfully validated, it was used in cadaveric testing. Three experimental phases were conducted on each cadaveric specimen. These phases were:

1. Native UCL testing
2. Transected UCL testing
3. Reconstructed UCL testing

Data was collected during all three testing phases. Phase I, native UCL testing, was conducted to observe the behavior of the native UCL prior to injury. The data collected in this phase was used as a control, or baseline, to use as a comparison to the data collected from the reconstructed phase group. This is helpful because the biomechanics of each specimen may vary due to anatomical differences. During phase II, transected UCL testing, we simulated UCL injury by transecting the ligament and then simulated the same flexion and extension cycles as in phase I. This step was helpful to further understand the function of the UCL and how the biomechanics of the elbow change when the UCL is not functioning. During phase III, reconstructed UCL testing, an attending surgeon at UMass Memorial Hospital performed reconstruction surgery on the transected UCL's of each cadaveric specimen. Data was collected and analyzed to determine if and how the reconstruction changes the biomechanics of the elbow. By collecting data from all three phases, we were able to compare the reconstructed UCL state to the native and transected states to understand the post-operative changes in the biomechanics, particularly the regions of joint contact.

2 Literature Review

In today's society, youth populations are becoming more involved in competitive athletics. In fact, approximately 55% of high school students participate in sports and in a survey conducted in 2013, baseball was found to be the third most popular sport played among these high school athletes (Patel et al., 2014).

2.1. Youth Sports Injuries

Due to an increase in youth sports participation in recent years, the amount of sports-related injuries in young populations has also grown proportionally. 65% of youths report that they are active more than 12 times a month while only 40% of adults report the same level of activity. Additionally, children are more likely to sustain injuries than adults due to their underdeveloped skills and coordination. In fact, 8% of youths drop out of sports each year due to injury. Unfortunately, there has been little research conducted on how to reduce injury, including injury prevention and understanding how injuries occur and their outcomes. Specifically, there is little knowledge regarding long-term effects of injuries and their treatments (D.J. Caine & Maffulli, 2005).

The most common long-term consequence of sports-related injuries in athletes is osteoarthritis (OA). Playing sports puts players with any former injury, muscular weakness, or joint abnormality at a high risk of developing OA later in life. This is because many motions in sports require a high level of joint loading which, when supplemented with any of the risks factors associated with OA, puts players at significant risk for developing OA (J. A. Buckwalter, 2003). The risk of developing OA is especially prevalent in young athletes because they are still growing (Maffulli, Longo, Gougoulias, Loppini, & Denaro, 2010). Developing OA earlier in life will not only reduce the quality of life for these young athletes, but will also place a financial burden on the healthcare system to care for these patients (D. J. Caine & Golightly, 2011).

2.2. Ulnar Collateral Ligament Injury

Sports that involve repetitive overhead throwing motions can be especially harmful to the shoulder and elbow of an athlete due to the high speeds at which these motions occur. Some examples of these sports are baseball, tennis, softball, volleyball, and javelin throwing. It has been observed that sports such as baseball, tennis, softball, and volleyball require specifically high levels of joint loading, putting these athletes at a greater risk of developing OA (J. A. Buckwalter, 2003). Of these sports, baseball is most commonly played among adolescents. In the United States, over 20 million youths play organized baseball per year. Out of these millions, 26% of youth and 58% of high school baseball players complain of elbow pain. The most common source of this discomfort is UCL injury. A study was conducted to evaluate the location of elbow injury in youths who participate in the Taiwan Little League. After surveying players, it was found that 41% of pitchers reported pain originating from the medial region of the elbow where the UCL is located (D.J. Caine & Maffulli, 2005). Large increase in adolescent participation of overhead throwing sports results in higher frequencies of UCL injuries ("**Docking technique to repair torn elbow ligament yields favorable results in teen baseball players**," Apr. 7, 2013). While UCL injury is most commonly observed in overhead throwing athletes, it is also a common injury to sustain as a result of elbow dislocation. In children, the elbow is the most frequently dislocated joint in the body (Bhandari, 2011).

The most popular treatment for UCL injury is surgical reconstruction of the ligament. Non-operative rehabilitation is used in some cases, but it is not as successful and therefore is far less practiced (Langer et al., 2006). Surgical options, however, have success rates of 63-97% depending on the technique used, making reconstruction surgery the gold standard of UCL

treatment. Since 2001, 75 major league baseball pitchers required UCL reconstructive surgery (Langer et al., 2006). Surgical success has been defined as allowing players to return to their pre-injury level of play for one year after recovery. The short-term analysis, however, does not evaluate whether UCL injury and reconstruction could contribute to developing chronic conditions later in life.

2.3. Ulnar Collateral Ligament Epidemiology

2.3.1. Anatomy

The elbow is comprised of three major anatomical structures: bones, muscles and ligaments. The elbow joint is located at the junction of three bones: humerus, ulna, and radius. The humerus is the bone in the upper arm that extends from the shoulder to the elbow. The ulna and radius are both located in the forearm and are oriented on the medial and lateral sides, respectively (Lerner, 2007). A diagram of the bony anatomy of the elbow can be seen below in **Figure 1**.

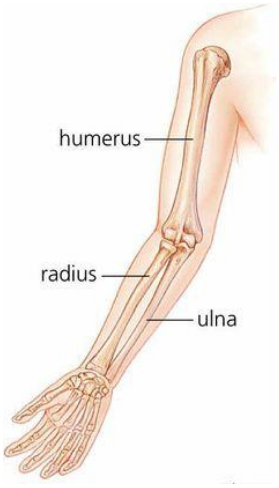

Figure 1: Bony anatomy of elbow (Iverson, 2014)

There are four main muscle groups that control elbow motion; these muscle groups are the biceps brachii, brachialis, brachioradialis, and triceps brachii. The biceps brachii, brachialis, and brachioradialis are located along the anterior side of the humerus while the triceps brachii are

along the posterior side of the humerus. To perform elbow flexion, or the pulling of the forearm towards the body, three of the four muscle groups are used. The primary muscle group used for flexion is the biceps brachii. The brachialis and brachioradialis supplement the biceps brachii to aid in flexion (Lerner, 2007). **Figure 2** below shows a diagram of these flexor muscles.

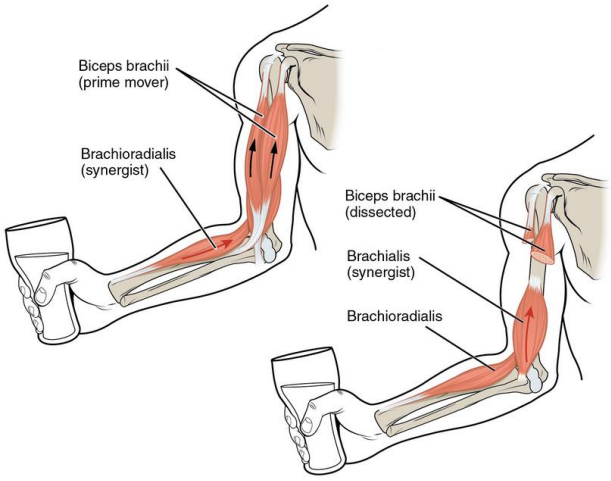

Figure 2: Muscles used in Elbow Flexion (Wikipedia, 2014)

To perform elbow extension, or to straighten the arm, the triceps brachii are engaged (Lerner, 2007). **Figure 3**, below, shows how the triceps brachii contract to extend the arm.

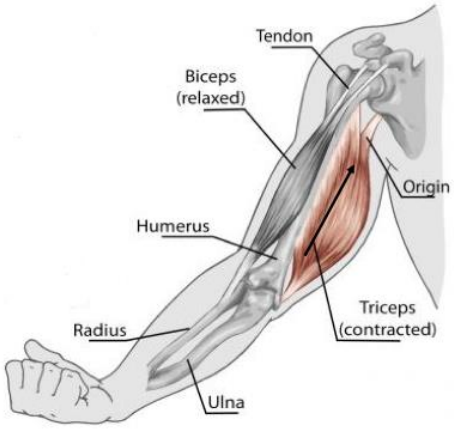

Figure 3: Muscle used in Elbow Extension ("shutterstock119687548copy," 2013)

The third major group of anatomical structures that aids in elbow function is the ligaments. The ligaments hold the bones of the elbow together and provide stability to the joint. They are fibrous and are comprised of collagen and elastin. The highly oriented fibers are woven together to provide stability in multiple directions. There are two main ligaments in the elbow joint: radial collateral ligament (RCL) and the ulnar collateral ligament (UCL). The RCL connects the radius to the humerus, while the UCL connects the ulna to the humerus. The UCL is comprised of three bands which have insertion points in the ulna and humerus (Lerner, 2007). **Figure 4**, below, shows the three bands of the UCL: anterior band, posterior band, and transverse band.

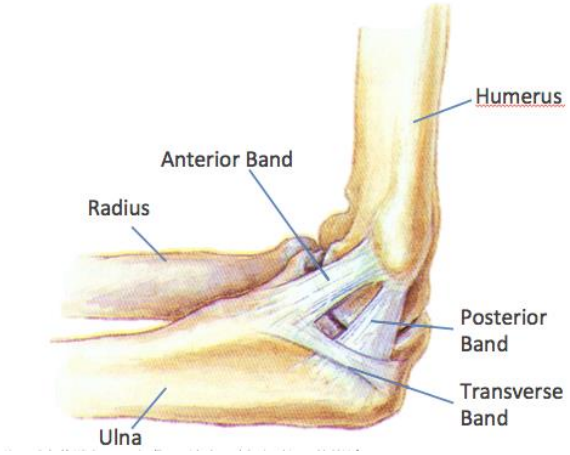

Figure 4: Three Bands of the Ulnar Collateral Ligament ("UCL Reconstruction (Tommy John Surgery)," 2014)

Out of these three bands, the anterior band provides the most stability to the elbow joint and therefore is often associated with UCL injuries. Release of the anterior bundle alone causes increased joint laxity (Lerner, 2007).

The posterior band is fan-shaped and provides little stability to the elbow (Lerner, 2007). The transverse band, also known as the oblique bundle, has attachment sites on the ulna alone and, therefore, does not aid in medial stability (Lerner, 2007).

2.3.2. UCL Injury Epidemiology

The UCL has two main functions which include providing stability to the elbow and resisting valgus stress. Valgus stress occurs when the forearm is moved laterally away from the body creating a space in the medial side of the joint, which is where stress is applied to the UCL. The diagram shown below in **Figure 5** depicts a valgus motion, as well as the opposing varus motion, of the elbow.

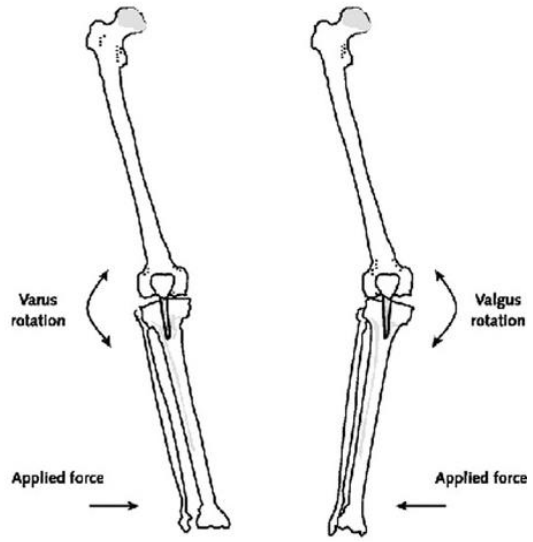

Figure 5: Varus and Valgus Rotation ("639 Musculoskeletal Problems," 2014)

During an overhead throw, high valgus stress is placed on the elbow. Studies have shown that valgus forces generated in professional baseball pitching place a near failure stress on the UCL. In other words, the load on the UCL during pitching is near its maximum capacity (Bruce & Andrews, 2014). The UCL is more likely to be injured during repetitive throwing due to muscle fatigue which results in stress transfer from the muscles to the UCL. This causes the UCL to bear an even greater load and eventually fail.

UCL injuries are classified into two categories: acute or chronic. Acute injuries of the UCL are sudden tears in the ligament resulting from some type of trauma to the elbow. Some patients report hearing a 'pop' as the injury occurs. Chronic injuries are caused by chronic attenuation and repetitive high valgus stress. Chronic attenuation is stretching of the ligament over time due to repetitive stress applied to the elbow from activities such as pitching (Bruce & Andrews, 2014).

2.3.3. Treatment Options

The UCL is the primary stabilizing structure of the elbow so injuries left untreated are career ending to the overhead throwing athlete. There are both operative and non-operative treatment options for UCL injury. For overhead throwing athletes, the most common treatment option is surgery. Non-athletes may also choose operative treatment over non-operative treatment if they have complete UCL tears or partial tears that did not heal properly. Surgical treatment can either involve direct repair or reconstruction of the ligament. Direct repairs are performed in the case of an acute avulsion. An acute avulsion occurs when the bone at the UCL attachment sites on the humerus or ulna breaks off, detaching the ligament. These injuries are less common than UCL tears and therefore reconstruction surgery is the most common form of operative treatment. Reconstruction is also more accepted than direct repair because it is better documented in studies that include high performance athletes. Reconstruction surgery has also yielded higher surgical success rates than direct repair surgery in recent years (Langer et al., 2006; P. Langer, 2006). In a comparative study conducted in 2000, it was found that reconstruction surgery had a surgical success rate of 81%, whereas direct repair had a surgical success rate of 63% (Azar, Andrews, Wilk, & Groh, 2000).

There are many types of reconstruction techniques that are currently practiced (P. Langer, 2006). Generally, a graft from the palmaris longus tendon, located in the forearm, is used to restore the elbow (Andrews, Jost, & Cain, 2012; "Johns Hopkins Sports Medicine Patient Guide to UCL Injuries of the Elbow (Ulnar Collateral Ligament)," 2014). The use of this tendon is advantageous because it is long enough to provide surgeons with the necessary 15-17 cm to perform the surgery. It also has a failure load of 357 N, which is greater than the UCL failure load of 260 N. This higher failure load ensures the new graft will have the ability to withstand the forces that the UCL originally endured. Another advantage is that this tendon does not cause functional deformities when removed from the forearm. However, approximately 10% of people do not have the palmaris longus which limits the supply of this graft (Andrews et al., 2012). Also, the surgery to remove it can cause damage to the median nerve (P. Langer, 2006). An important aspect of this graft is that it is a tendon, not a ligament, and therefore differs in composition and function from the native UCL. Tendons do not have as much elastin as ligaments and do not crimp as much. Both of these factors would make the palmaris longus tendon less elastic than the native UCL (Franchi, Ottani, Stagni, & Ruggeri, 2010). Crimp, seen in ligaments, is the pleating of the collagen fibers when the ligament is relaxed. When a force is applied, these pleats straighten. This crimping allows the ligament to provide stability without restricting motion. Using a tendon as a graft for UCL reconstruction can, therefore, be considered a disadvantage since the differences in the composition and function of these structures may lead to a change in the biomechanics of the elbow as a whole.

The first reconstruction technique was developed in 1974 and is called the Jobe, or Tommy John, technique (Langer et al., 2006). The Jobe technique involves drilling two holes into the ulna and

two holes into the humerus. The palmaris longus graft is then fed through the holes in a figure eight pattern and then sutured to itself as seen in **Figure 6** below.

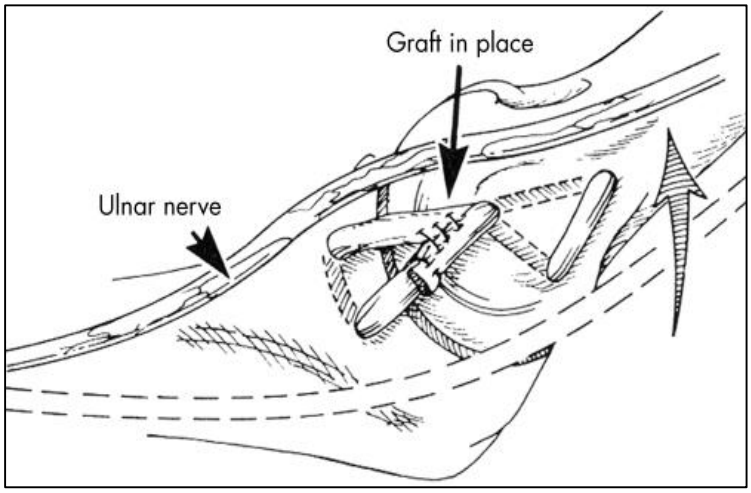

Figure 6: Jobe Technique (Langer et al., 2006)

In the original article, released in 1986, Jobe recorded that 10 out of 16 patients were able to return to pre-injury level of play (Jobe, Stark, & Lombardo, 1986)**.** With modifications and practice over the years, this technique has become a more successful procedure. In a systematic review published in 2008, 76% of surgical success was found using the Jobe technique (Vitale & Ahmad, 2008). A common complication with the Tommy John surgery is ulnar nerve paresthesias, which can cause residual pain and discomfort (P. Langer, 2006).

Later developments of the Tommy John surgery lead to the muscle splitting technique. When the Jobe and muscle splitting technique are used together it is referred to as the modified Jobe technique. Rather than detaching the entire flexor pronator mass, the muscle splitting technique involves splitting the muscle to get to the UCL. By splitting the muscle, the surgeon can avoid handling the median and ulnar nerve and reduce the side effects of the procedure(P. Langer, 2006). In a study conducted in 2012, the modified Jobe technique was performed on 120 patients

and yielded an 87.5% surgical success rate (Dugas et al., 2012). In another study performed to analyze the success of this technique, it was found that only 5% of the 83 patients in the study had residual pain or denervation due to ulnar nerve complication (Thompson, Jobe, Yocum, & Pink, 2001). Due to its success in reducing ulnar nerve complications, the muscle splitting technique is commonly used with other surgical reconstruction techniques.

The Jobe technique was further modified to reduce ulnar nerve complication with the American Sports Medicine Institute (ASMI) modification. This modification included two changes from both the muscle splitting technique and the Tommy John surgery. First, to get to the UCL, the flexor carpi ulnaris (FCU) muscle is removed anteriorly. The FCU muscle is located medially, directly over the UCL, and extends down the length of the forearm. Second, an ulnar nerve transposition (UNT) is performed subcutaneously, or beneath the skin. A UNT is when the ulnar nerve is moved to a new location. It is commonly performed to treat cubital tunnel syndrome which is a pain syndrome caused when the ulnar nerve becomes trapped between the humerus and the ulna (Rogers, Bergfield, & Aulicino, 1991). This procedure is sometimes performed during a UCL reconstruction to reduce potential ulnar nerve entrapment, which can arise from improper placement of the nerve. Previously, UNT was performed under the muscular tissue. The USMI modification, however, places the ulnar nerve on top of the muscle tissue and below the skin (P. Langer, 2006). An illustration of the UNT performed in this modification can be seen in **Figure 7** below.

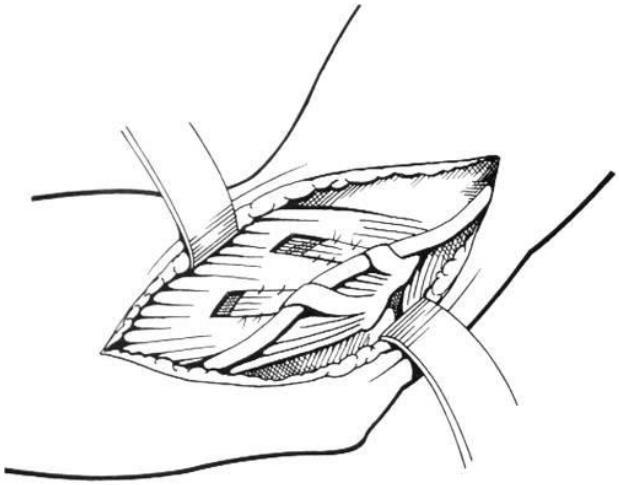

Figure 7: Photographic representation of the USMI modification (P. Langer, 2006)

In a study conducted in 2000, 79% of patients achieved surgical success with the ASMI modification and only one patient needed postoperative revision of the ulnar nerve location (Azar et al., 2000).

Another common technique is the docking technique. Like the Tommy John surgery, this technique uses a ligament graft, but instead of suturing the graft to itself in a figure eight shape, the graft is sutured over a bone bridge in the humerus in a triangular shape (George A. Paletta et al., 2006), as seen in **Figure 8** below.

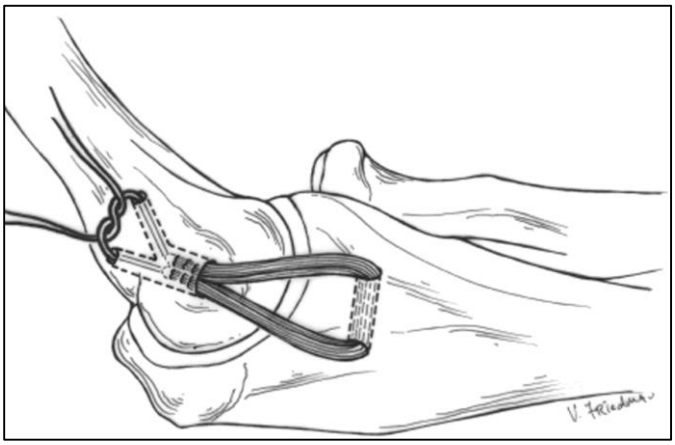

Figure 8: Docking Technique (George A. Paletta et al., 2006)

Studies using this technique have reported increased surgical success rates of 92% and 97% (Rohrbough, Altchek, Hyman, Williams, & Botts, 2002). In a study conducted to compare the Jobe and docking techniques, the docking procedure was found to offer initial biomechanical advantages over the Jobe technique (George A. Paletta et al., 2006). The docking technique and the native UCL had a higher maximal moment to failure, 14.3 Nm and 18.8 Nm respectively, than the Jobe procedure (8.9 Nm) (George A. Paletta et al., 2006).

UCL reconstruction was further modified with the invention of the inference technique. The inference technique is different from the Jobe technique in that it secures the tendon graft through one single bone tunnel in the humerus and ulna with inference screws. By securing the tendon graft through one bone tunnel, it is no longer secured over a bone bridge. This eliminates the chance of bone bridge fracture. An additional advantage to this technique is that its simplicity reduces the handling of the ulnar nerve and, therefore, possible ulnar nerve complications (P. Langer, 2006). An image of the inference technique can be seen below in **Figure 9**.

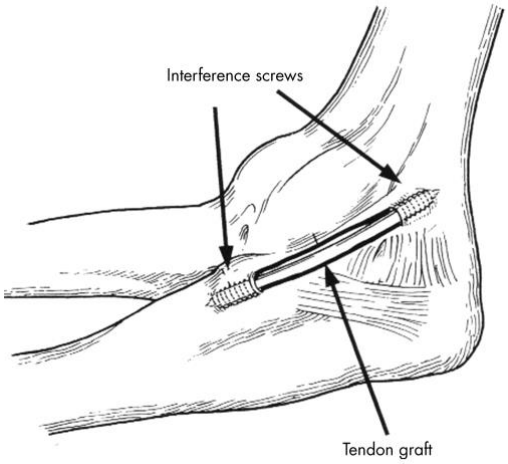

Figure 9: Inference technique method (Watson, McQueen, & Hutchinson, 2013)

The UCL reconstruction studies mentioned previously only investigated the short-term effects of UCL surgery to determine if players would be able to return to their sport. Unfortunately, long-term effects of these surgeries have yet to be investigated (Anderson, Marsh, & Brown, 2011).

2.4. Chronic Conditions

Without the knowledge of how UCL reconstruction affects elbow longevity, there is currently no way of knowing whether the growing number of young athletes undergoing these surgeries will develop complications later in life. One major concern for patients who have undergone joint reconstruction is the development of OA.

2.4.1. Osteoarthritis

OA is a chronic condition caused by joint degeneration. This degeneration can cause both joint pain and dysfunction. Joint degeneration begins with the loss of the articular cartilage of a joint; the articular cartilage covers the bones of the joint and allows the joint to move smoothly through its full range of motion painlessly. OA is the most common joint disease (J. Buckwalter, 2006). Although the actual cause of OA is still unknown, there are many risk factors associated with its development.

2.4.2. Risks

Although the epidemiology of OA is not well known, there are many known risk factors associated with its development. Some of these risk factors include increased age, excessive joint loading, joint abnormalities, joint injuries, excessive articular surface contact stress, and joint laxity (J. Buckwalter, 2006). Additionally, repetitive joint overuse, joint injury, posttraumatic joint instability or misalignment, and joint abnormalities can all put mechanical burdens on the elbow

which will eventually cause damage to the articular surfaces (Chammas, 2014). Furthermore, past clinical experience and epidemiologic studies show that ligament and joint capsule tears increase the risk of joint degeneration that causes posttraumatic osteoarthritis (PTOA). Specifically, the results of a study regarding knees showed that the risk of OA increases as much as 10-fold after a significant ligament injury (Anderson, Chubinskaya, et al., 2011).

Overhead throwing during competitive sports often inflicts near-failure stresses on the ulnar collateral ligament (Lynch et al., 2013; Seiber, Gupta, McGarry, Safran, & Lee, 2009). Repetitive loads of such high magnitudes can increase the risk of degeneration of the cartilage in those joints (J. Buckwalter, 2006). Participation in these sports also increases the risk of injury to the elbow and associated ligaments. Ligament injuries may lead to joint instability and other changes to joint contact mechanics including the dispersion of inflicted stresses. Evidence suggests that alteration of load distribution can speed up the initiation and progression of OA (Goldring, Laboratory for Cartilage Biology, Hospital for Special Surgery, Goldring, & Laboratory for Cartilage Biology, 2014). While there have been no upper extremity studies conducted to determine if ligament reconstruction relates to the development of OA, there have been studies conducted on lower extremities. In an ankle study conducted by Donald D. Anderson, it was observed that localized thinning of articular cartilage corresponds to increased contact stresses in that area (Anderson, Marsh, et al., 2011). Specifically, cartilage loss is linked with over exposure to contact stresses above 2.0 MPa-s (Anderson, Marsh, et al., 2011).

2.4.3. Treatment Options

There is no cure for OA, however several treatment options aim to relieve symptoms and improve the functionality of the joint. Treatments can include any of the following: patient education,

physical therapy, weight control, medications, and joint replacement ("EngArc - L - Tensile Test," 2014). Patient education is important because awareness of the condition and ways to avoid its progression can aid in the management of symptoms. Physical therapy teaches muscle building and cardio exercises to patients. These exercises increase stability of the rehabilitating joint by strengthening the muscles that surround it and decrease the risk of obesity. Weight control decreases the loads on the joint and has also been reported to decrease pain intensity. Medication is another way of treating OA; typically medications such as topical or oral non-steroidal anti-inflammatory drugs (NSAIDs) are used to reduce inflammation, which in turn reduces the pain. With highly developed OA, anti-inflammatory drugs are often supplemented with other pain-relieving medications such as opioids ((UK), 2008; Creamer & Hochberg, 1997).

Unfortunately, these treatment options do not cure OA, they only mask the symptoms (J. Buckwalter, 2006). Another option to treat OA is joint replacement surgery. During this procedure, the affected elbow is replaced with an implant. Unfortunately, joint replacement is not a desirable treatment for younger adults since prostheses have a limited lifespan (Anderson, Chubinskaya, et al., 2011). For young patients, pain management and joint functionality are the focus of treatment in order to delay joint replacement until patients are older (Chammas, 2014). With no successful long-term treatment of OA, reducing the risk of developing this condition for young athletes is of great importance.

2.5. Cadaver Testing

The first step in reducing the risk factors associated with chronic conditions is awareness. Studies have been conducted to better understand the elbow joint and tissues that encapsulate it. The

gold standard models used in these biomechanical studies are cadaveric specimens. There are several advantages and drawbacks to using cadaver models for scientific studies, most of which are dependent upon the method of preservation.

Two main techniques for preservation of these specimens for testing are embalming and freezing. Embalmed cadavers are not ideal for biomechanical studies due to effects of the chemicals on the material properties of the soft tissue (Crandall et al., 2011). Fresh-frozen cadavers are frozen at the time of acquisition and thawed immediately prior to testing. This technique is more commonly used since it allows for the retention of mechanical properties of the hard and, to an extent, soft tissues (Crandall et al., 2011).

There are various advantages to using cadaver models for research applications. Using cadavers for biomechanical experiments is beneficial because identical testing can be performed on multiple experimental groups. This allows for accuracy and precision of the data acquisition process. The most important advantages of cadaver testing, however, are that they provide an exact representation of human anatomical structures as well as the opportunity to accurately learn more about the complexity of the human body (Crandall et al., 2011).

Like any study, there are limitations to those using cadaver specimens. While they provide the most accurate model for human biomechanical studies, there are certain drawbacks that are associated with the use of cadavers. Cadaver testing may require a considerable amount of time and money due to high costs of specimens and necessary preparation procedures. Due to their biohazardous nature, specific protocols and lab training are required when using cadaver specimens. This may increase expenses and time spent on the study. Availability is often a

limitation and donor specimens are typically biased toward older populations, some having pre-existing pathologies that may impact the related study. A major limitation of cadaver specimens is that, while conducting the experiment, there is no way to account for natural muscle contraction or a physiological response since the tissue is not living. This is a critical limitation in which the analysis of the data must take note of and account for (Crandall et al., 2011).

There are specific preparations that must be considered when conducting a cadaveric study. Since cadavers are biohazardous, personal safety preparations, such as lab training, must be completed prior to testing (Crandall et al., 2011). Another aspect of cadaver studies that must be considered for planning purposes is that fresh-frozen specimens have a limited number of freeze/thaw cycles. They may be frozen and re-thawed up to 5 times; however, 3 is the optimal amount of cycles and any cycle beyond 5 may result in compromised mechanical properties of the soft tissue (Tan & Uppuganti, 2012). Dehydration of the tissues must also be prevented during testing to preserve the material properties. This may be done by simply spraying the tissue with a saline solution periodically during testing.

If a cadaver study is being conducted to test a tendon or ligament, preconditioning of the tissue should be considered as well. Preconditioning is the process of changing the orientation of the collagen fibers in the tendon or ligament from a crimped state to an aligned state before testing. This is done by subjecting the tissue to various stress cycles in order to straighten and stretch the crimped fibers. A study conducted by Scott et. al, demonstrated that preconditioning the tissue prior to testing reduces variability of subsequent cycles due to an increase in the initial reference length of the tendon or ligament (Scott, Nicole, Sue, & James, 2011). Another study which

focused on the effects of preconditioning demonstrated that optimum clinical preconditioning of a tendon or ligament considerably improves the tensile properties of the tissue (Teramoto & Luo, 2008). However, extended duration of this process will lead to microstructure fractures resulting in an adverse effect (Scott et al., 2011). This is an important notion that is directly related to the concept of a player "warming up" prior to playing at a competitive level in order to avoid injury. Preconditioning is a practice that is recommended in a clinical setting to gather accurate and precise data.

The use of cadaver specimens for biomechanical studies has its advantages and drawbacks; however they are the most accurate existing models to date and have been used as a gold standard in various medical and scientific studies conducted to learn more about the human body and ultimately improve the quality of life for future patients.

2.6. Previous Cadaver UCL Testing

There have been numerous cadaver studies conducted to learn more about anatomical joints, including testing of the UCL. The biomechanics of the ulnar collateral ligament after reconstructive surgery have been revealed in several studies performed with cadaver specimens. In a 2011 study performed by Paletta et. al, the biomechanical properties of reconstructions performed using the Jobe and docking techniques were compared revealing the mechanical advantages of the docking technique (George A. Paletta et al., 2006). In another study which focused on the UCL, Duggan et. al. searched to understand the contact area and pressure distributions of the lateral compartment of the elbow under valgus loading (Duggan Jr, Osadebe, Alexander, Noble, & Lintner, 2011). In studies such as these, the biomechanics of the elbow are

explored under various conditions and efficiencies of the UCL; however, these studies are conducted under static conditions. The lack of a dynamic setup, which simulates a physiologically relevant environment to test the UCL and elbow joint, yields results that may not be as accurate as possible. Designing a device capable of simulating joint extension and flexion motions in a dynamic and cyclic manner is ideal.

Dynamic joint simulators have been produced to explore joint stability and motion pathways as well as to improve and validate rehabilitation and reconstructive protocols (Dunning, Gordon, King, & Johnson, 2003). Active upper extremity joint simulators have been designed for research purposes. Some of these active systems are load-controlled meaning a controlled magnitude is applied to the bone or tendon of the specimen to actuate motion (Dunning et al., 2003). Johnson et al. used a load-controlled device that applied calculated loads to relevant tendons with the use of pneumatic actuators in their passive vs. active testing study (Johnson et al., 2000). Other systems, referred to as motion-controlled simulators, use a motor or actuator to produce a controlled displacement of tendons to cause flexion and extension of the specimen. A motion-controlled device was designed in the study conducted by Dunning et. al and used to produce elbow motion via tendon loading. Systems that use passive motion to simulate elbow flexion and extension by applying free-hanging weights to muscles and manually moving the forearm of the specimen have also been used in the past. However, passive testing of the muscles during biomechanical studies is much less accurate than active testing (Johnson et al., 2000). Also, in a different study conducted by Dunning et. al. that compared the two methods, the results from active actuation exhibited no difference in data repeatability based on forearm position or load magnitude. Passive testing, on the other hand, yielded high variability of data (Dunning, Duck,

King, & Johnson, 2001). This is a crucial difference because repeatability in an experiment is of the upmost importance.

The objective of our UCL biomechanical study is to combine technology used in previous cadaveric UCL studies with the technology used in previous joint simulator studies. We designed a motion-controlled device to simulate dynamic motion of the forearm, with the humerus fixed horizontally, to study the changes in elbow biomechanics after UCL reconstruction. A crucial advantage of our study is the dynamic and cyclic testing of the elbow joint. We simulated flexion in a horizontal plane, as opposed to the vertical plane in which most elbow simulator studies have done. Motion-controlled actuation using an Instron was utilized to guarantee accuracy and repeatability of all results. The joint contact mechanics of the elbow was closely studied using a Tekscan sensor inserted into the joint to map the pressure distributions throughout the joint space before and after reconstruction of the UCL. This information was used to determine whether or not the articular profile was altered and whether degradation will occur years after the reconstructive procedure. This type of investigation of UCL reconstructions has never been conducted in another UCL cadaver study. All of these unique advantages of this study helped us achieve our main goal to determine whether or not UCL reconstruction alters the biomechanics of the elbow, which may lead to the development of chronic conditions such as OA.

2.7. Technology

To observe the joint biomechanics of the elbow before and after UCL reconstruction, the team used various technologies to help conduct testing and collect data. The machines and equipment used are described in this section.

2.7.1. Material Testers

Material testers are machines designed to test the material properties of a specimen. Below is a picture of the crucial components contained in any material tester.

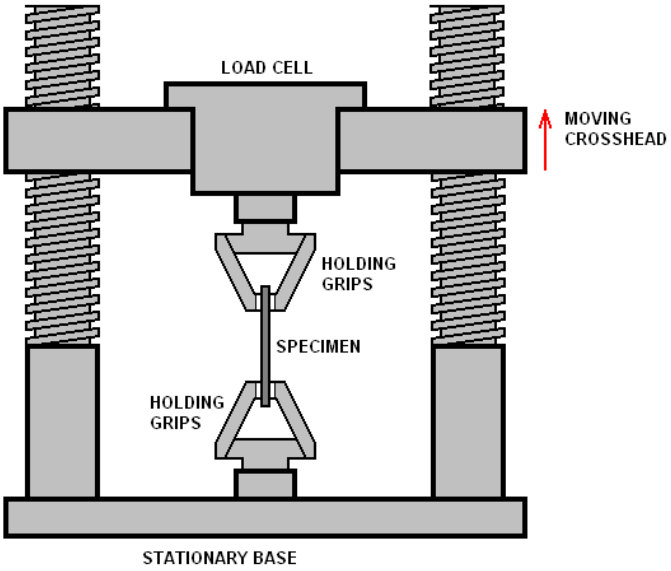

Figure 10: Basic Material Tester ("EngArc - L - Tensile Test," 2014)

As seen in **Figure 10**, a material tester holds a specimen and uses a load cell and moving crosshead to measure material properties of the specimen. The moving crosshead is able to move up and down at set rates. It can also measure displacement and force, which can be used to calculate stress and strain. For our study, it was used to accurately manipulate the muscles in a controlled manner by moving the crosshead at validated rates.

Currently, there are many different types of material testers on the market. Two main companies known for their material testers are Instron and Chatillon. Instron and Chatillon produce very similar machines. The main difference between the two companies is that Chatillon markets their setup as a motorized stand in which a digital force gauge could be used while Instron markets their setup as a motorized stand with the load cell as a part of the machine ("Instron : Materials

Testing Machines for Tensile, Fatigue, Impact & Hardness Testing," 2014; "Testers & Stands | Chatillon Force Measurement," 2014).

We used an ElectroPuls E1000 All-Electric Test Instrument, as seen below, as an actuator attached to flexor tendons to mimic the contraction of the muscles.

Figure 11: ElectroPuls E1000 All-Electric Test Instrument ("Testers & Stands | Chatillon Force Measurement," 2014)

This model is one of the material testers from Instron. With the current load cell on it, the machine has a dynamic load capacity of ±2 kN and can be used in a vertical or horizontal configuration ("Testers & Stands | Chatillon Force Measurement," 2014). This specific model was used because it was made available to us in Gateway Park, where the cadaveric specimens were being stored. Having access to this machine in the lab was key to staying within budget since purchasing a machine would far exceed the team's budget.

2.7.2. Pressure Sensor

To measure the pressure observed across the articular cartilage, we needed a sensor that could fit into the small joint space and accurately map the pressure array. There were two main types of devices to measure the pressure over the joint that we considered using: FujiFilm and Tekscan.

Fujifilm is a pressure sensitive film, as seen below in **Figure 12**, that changes color as pressure is applied to it.

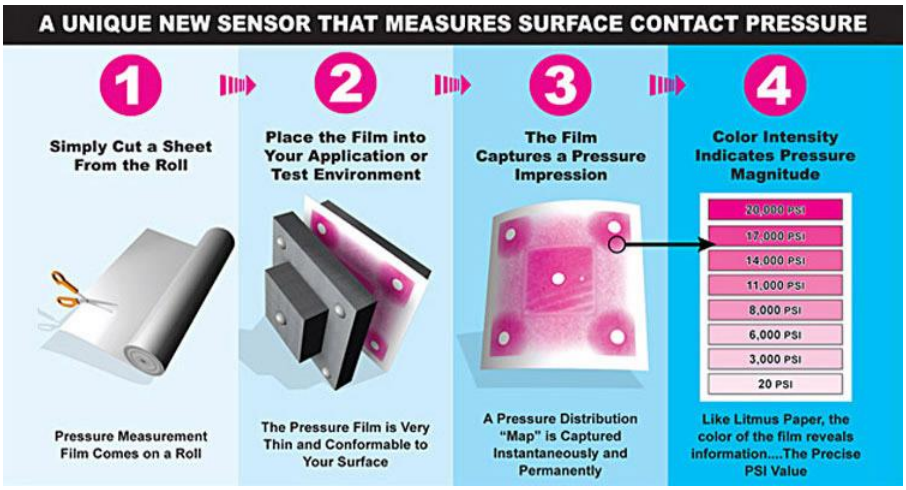

Figure 12: FujiFilm Prescale Sheet (Institute, 2014)

This film is between 100-200 µm thick, which could easily be placed into a joint space. The film consists of microcapsules that are broken as increasing pressure is applied. As seen below in **Figure 13**, inside the microcapsules is a solution that, when released, reacts with the color-developing layer to create a color change.

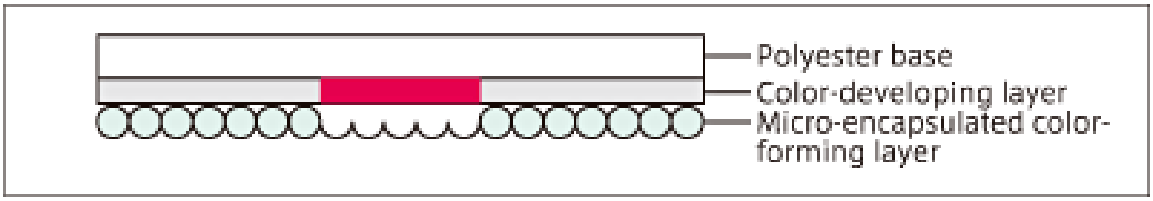

Figure 13: FujiFilm Composition ("Prescale Sheet Type | Fujifilm Global," 2014)

This method of measuring pressure would show the distribution of contact within the joint space by displaying an array of colors and using the included scale in which colors indirectly correlate to a pressure (Institute, 2014). Although this would give us numerical data to an extent, the accuracy becomes a concern due to human error since the system depends on qualitative properties being properly assigned to a point on a quantitative scale. Moreover, time would have to be dedicated to converting the film color into numerical data, which would slow down the testing and analysis process significantly. Additionally, it could not be used to show how pressure changes during a cyclic motion because once contact is made, the film is no longer useful. Due to these limitations, we decided to use Tekscan pressure sensors.

Tekscan pressure sensors are sensors that output an array of the varying pressures across the joint into a data sheet. These sensors are to be used with a Tekscan pressure measurement system and sensor driver for the particular sensor. Tekscan sensors come in different sizes. They vary in maximum pressures; their maximum pressure is typically 125 psi but can go up to 25,000 psi. With the output of numerical pressures displayed on the computer interface, one can easily analyze changes in pressure during dynamic testing ("Pressure Sensors in Various Sizes and Resolutions," 2014). Another benefit of Tekscan sensors is that they can be reused. We were given access to Tekscan sensors, the measurement system, and drivers through the advisor, Professor Karen Troy.

2.7.3. Sensor Implantation

To insert the Tekscan sensor into the small joint space we used a similar technique to the one described in a previous cadaver study conducted by Duggan et. al. In this study, a thin sensor was inserted into the radiocapatellar joint to measure contact pressures in the lateral compartment

of the elbow. To insert the sensor, an incision was made in the joint capsule posterior and in line with the UCL. Another incision was made on the lateral border of the olecranon to gain access to the radiocapatellar joint. Passing sutures were inserted through these incisions and were used to gently pull the sensor from the anterior side into the radiocapatellar joint while flexing and extending the arm by moving the forearm. We attempted to insert the sensor into the ulnar side of the joint as well. This proved to be extremely difficult, however, since this side is significantly tighter than the radial side. The sensor was fixed in the joint by suturing it to the skin and tying the passing sutures around the humerus from the posterior side (Duggan, Osadebe, Alexander, Noble, & Lintner, 2011).

2.8. Summary

Increased adolescent participation in competitive sports has resulted in an increase in sports-related injuries. Competition that involves overhead throwing motions such as volleyball, tennis, and more predominantly baseball have an increased occurrence of elbow injuries. The most common of these elbow injuries occur to the UCL, which is the primary stabilizing ligament in the elbow.

Treatments for UCL injuries typically include rehabilitation and surgery. Surgical reconstructive treatments are increasing in popularity due to the high success rates of these procedures. Over the years, various reconstructive techniques have been adopted. The two most commonly used are the Jobe and docking techniques.

Many cadaver studies have been conducted regarding the different reconstruction methods and their outcomes as well as success rates. Typically, these studies are done using static testing,

occasionally simulating motions by fixing the orientation of the elbow, forearm and wrist under given loads. While there have been several cadaver studies done regarding the UCL, no connection between reconstruction and early onset chronic diseases have been made.

We have conducted our own cadaver study to demonstrate and understand the changes in joint contact mechanics of cadaveric elbow specimens. We have designed a testing fixture that allows for dynamic testing of native, transected, and reconstructed cadaveric UCLs under physiologically relevant loads of the biceps brachii, brachialis, and triceps brachii muscles. Using the data collected on the joint contact mechanics of each experimental group, and the information gathered in the literature review correlating joint contact mechanics with OA, we will analyze the long term implications of UCL reconstruction surgeries.

3 Project Strategy

In order to design and test an elbow flexion/extension simulator, a project strategy was created. In this chapter, the process used to define project objectives and create the project strategy was documented. In the first section of this chapter, the procedure used to refine the client statement is discussed. In the next section, project objectives and constraints derived from the client statement are shown. Lastly, the planning and execution of the project will be discussed in the final section, entitled project approach.

3.1. Initial Client Statement

Before the project approach could be planned, we had to first define the project topic using the client statement. This was to ensure that the client's objectives would be fulfilled and constraints

would be adhered to throughout the course of this project. The following initial client statement was given to our team directly from the advisor, Professor Karen Troy (Troy, 2014):

"Design and fabricate a testing fixture for cadaveric specimens to simulate elbow flexion/extension before and after ulnar collateral ligament injury.

Goals: The fixture should simulate the range of motion of elbow flexion that would occur during a baseball throw. It must allow for the insertion of a small pressure sensor (Tekscan) into the elbow joint space during motion. It should include any muscle forces that are important during throwing. (Muscle forces may be simulated by suturing to the tendons and applying weights or other traction).

Constraints: The specimens are complete forearm/hand specimens with the elbow intact, and the fixture must not damage the forearm and wrist. Total cost must be less than $1000. It must interface with the Instron Materials Testing Machine located in the 3rd floor laboratories in Gateway Park."

3.2. Objectives

With the information provided in the initial client statement, four main project objectives were created. Below there is an objectives tree shown in **Figure 14**. The primary objectives are in bold type font. It is important to note that in this visual diagram two of the main objectives, precision and accuracy, are grouped together because they have the same secondary objectives.

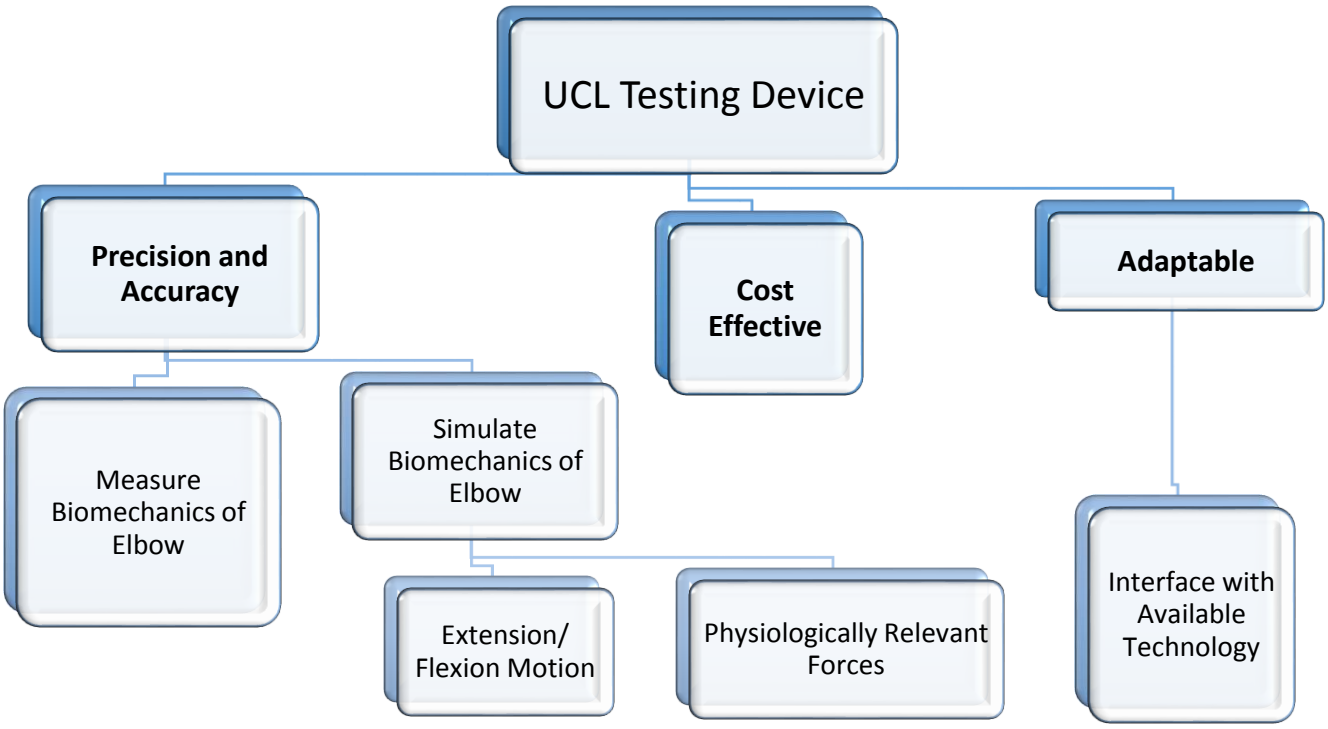

Figure 14: Objectives Tree

A pairwise comparison chart, as seen below in **Table 1**, was used to rank the objectives.

	Accuracy	Precision	Adaptability	Cost Effective
Accuracy	X	0	0	0
Precision	1	X	0	0
Adaptability	1	1	X	0
Cost Effective	1	1	1	X
Total	3	2	1	0

Table 1: Pairwise Comparison Chart of Objectives

Based on the pairwise comparison chart, the objectives were ranked from highest to lowest importance in the following order:

1. Accuracy of testing device and procedures
2. Precision of testing device and procedures
3. Adaptable to equipment and technology currently available to the team
4. Cost effective by utilizing available resources

First, accuracy was determined to be the most important primary objective for this study because without physiological relevance, the data will not be applicable. This is also the most important objective because the advisor, Professor Karen Troy, plans to use the data collected to validate a computer model of the elbow joint. For these reasons, accuracy is of utmost importance. The secondary objectives associated with this primary objective were to utilize relevant muscle tendons to accurately measure and simulate the biomechanics of the elbow during the flexion/extension motion. Loading the muscles to create flexion/extension makes the system more physiologically relevant. This motion was performed in each of the three experimental phases, previously described, to understand how the UCL reconstruction alters the biomechanics of the elbow.

Precision of the devices and testing procedures was determined to be the second most important objective. As with the first objective, the secondary objectives of precision were to measure and simulate the biomechanics of the elbow with accuracy utilizing relevant muscle forces to simulate the flexion and extension motion. The ability to produce repeatable data that is statistically relevant is crucial to the success of the study. The device was designed to allow for the collection of data from the Instron and Tekscan sensors as precisely as possible and results of the experiments have been made as reproducible as possible by keeping controls constant throughout the process and using active actuation. We assured that the device also simulates a reproducible motion by fixing the ulna and radius using the forearm fixation plate in order to prevent pronation of the forearm.

Adaptability of the device was determined to be the third most important primary objective. Within this objective, there is a secondary objective which states that the device will interface

with available technology. To adapt to the resources available, the device connects to the Instron actuator and Tekscan system supplied by WPI.

The objective ranked last was cost effectiveness. Since there was a team budget, we had to ensure our expenses did not exceed this limit. Making the device adaptable to available equipment allowed us to save money and therefore this objective was not a first priority.

We faced many challenges when attempting to achieve all of the above objectives, particularly when simulating the desired motion in a controlled manner. The overall success of this project was determined, however, by our ability to collect precise and accurate baseline data of the flexion/extension motion in a repeatable process.

3.3. Constraints

Different kinds of constraints influenced the progression of this project. Design constraints were considered when attempting to meet the previously described objectives while project constraints were considered in order to meet the overall project goals.

3.3.1. Design Constraints

There were various constraints we considered when creating conceptual designs that fulfill the primary objectives for the UCL testing device. Initially, avoiding damage to the wrist or forearm was a large constraint. This constraint was given to us by our advisor, Professor Troy, because the wrist and forearm of these cadavers were used for another study. We were able to work closely with those conducting the other study and make changes in our design to accommodate them. Time was a major constraint for this project as we only had the 2014-2015 academic year to achieve all of the project objectives and complete the cadaveric study. The budget supplied by the advisor and MQP program was one of the more minor constraints since much of the needed

equipment was made available to us. With an advisor budget of $1,000 from Professor Troy and an MQP budget of $468 from WPI, there was a total project budget of $1,468 to create the device and perform experimental testing. Our advisor supplied the cadaveric specimens so they were not included in the budget.

3.3.2.Experimental Constraints

A major component of this project was the design implementation, which occurred in a cadaveric biomechanical study. There were several constraints we considered when creating the testing protocols. There was limited lab access as the labs are shared among peers and professors within the WPI community. Also, a major experimental limitation was the number of tested cadaveric specimens. Due to time constraints, we were only able to successfully achieve design implementation using one specimen. With such a small population, systematic errors may be difficult to identify, however this level of testing provided validation for our system. Other experimental constraints were due to the challenges and limitations of working with cadavers as previously described. These limitations include limited freeze/thaw cycles, a potential for rigor mortis to occur and the need for manual hydration of tissues (Tan & Uppuganti, 2012). Additionally, an obvious but crucial limitation to cadaver studies is the lack of physiological responses such as healing and muscle contractions. All of these limitations were accounted for when planning the experimental approach.

3.4. Revised Client Statement

After several weekly meetings with Professor Troy, the team refined the client statement to the following:

Design and fabricate a testing fixture for cadaveric specimens to simulate physiologically relevant elbow flexion/extension before and after simulated UCL injury, as well as after reconstruction surgery. Use findings to understand the effects of UCL reconstruction on joint contact mechanics. Testing must not exceed a cost of $1,468 and must not damage the forearm or wrist.

The two main aspects of the initial client statement that were altered due to clarifications from Professor Troy were the type of motion to be simulated and what the information will be used for. The type of motion was changed from a baseball pitch to more easily replicated motions. A baseball pitch was determined to be too challenging to simulate due to the high speed at which it occurs and the complexity of the motion. To increase the feasibility of the project, this portion of the client statement was revised to instead simulate physiologically relevant flexion and extension. This motion was determined to be beneficial for validating an electronic model of the elbow in which Professor Troy is interested in making. This motion was also chosen because it closely resembles acts of daily life (ADLs). Instead of using the data from this study to infer about long term effects of UCL reconstruction as we originally planned, the data was used to identify the changes of joint contact mechanics that occur after UCL reconstruction. These changes were used to validate predictions regarding the longevity of elbow joints with reconstructed UCLs. Lastly, a minor change to the client statement was that the budget changed from $1,000 to $1,468 to account for the allotted MQP project budget of $156 for each student.

3.5. Project Approach

To complete our objectives, a detailed project approach has been created for each term.

3.5.1.A-term

The main goals for A-term were to finalize the project topic, complete initial background research and to begin the design phase of the project. The timeline to complete these main goals can be seen in the Gantt chart below.

A-term							
Task Completed	Week #						
	1	2	3	4	5	6	7
Research							
Chapter 1							
Chapter 2							
Conceptual Designs							
Chapter 3							

Table 2: Gantt Chart for A-term

To gain in-depth background knowledge for this project, we worked continuously throughout the term to research necessary topics pertaining to UCL injury and reconstruction. The first week was used to primarily understand and finalize the project topic. In the second to fourth week the introduction (Chapter 1) of the report was written. The third to seventh week were used to continue to collect research and write the literature review (Chapter 2). Once a base of background knowledge was obtained in week four, we began to brainstorm conceptual designs. The project strategy (Chapter 3) was written from the fourth week to the seventh week.

3.5.2.B-term

Once the preliminary organization and research portion of the project was completed in A-term, the main goal for B-term was to complete the design portion of the project. The timeline to complete the design portion is shown in the Gantt chart below.

B-term							
Task Completed	Week #						
	1	2	3	4	5	6	7
Research							
Conceptual Design: Humerus Fixation							
Conceptual Design: Pulleys							
Conceptual Design: Actuator							
Draft best design in SOLIDWORKS							
Build Prototype							
Mock Testing of System							
Refine System Prototype							
Second Mock Testing of System							
Chapter 1-3 Revisions							
Chapter 4							

Table 3: Gantt chart for B-term

Throughout the term we continued researching as needed. This research was mostly pertaining to additional reconstruction methods as well as existing cadaveric testing devices in order to aid the design process. In weeks 1-5, we continued with the conceptual design stage. An initial conceptual design was chosen and used to create prototype I (see **Figure 24**). This design was repeatedly revised. Once the design was finalized, it was drafted in SOLIDWORKS. Having the design in SOLIDWORKS allowed for the team to better communicate design ideas and facilitated prototype building. In the fourth and fifth week, prototype II was built (see **Figure 25**). Next, we moved on to mock testing. Mock testing was conducted using sawbones to simulate flexion and extension of the elbow. This was done to make sure that the design functions properly before using the expensive cadavers. In the sixth and seventh week, prototype II was refined based on

flaws identified during mock testing. This led to the development of prototype III (see **Figure 26**). Additional mock testing of prototype III occurred in the seventh week. The conceptual designs (Chapter 4) portion of the report was written in weeks five through seven. Any revisions to Chapters 1-3 were made mostly throughout the term.

3.5.3.C-term

The main focus of C-term was building and validating the final design.

C-term							
Task Completed	**Week #**						
	1	**2**	**3**	**4**	**5**	**6**	**7**
Research							
Motion Capture Study							
Building Setup/Revisions							
Chapter 5							
Chapter 7							
System Testing							
Chapter 6							
Chapter 8							

Table 4: Gantt Chart for C-term

In the first weeks of C-term, revisions were made to the prototype and a final working design was eventually created. System testing began in the fourth week and continued through the seventh week of the term as revisions to the setup were made. A motion capture study was conducted and the data analyzed in order to validate actuation rates. During C-term, we also focused on writing all remaining sections of the report. These sections are as follows: Results (Chapter 5), Discussion (Chapter 6), Final Design and Validation (Chapter 7), Conclusions and Recommendations (Chapter 8).

3.5.4.D-term

The primary focus of D-term was to validate the final design and experimental system, complete design implementation, and finalize the report and compile the final presentation. A Gantt chart of our progress can be seen below.

D-term							
Task Completed	**Week #**						
	1	**2**	**3**	**4**	**5**	**6**	**7**
Design Validation: Sawbones							
Design Validation: Cadaver							
Setup Validation							
Design Implementation							
Finalize Report							
Compile Presentation							

Table 5: Gantt Chart for D-Term

In the first two weeks of D-term, we began design and setup validation by testing the system using artificial sawbones. After this round of mock testing, several adjustments were made to the design and setup and then the system was tested using a cadaver specimen. More adjustments were made to remedy issues identified in the system after this round of mock testing. When the design and setup were validated and functioning properly, design implementation was conducted in the form of a biomechanical study in which a cadaver specimen was tested under various UCL efficiencies to observe changes in joint contact mechanics. Throughout the process of validating the system, the report was being edited and completed. By week 5, we began compiling the presentation for Project Presentation Day on April 23rd. After presenting, the report was finalized and submitted.

3.5.5.Financial Strategy

The team had an overall budget of $1,468 to complete this project. A general outline of how we utilized the project budget is as follows:

Item	Price ($)
Hardware and Materials	302.51
Sawbones	111.00
Vise	84.97
Acrylic sheet	65.00
Wood Baseboard	10.98
Lab Notebooks	12.00
TOTAL	**586.46**

We were able to complete our design objectives while staying under budget. We had an extra $881.54 left of our budget at the completion of the project.

4 Design Alternatives

Using the client statement, project objectives and constraints as a guide, we began the design process. Many conceptual designs were created and refined until a working prototype of the final conceptual design was built. Instead of building one device, we created a system consisting of several components. These components included humeral fixation, forearm fixation, and actuation. All of these separate components interface with one another to work in succession as one system to fulfill the design objectives and simulate cycles of elbow flexion/extension.

4.1 Needs Analysis

After consulting literature and having several conversations with Professor Troy and Dr. Joshua Johnson, a post-doc research assistant, the team discussed the specific needs that the elbow simulator must meet. First, the design had to simulate elbow flexion within the range of 30° to 120^{o}, since this is the range of motion in which the UCL is the primary stabilizing structure within

the elbow. Next, this motion had to be restricted to cycles of flexion and extension only, while preventing any other degrees of freedom. The specific motions that needed to be prevented included pronation of the radius over the ulna as well as varus-valgus movement. Controlling the kinematics of the elbow and forearm allowed for a more precise and repeatable data acquisition. The device also needed to maintain as much physiological relevance as possible while simulating cycles of flexion and extension and allowing for data collection within the joint space.

4.2 Functions and Specifications

- **Simulate cycles of flexion from 30° to 120°**
  - This is the range of flexion in which the UCL is the primary stabilizing structure within the joint.
- **Simulate a physiologically relevant motion**
  - Apply loads to the tendons of flexor and extensor muscles to actuate motion.
  - Apply a static free-hanging weight onto the tendon of the extensor muscle to simulate co-contraction.
- **Prevent pronation of the radius about the ulna**
  - Constricting the motion of the elbow and forearm strictly to a single plane during flexion will allow for more precise and repeatable data acquisition.
- **Must not damage the wrist or forearm**
  - Since cadaver specimens are so costly, several experiments will be conducted using this specific batch of specimens and therefore our design must not inhibit the other studies.

4.3 Conceptual Designs

The design of the device was created one component at a time. The first component we focused on was humeral fixation. Researching previous UCL cadaver studies helped us brainstorm several conceptual designs to secure the humerus. The next component of the system we focused on was forearm fixation. This component is important because it prevents pronation of the forearm creating a controlled motion. Finally, the last component of the system was actuation. We had to choose a mode of actuation and design a working interface between the device and actuator. Several conceptual designs were brainstormed for each component of the system. After

conceptual designs were chosen, prototypes were built and refined during mock testing until we arrived at a final, validated system.

4.3.1 Humeral Fixation

In our first conceptual design for humeral fixation, we planned to use a rod inserted into the humeral canal. This method has been seen in various cadaver studies conducted in the past. However, we quickly decided fixing a rod into the humeral canal would not be an option for our study because it was unknown what the humerus lengths of the specimens would be and it may have caused too much damage to the specimens. A sketch of this method for humeral fixation is seen below in **Figure 15**.

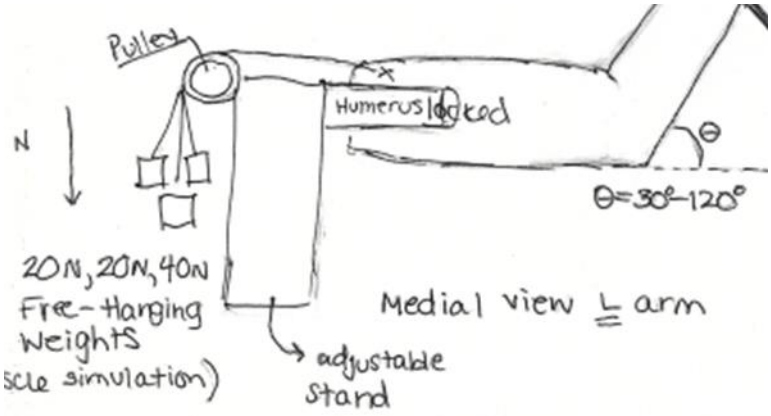

Figure 15: Rod humeral fixation

The next method we considered for humeral fixation was potting. We learned about this method from our advisor. Potting is a process in which the bone (humerus) is set in bone cement (PMMA) using two substances poured into a mold and cured over time. This creates a solid mass encasing the bone, which can then be drilled into with screws or mounted using other equipment in the lab. This method is often chosen because it is relatively inexpensive and any mold can be used, which allows for flexibility and creativity with the design. We considered using these aspects of potting to our advantage by creating channels through the PMMA to pull cables attached to

tendons through in order to maintain natural lines of action of the muscles. The cables would run through the channels in the PMMA and onto pulleys. From the pulleys, the cables would attach to the actuator. **Figure 16** below shows sketches of this concept of fixation.

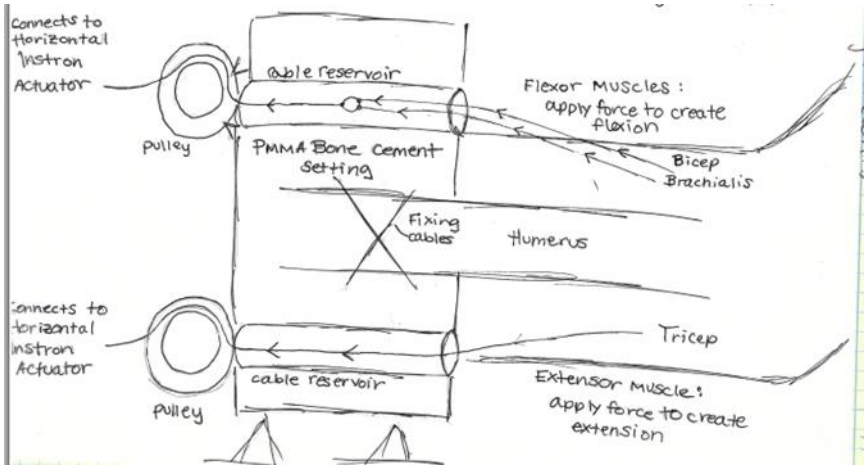

Figure 16: Channels in potting fixture

There are disadvantages associated with using PMMA bone cement to fix the humerus. This method can be messy and PMMA takes time to cure. Also, the end result may be imperfect which would be undesirable for this study because it would affect the accuracy of the channels. The team eventually spoke with Dr. Joshua Johnson regarding the disadvantages of using PMMA bone cement for humeral fixation. He informed us that for his study he would be fixing the humerus by drilling and bolting it to the testing table. To increase efficiency of our testing setup and save resources, we chose to use this same method to collaborate our design with his.

In order to use bolts for the humeral fixation, we had to create a device that allows the specimen to be secured to the humeral fixation device while leaving room to interface with multiple pulleys. This lead to our final conceptual design for humeral fixation, which involved placing a PVC pipe around the bone and securing it to the humerus of the specimen using bolts. Pulleys would then be mounted on the outer surface of the PVC pipe and the entire setup secured with

a pipe vise. Nylon cables would run from the muscle tendons, through a system of pulleys and to the actuator. **Figure 17** below shows a sketch of the conceptual design for PVC fixation.

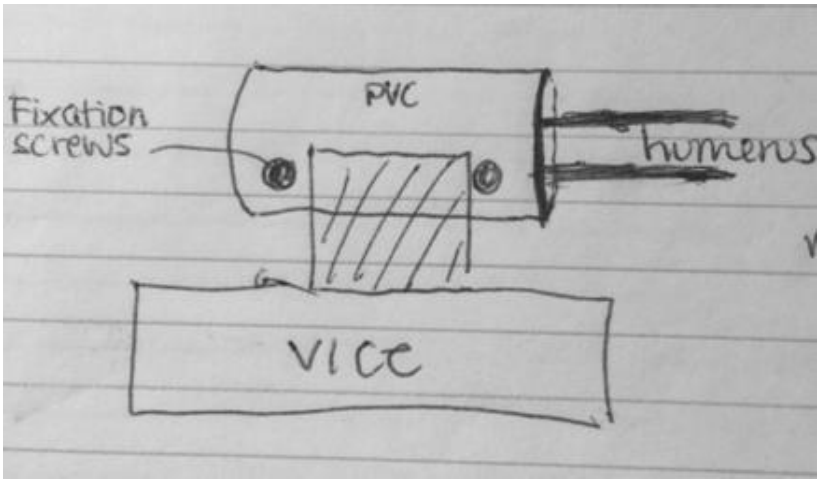

Figure 17: PVC humeral fixation

Furthermore, a slot will be cut into the PVC pipe to allow the attachment of the humerus fixation bolt to be adjustable. This method will further increase experimental set up efficiency because one PVC pipe with pre-mounted pulleys will be able to be used for every specimen. Otherwise specimen specific PVC pipes would need to be created for all cadavers prior to testing. **Figure 18** shows a CAD model of the final conceptual design for humeral fixation.

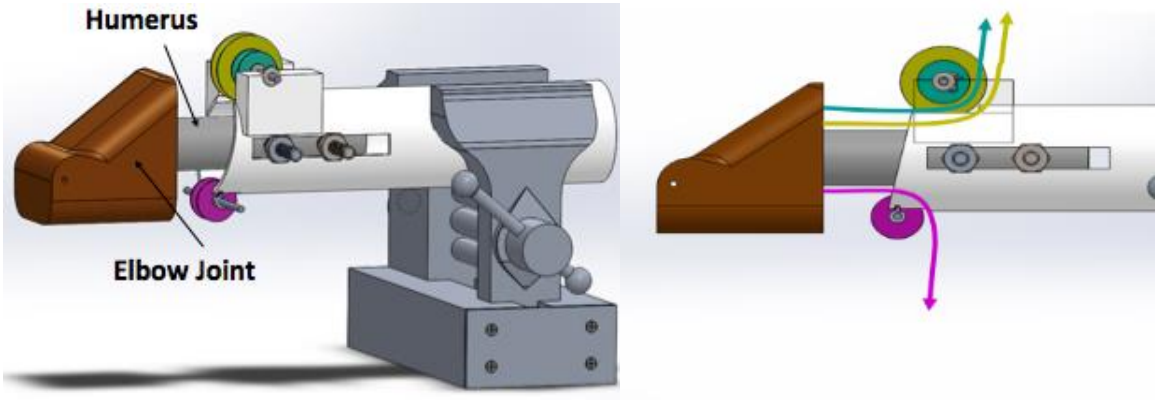

Figure 18: Final Conceptual Design for Humeral Fixation

4.3.2 Forearm Fixation

During our first meeting with Dr. Johnson we also discussed the concept of forearm fixation. He explained to us that controlling the kinematics of the forearm as much as possible would be crucial for maintaining consistency in our study. Ensuring a consistent motion pathway for each cadaver specimen minimizes the variables that have to be taken into consideration when analyzing the data. To do so, he explained that we must constrict the forearm to the defined neutral position to prevent pronation of the ulna and radius during flexion and extension. The neutral orientation that we have defined for the forearm will be a supinated position at 30° of flexion.

When conducting our initial brainstorming for conceptual designs prior to meeting with Dr. Johnson, we considered the use of a track to constrict and guide the motion of the forearm. This design includes two rigid acrylic sheets that would be fixed to the table on the medial and lateral sides of the forearm specimen, which would act as the forearm guides. There would be a track carved into the plastic in which pins that have been inserted into the wrist of the cadaver would slide back and forth while an actuator would pull the wrist to simulate flexion. Free-hanging weights would attach to the tendons of relevant flexor and extensor muscles in this design, however, loads applied to the wrist by the actuator would be what drive the motion. **Figure 19** below shows the sketch of this design.

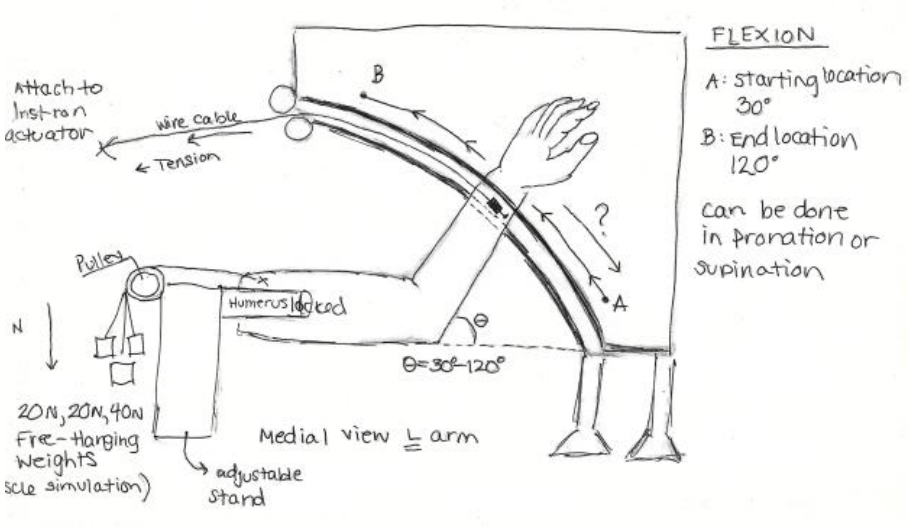

Figure 19: Track forearm fixation

This idea was not chosen for several reasons. First, we were concerned about the friction between the pins and the track. Also, it would have been difficult to create a cyclic motion since this setup simulates flexion but not extension. Finally, after speaking with our advisor, Professor Karen Troy, we decided it would be more physiologically relevant to attach the actuator directly to the tendons of flexor and extensor muscles to simulate the desired motion instead of using a track to pull the forearm through the motion.

During our meeting, Dr. Johnson described how he planned to fix the forearm for his own study, which involved cutting away the soft tissue on the distal end of the forearm and bolting the ulna and radius to a forearm plate. **Figure 20** below shows a sketch of our initial conceptual design to fix the forearm. This design utilizes the bolts used in Dr. Johnson's study and two small acrylic plates on the posterior and anterior sides of the specimen.

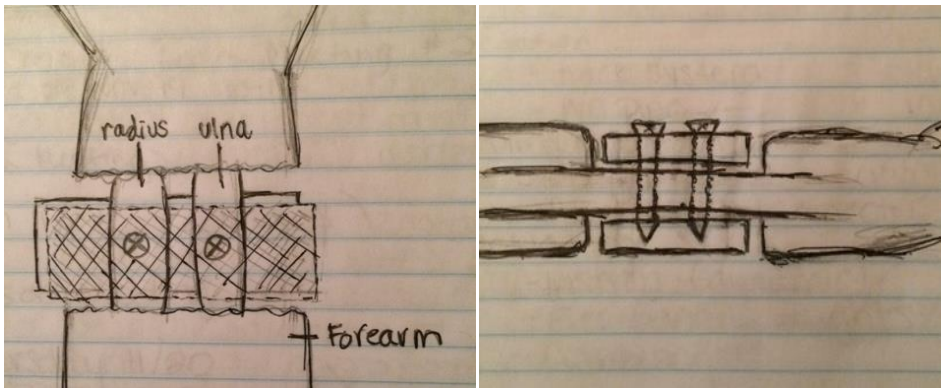

Figure 20: Original Forearm Fixation

The protocol of Dr. Johnson's study quickly changed to dissecting and drilling through the proximal end of the forearm instead of the distal end. To accommodate this, we adjusted the location of the bolts through the radius and ulna. During a subsequent meeting with Dr. Johnson, we discussed the specifications of our final design for the forearm fixation component of the system. The final design includes one large acrylic forearm plate, two small acrylic forearm plates, and two large acrylic forearm guides. The large forearm plate, referred to as **Plate A**, is 20.5 cm long, which is just short of the length of the longest forearm specimen. **Plate A** has a small 5 cm by 5 cm cutout through the face of the plate that is coincident with the proximal end of the forearm. This region is where the soft tissue would have been dissected as per Dr. Johnson's protocol, however, after the plate was machined there were last minute changes made. The procedure of the new protocol no longer involved drilling holes into the proximal ends of the radius and ulna. Therefore, minor changes were made to our final design in which holes in the radius and ulna are no longer necessary. The plate with the cutout was still used as **Plate A** for the setup of our study because the change in protocol did not impact its functionality. A CAD model of Plate A can be seen in **Figure 21** below.

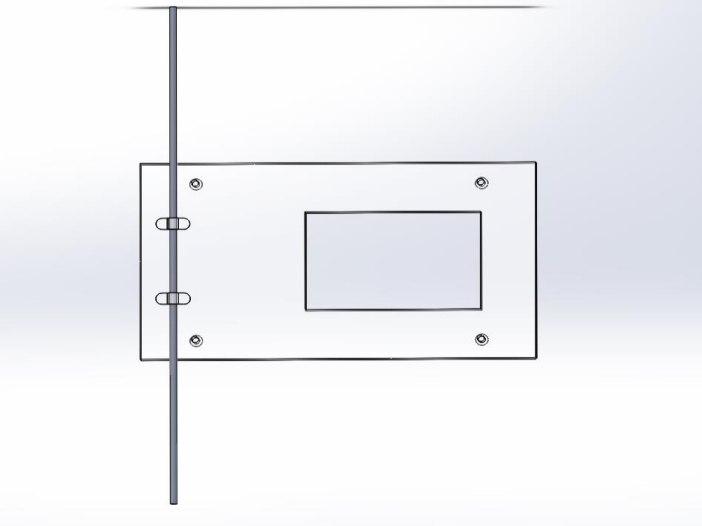

Figure 21: Plate A

The two smaller acrylic forearm plates (Plate B and Plate C) are 5 cm by 10 cm. These smaller plates were used to secure **Plate A** to the posterior side of the forearm of the specimen. While the specimen was held in a supinated position, Plates B and C were bolted to **Plate A** on the anterior side of the proximal and distal ends of the forearm, respectively. The bolts were tightly fastened on the medial and lateral sides of the wrist as well as just below the elbow so as not to penetrate the tissue of the specimen since this region was not dissected in the previous study as initially intended. A CAD model of this final conceptual design for forearm fixation is shown below in **Figure 22**.

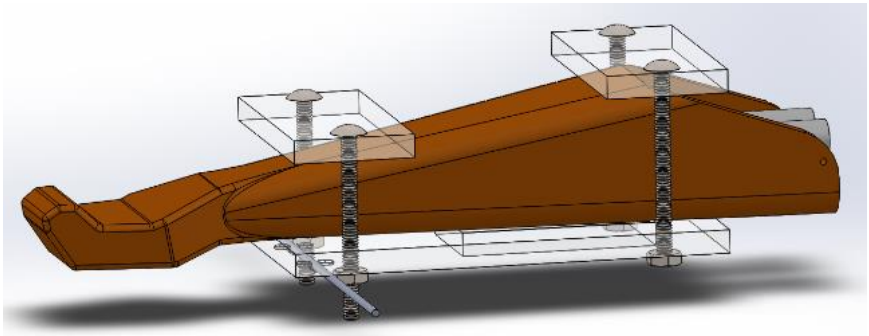

Figure 22: Final Conceptual Design for Forearm Fixation

Plate A will work in conjunction with the large acrylic forearm guides in order to provide additional stability to the setup by further preventing pronation of the forearm. The final design of the forearm guide has a track in which a metal rod clamped to the distal end of **Plate A** will slide through during flexion and extension of the specimen. This design will guide the motion of the forearm and resist pronation as well as varus and valgus motion. See **Figure 23** below for a CAD image of the humeral fixation and forearm fixation interface.

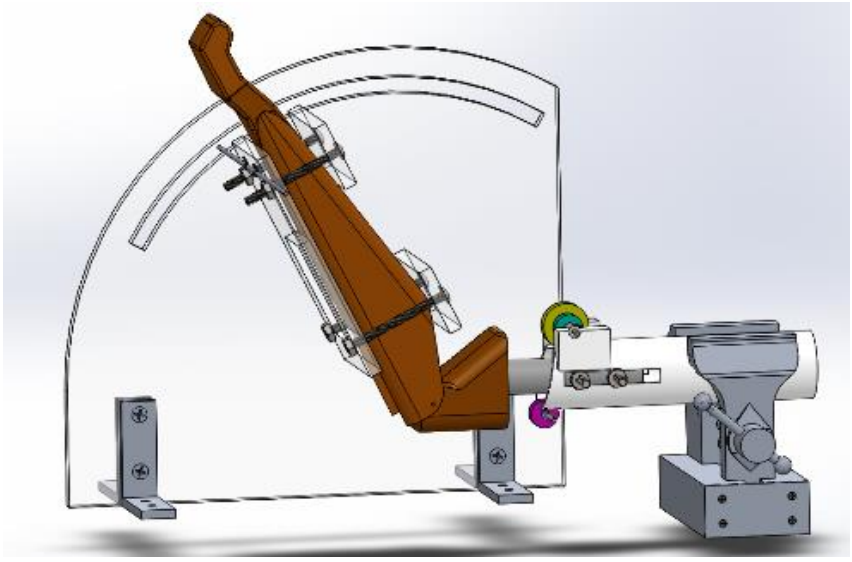

Figure 23: Humeral Fixation interface with Forearm Fixation (only one guide shown)

4.3.3 Actuation

The next component of the system is actuation. There are a number of methods that can be used to drive a specific motion. Actuation is generally categorized as either passive or active. We considered both methods when discussing how to simulate cyclic flexion and extension for this study. Passive flexion simply involves applying free-hanging weights to relevant muscles and manually moving the forearm of the specimen at an arbitrary rate through a specific range of degrees of flexion. This technique is extremely simple and inexpensive, as it does not involve complex equipment or technology. The issue with this method, however, is the lack of

repeatability of the elbow kinematics since there is no control over rates and magnitudes used to actuate the motion (Dunning et al., 2001). Since the primary goal of our study was to identify shifts in the regions of concentrated contact pressure along the articular surface, consistency of the specimens' motion pathways was crucial. If the kinematics of the specimen were altered between cycles, it would be impossible to observe any changes to the articular geometry. Active loading produces precise motion pathways as well as more consistent data samples. In a study conducted in 2000, passive control was observed to produce greater variability in flexion amongst trials of forearm supination, whereas active forearm supination was observed to produce 30.6% less variability (Johnson et al., 2000). The smooth and repeatable motions that occur under active actuation would result in a more physiologically accurate model, making this method even more desirable for the UCL study (Johnson et al., 2000). Given all the advantages of active control over passive control regarding accuracy and precision, we decided to use active actuation to produce cyclic flexion and extension. There are a number of differing methods that can be used to create active actuation, however, given the budget and time constraints of this project, the team decided to use an Instron as it was readily available and owned by the Institution. See the technology section for more details regarding this piece of equipment.

Actuation was conducted by applying active loads to cables that were sutured to relevant flexor muscle tendons. The flexor muscles that were used were the biceps brachii and brachialis because they provide the primary forces responsible for flexion as well as intrinsic elbow stability (Seiber et al., 2009). The brachioradialis, another flexor muscle, was not used in our study because it is not a primary flexor muscle. The cables attached to the biceps brachii and brachialis muscles ran from the tendons, through the appropriate pulleys and finally to the Instron which

actuated flexion. These muscles were actuated by the same Instron and at the same rates and magnitudes since there was only one available actuator. However, previous cadaver studies have loaded these muscles with equal ratios while testing in a static state and therefore using the same actuator had minimal negative impact on our study (Seiber et al., 2009). The extensor muscles that were used in our study were the triceps brachii. A cable was sutured to the triceps brachii tendons, which extended through a pulley system and held a free-hanging weight. The purpose of this static load applied to the triceps brachii was to simulate extension when the Instron reversed direction after flexion. This weight also simulated co-contraction during flexion and extension making the design more physiologically relevant. The location and size of the pulleys affected the lines of action of all the muscles and increased the level of physiological relevance. Therefore, an average line of action was calculated for each muscle group and used in this study by using measurements of the cadaver forearms and the program OpenSim. From this program, the origin, insertion sites and wrapping points of the muscles were located and used to determine the correct angle in which the lines of action each muscle had to maintain.

4.4 Building Prototypes

During the process of finalizing the conceptual designs for humeral fixation, forearm fixation and actuation, we began to build prototypes to aid in the design process. These prototypes were tested and refined through a series of mock testing until we arrived at a final working system.

4.4.1 Prototype I

Prototype I consisted of a PVC pipe with mounted pulleys used for humeral fixation. The PVC pipe was secured to a wooden dowel which was used as a substitute humerus. Using artificial sawbones as a guide to choose the diameter of the pipe, we bought PVC pipes with diameters of 1-1/2” and 3-1/2” sizes. The smaller size fit tightly around the dowel while the bigger size allowed

for other components to possibly fit on the interior of the PVC pipe. The team quickly realized that using the interior space left with the bigger pipe would interfere with the operation of the pulleys and cables. **Figure 24** below shows the initial prototype built using PVC to fix the humerus, which is represented by the wooden dowel.

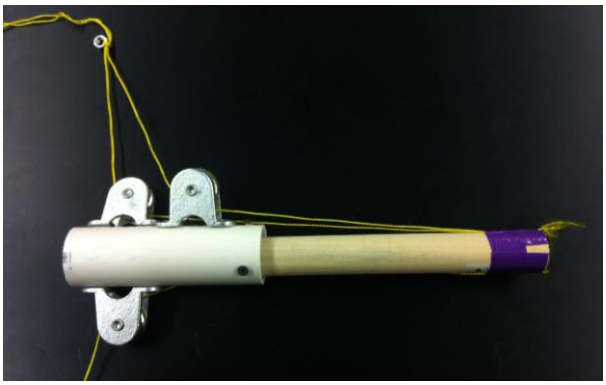

Figure 24: Prototype I

4.4.2 Prototype II

During the production of the initial prototype, we observed a number of issues that were solved to refine this design. First, smaller screws were used to mount the pulleys onto the surface of the PVC pipe so the sharp tips would not come into contact with the humerus. We also observed that we could offset the pulleys less, as long as the cables did not come into contact with other components, to maintain the lines of action of the muscle tendons and sutured cables as accurately as possible. Finally, a longer PVC pipe was used in the second prototype to leave space for a vise to secure the device to a table during testing. **Figure 25** below shows the second prototype that was built using the artificial sawbones instead of the wooden dowel.

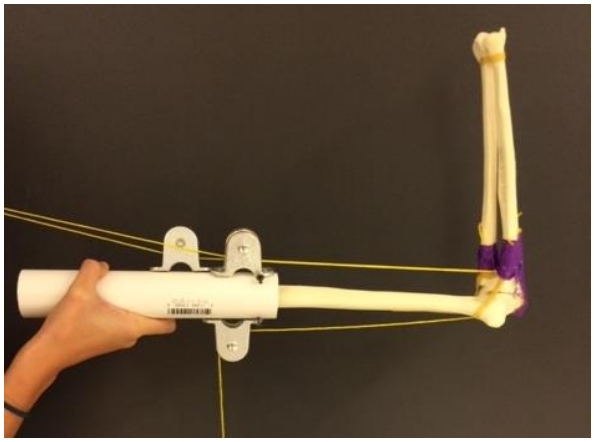

Figure 25: Prototype II

4.4.3 Prototype III

This prototype included both the humeral and forearm fixation components and was made with cardboard to demonstrate the concepts of the final design. Prototype II did not completely eliminate the possibility of the PVC pipe slipping or rotating out of the vise. For the next humeral fixation prototype, we planned to use grip tape found at Home Depot to reduce the possibility of the PVC slipping out of the vise. If additional stability was then needed, we would secure screws through the PVC pipe on either side of the vise to ensure it would not move horizontally. Although, at this point we no longer felt that this additional support would be necessary as there was no observed linear motion during the preliminary tests.

The team met with Dr. Johnson a second time to review prototype II. It was during this meeting that he made several suggestions to improve the humeral and forearm fixation components of our final conceptual design. Regarding humeral fixation, he suggested that we replace the screws we used to fix the humerus to the PVC pipe with a bolt since he plans to be drilling horizontally through the bone. Also, to make this design adjustable for each cadaver, we cut identical slots into the sides of the PVC pipe to ensure the device would fit onto every specimen. He also made little suggestions regarding forearm fixation. All of his suggestions were taken into consideration

when building our working prototype of the final conceptual design. The main challenge we encountered with this prototype was associated with the forearm fixation. When bolting the ulna and radius of this prototype, we initially held the sawbones flat which altered the orientation of them within the joint space. It was unclear whether or not this would be an issue when using an actual cadaver specimen. A picture of prototype III is shown below in **Figure 26**.

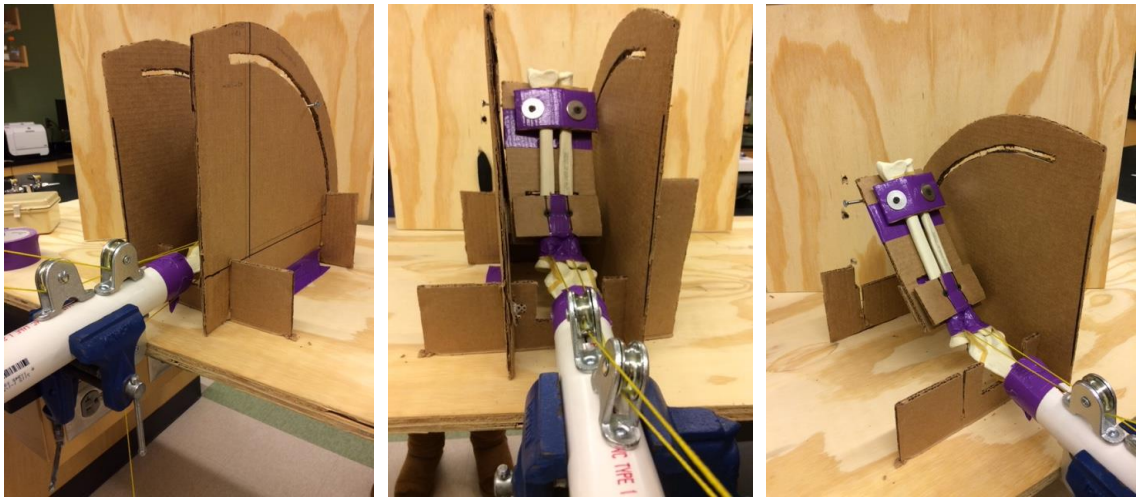

Figure 26: Prototype III

4.5 Data Analysis

The team collected data on the joint contact mechanics within the elbow during dynamic testing. Calibrated Tekscan sensors were inserted into the joint space of each specimen and data was collected through all three experimental phases. The primary parameters we collected were the total pressure across the joint space and the contact areas in which the pressure occurred on the articular cartilage. These sensors output an array of pressures over time, which is vital to our dynamic setup. The qualitative colors in the output arrays were matched to associated pressures from the calibration process. The main challenges presented by this technology was inserting the sensor into the extremely tight joint space and the possibility of the sensor moving or slipping during dynamic testing. To address these challenges, passing sutures were used to aid in the

insertion of the sensor and tied around the humerus to keep it in place. Due to the tightness of the joint, the sensor was inserted into the radiocapatellar side only. We also had to ensure that the force generated in the joint space would not damage the expensive sensors. We did this by calculating theoretical joint reaction forces using free body diagrams prior to testing and comparing those calculations to the limitations of the sensors. These theoretical forces did not exceed the capabilities of the sensors (maximum pressure is 13.8MPa) and therefore we proceeded to use them in our experiment ("Pressure Sensors in Various Sizes and Resolutions," 2014). The methods and results of the theoretical calculations can be seen in section **5.1.3**.

4.6 Feasibility Study

After completing the majority of the design process, the team conducted a feasibility study to determine whether or not we would still be able to meet the project objectives successfully. To do so, the team evaluated several influential factors such as materials, finances, time, available resources and manpower as well as external factors such as the client and schedule of outside partners to determine feasibility of the design.

Initially, the team acknowledged and considered several constraints when beginning the design process. Some of these constraints included budget, readily available resources, and time. Throughout this project, the budget did not prevent any progression of the design since most of the necessary equipment was already available in the Gateway lab (i.e. Instron) or purchased for use in this project as well as the lab in the future (i.e. Tekscan). The given project budget of $1,468 was more than enough to complete the project objectives as needed. At the point of the feasibility study, the major project constraints that may have prevented the team from achieving all of the intended project goals were time and knowledge. The team would have ideally

completed cadaveric testing by the end of February, however due to unexpected hurtles including inclement weather and last minute setup changes, design validation using a cadaveric specimen was not achieved until the end of March. After performing series of testing with a cadaver, we refined the setup once again. The team was unable to perform testing on a large sample of specimens; however, the design component of the project has always been prioritized over design implementation. While this yielded a less robust data sample, the main project objectives regarding the design and fabrication of an elbow simulator apparatus were successfully achieved.

4.7 Conclusion

In conclusion, we considered many design alternatives throughout the design process in order to create a final working prototype that was used as a guide to create our final working system. The fixture successfully tested the joint contact mechanics of the elbow during flexion and extension before injury and before and after UCL reconstruction while maintaining physiological relevance and staying within the $1,468 budget.

5 Results

After completing the conceptual design and building a series of working prototypes, preliminary testing and validation of the setup was required to verify that the design met the client's needs and performed all the necessary functions under the correct specifications. In order to do so, preliminary studies were conducted to validate parameters that were later used to verify that the design and setup met all project objectives. Once the function of the design was validated, we performed design implementation by testing a cadaveric elbow specimen in our biomechanical study.

5.1 Design Validation

5.1.1 Pulley Locations

One major design objective was to maintain physiological relevance while simulating a flexion/extension motion. To meet this objective, the motion was actuated by applying known forces to specific muscle tendons in each specimen to allow for a more natural movement. This was done by suturing the muscle tendons to a cable and then applying tension to the cable via active actuation. However, in order to truly maintain the physiological relevance of this system, it is necessary to maintain the muscle lines of action during the simulated motion. To preserve the lines of action of each muscle group used in this study, pulleys were incorporated into the design to control the orientation of the cable and feed it to the actuator. The location of these pulleys, specifically the distance away from the epicondyle and height from the humerus, were carefully calculated and these calculations were validated via setup validation testing.

The overall concept used to validate the pulley locations consisted of a simple slope equation problem. If the muscle locations of the origin and insertion points could be found when the arm is at 0° of flexion, or extended straight out, then these points could be used to calculate the slope of the muscle lines of action. With the slope identified, the pulley location could be placed anywhere along that line.

Applying this method to the cadaveric specimens proved challenging, however, since all specimens were amputated mid-humerus. This meant that the muscle insertion points were no longer intact and could not be used to determine the muscle lines of action. To solve this problem, OpenSim software was used to estimate the location of each muscle insertion point for each specimen. OpenSim is a biomechanical software system that contains musculoskeletal

models that are used for research. The calculations in this study were computed using the Arm26 model, which was scaled to the size of each specimen. From the scaled models of each cadaver, muscle origin and insertion points were located and used to calculate the slope of the muscle line of action.

A scaling factor was calculated and applied in OpenSim to scale the Arm26 model for each cadaveric specimen. First, the forearm length of each specimen was measured. This distance was measured from the lateral humeral epicondyle to the radial styloid. Next, the length of the forearm of the Arm26 model was found. The scaling factor was calculated by dividing the cadaver forearm length by the Arm26 model forearm length, which can be seen in the equation below.

$$\frac{Cadaver\ Forearm\ Length}{Arm26\ Model\ Forearm\ Length} = Scaling\ Factor$$

This scaling factor was applied to the model for each cadaver in order to estimate the location of the muscle origin and insertion points for each specimen.

Each of the three muscle groups used to actuate flexion and extension in this study presented unique sets of limitations in the OpenSim model. For this reason, different assumptions were made for each muscle group. The method used to find the slope of each muscle group and the assumptions used to calculate this slope is documented in the following sections.

Biceps Brachii

One of the muscle groups used to actuate flexion was the biceps brachii and therefore the line of action needed to be identified. In OpenSim, muscle groups are depicted as one line that is representative of the center of the muscle belly. Additionally, muscles do not follow one direct

path. Instead, they have multiple wrapping points where the direction of the muscle changes. Therefore, to calculate the slope of the biceps brachii, two of these wrapping points needed to be chosen to isolate a straight line in which a slope can be calculated. The two points chosen for this purpose are highlighted in **Figure 27** below.

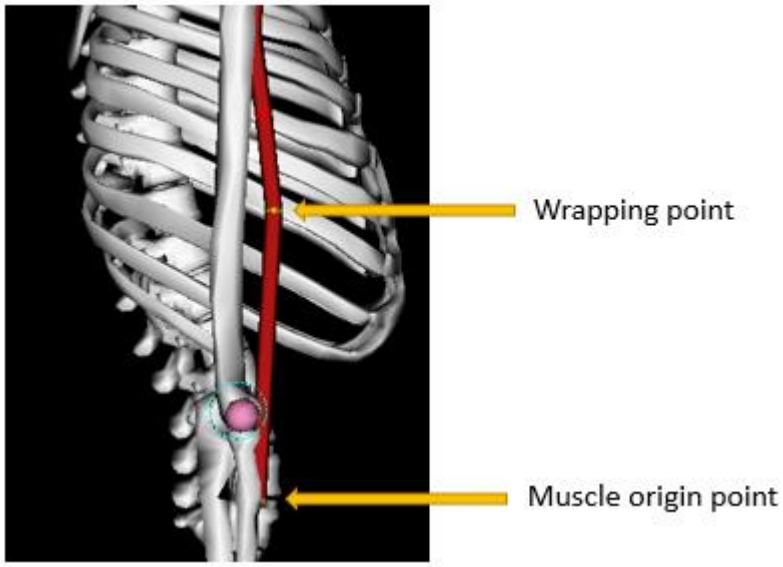

Figure 27: Biceps brachii wrapping points chosen for muscle lines of action calculation highlighted in yellow

The first point was chosen because it is the muscle origin point and the second was chosen because it is the last point before the muscle group splits into two separate bicep muscles. The splitting of the muscle group can be seen in the **Figure 28** below.

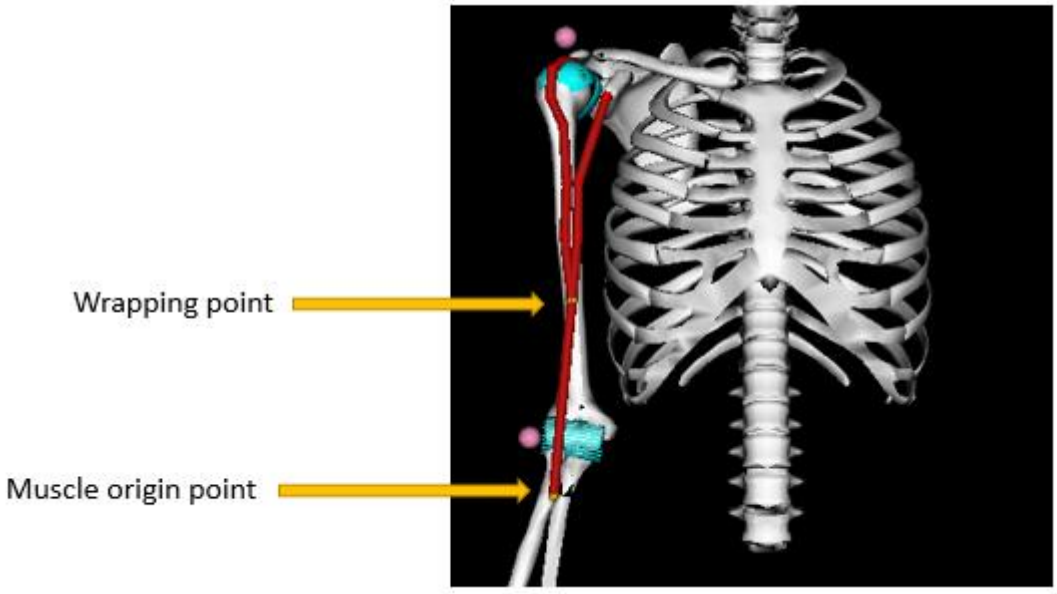

Figure 28: Wrapping points (highlighted in yellow) chosen for muscle lines of action showing the splitting of the muscle group

The x, y, and z coordinates of these two wrapping points were taken for each scaled model in reference to the lateral humeral epicondyle. They were then all averaged. The averaged x and y points were used to calculate the slope. This axis system can be seen below.

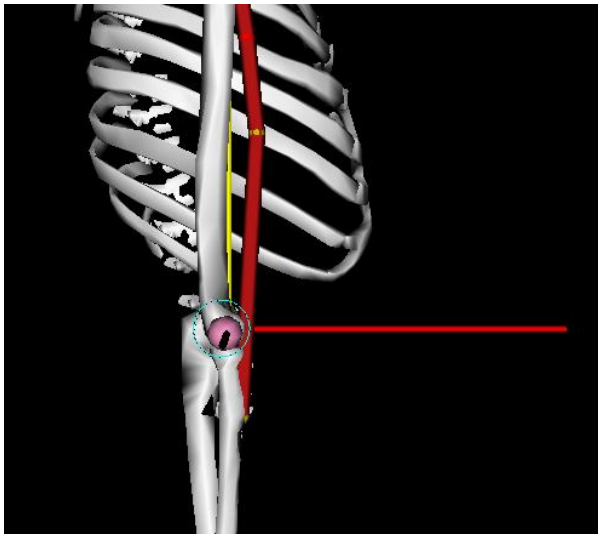

Figure 29: Axes of the coordinate system where the x-direction is shown in red and the y-direction is shown in yellow

The slope was calculated using the following equations where point 1 is the origin point and point 2 is the wrapping point selected:

Point 1 = Muscle origin
Point2 = Selected wrapping point
m = slope
b = y-intercept
y = distance vertically from muscle origin
x = distance horizontally from humerus surface

$$m = \frac{Point\ 2_y - Point\ 1_y}{Point\ 2_x - Point\ 1_x} \quad \text{Eq. 1}$$

$$b = Point2_y - m(Point2_x) \quad \text{Eq. 2}$$

From there, it was assumed that the point at which the coordinates were being taken was at the surface of the humerus. In this way, the pulleys could be placed for any *distance x* away from the humerus while the *y* distance was defined as the vertical height of the pulley from the muscle origin. For simplicity, this distance was subtracted from the *y distance* from the lateral humeral epicondyle to the muscle origin. This distance was then used as the *distance y* from the lateral humeral epicondyle. To find the slope, the following values were obtained from OpenSim and used in equations 1 and 2.

$$m = \frac{10.98571\ \text{cm} - (-4.62143\ \text{cm})}{1.592857\ \text{cm} - 0.721429\ \text{cm}}$$

$$m = 17.90984$$

$$b = 10.98571 - 17.90984(1.592857)$$

$$b = -17.5421$$

The pulley was chosen to be 1.65 cm (*distance x*) from the humerus so the *distance y* was found with the following equation:

$$y = m(1.65\ cm) + b$$
$$y = 17.90984(1.65\ cm) - 17.5421\ cm$$
$$y = 7.5\ cm$$

With these calculations, the location of the pulley for the biceps brachii was chosen to be 1.65 cm (*distance x*) from the humerus and 7.5 cm (*distance y*) from the lateral humeral epicondyle.

Brachialis

The other flexor muscle group used in this study was the brachialis. The same method and equations used for the biceps brachii were also used to calculate the slope for the brachialis. The location from which the coordinates were taken in reference to was still assumed to be at the surface of the humerus. However, in OpenSim the brachialis only has the muscle origin and insertion points so no assumptions were made using wrapping points. One other difference was that the coordinates were taken with the arm position at 90° of flexion as opposed to 0°. This was because at 0° of flexion the brachialis is curved around the elbow joint preventing the calculation of the slope. At 90° of flexion, the brachialis is straight and thus the slope can be calculated. The only difference this change in arm position made was that the *distance y* found from the slope equation was assumed to be the distance from the lateral humeral epicondyle. Equations 1 and 2 were applied to find the slope and y-intercept. From there, the pulley location was chosen to be 1 cm (*distance x*) from the humerus and 7.5 cm (*distance y*) from the lateral humeral epicondyle.

Triceps Brachii

The third muscle group that was used to actuate dynamic flexion and extension were the triceps brachii. These muscles function to aid forearm extension as well as muscle co-contraction. As with the biceps brachii and brachialis, the same method and equations were used to find the pulley location for the triceps brachii. These coordinates were taken when the arm was at 0° of flexion. The two points used were the muscle origin point and the second wrapping point. These points can be seen highlighted in yellow in **Figure 30** below.

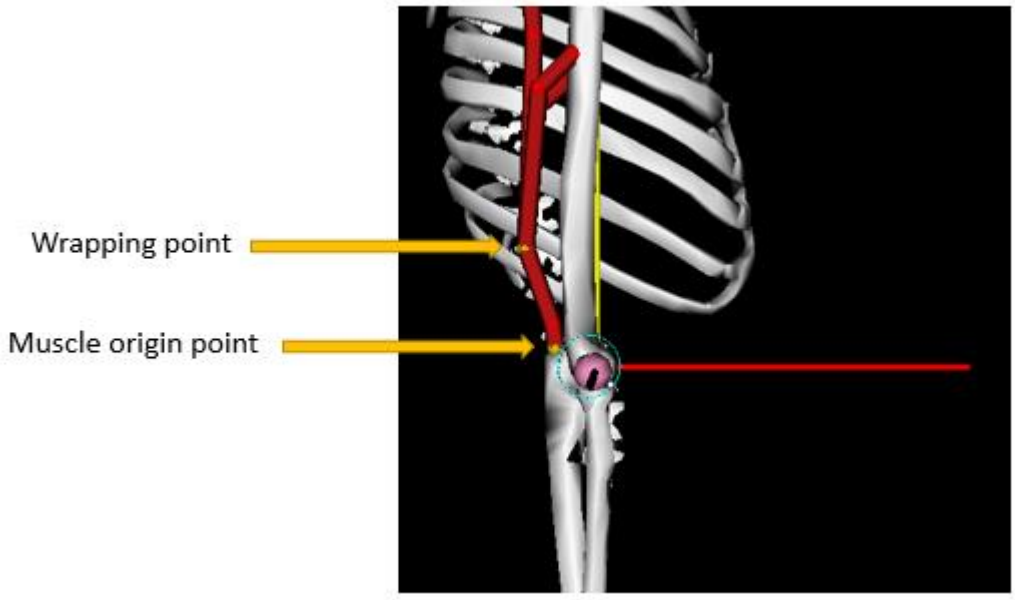

Figure 30: Triceps brachii wrapping points chosen for muscle lines of action calculation highlighted in yellow

The second wrapping point was chosen over the first because it remained closer to the general muscle line of action. When using these points, however, it had to be assumed that the muscle path stayed in a straight line in the region between the two points. This meant ignoring the first wrapping point altogether. For the triceps brachii, the *x distance* found in the slope calculations was the *distance x* from the anterior side of the humerus. To find the pulley *distance x* from the posterior side of the humerus, the average diameter of the human humerus was used (Qu,

1992).This humerus diameter value was subtracted from the *distance x* in the slope calculations to find the *distance x* of the triceps brachii from the posterior side of the humerus. Equations 1 and 2 were applied to find the slope and y-intercept. From these calculations, the *distance x* from the posterior side of the humerus was 1 cm and the *distance y* from the lateral humeral epicondyle was 6.1 cm.

5.1.2 Polhemus Motion Capture

A validation study was conducted to validate appropriate rates to perform the flexion/extension motion. To maintain physiological relevance, the team chose to model these rates after one slow and one fast act of daily living. The slow action chosen was drinking from a cup, whereas the fast motion was using a hammer. The Polhemus G4 motion tracking system was used to record and analyze the kinematics of a volunteer while performing these model activities. The Polhemus G4 system tracks motion in six degrees of freedom: x, y and z position values and azimuth, elevation, and roll rotational values.

To set up this study, sensors were placed on the subject's wrist, lateral humeral epicondyle and shoulder. The location of each sensor in space was recorded while the subject performed trials of each of the described motions. To keep the motion in one plane, a board was placed upright next to the subject's arm to guide the movement. An image of this setup can be seen below in **Figure 31**. For each trial, the subject performed the activity 10 times. Three trials for each rate were recorded.

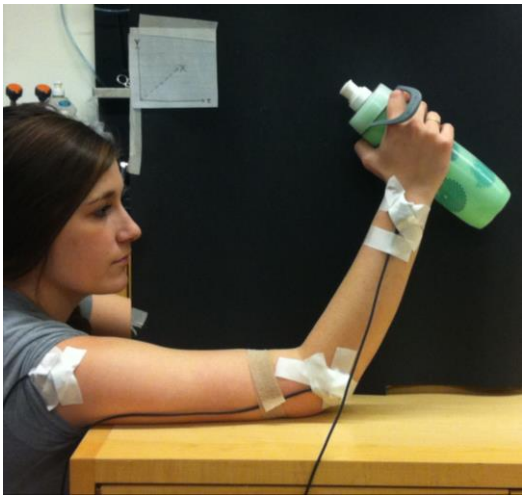

Figure 31: Motion capture study subject setup

Once the data was collected, it was then processed using MATLAB to calculate linear velocity. To calculate linear velocity, the change in position was calculated over time. MATLAB was used to first separate the data by sensor and then to find the angle between two vectors for a specified range of each cycle of the motion. The vectors were created from data points taken at the same time interval from the wrist and elbow sensors. After initially observing the Y-Direction vs. Time plot (seen in **Figure 32**), the range of 5 inches to 8 inches was chosen since all of the cycles fell within this region.

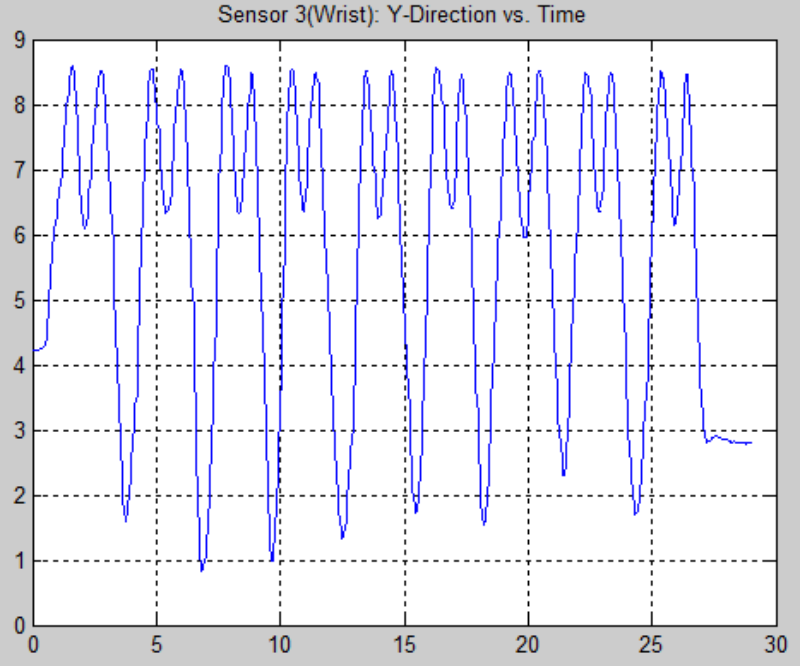

Figure 32: Wrist sensor Y-direction in inches vs. time in seconds

For each ascending portion of the cycle, the time point in which the Y-value was equal to 5 or 8 inches was indexed. Then the Z-values at these time points were extracted. The data at these time points were also extracted for the y and z values collected from the elbow sensor. These points were used to find the vectors from the elbow to wrist sensor in the y and z direction. By performing a dot product calculation, the angle between the two vectors was found. This angle was divided by the time region to find the angular velocity. A figure of the set up with labeled sensors and a corresponding image showing the two vectors and theta found to calculate angular velocity can be seen below in **Figure 33.** In this diagram, the green circle represents the elbow sensor location and the blue dashed lines represent the arc created by the wrist sensor during flexion and extension of the forearm.

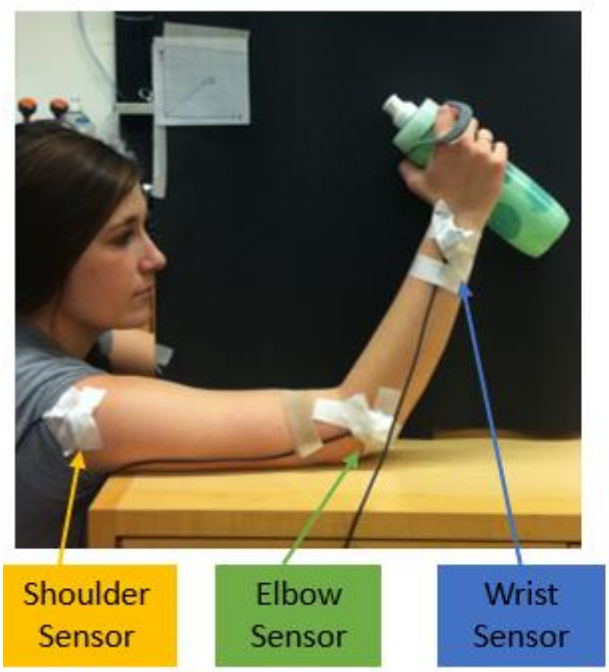

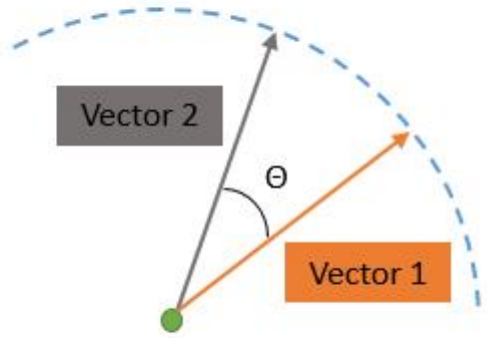

Figure 33: Image showing labeled sensors (left) and diagram of vectors and theta used to calculated angular velocity (right)

Linear velocity was computed by multiplying the angular velocity by the radius of the muscles. The muscle radius used was the biceps brachii distance from the lateral humeral epicondyle to the muscle origin found in OpenSim. These linear velocities were found for each cycle and averaged together. These averaged values were collected for each of the three separate trials conducted and were averaged together again to find the rates. The final slower drinking rate was 3.6 in/s or 91.4 mm/s and the final faster hammering rate was 11.9 in/s or 302.26 mm/s. The full MATLAB script used for this analysis can be seen in **Appendix A**.

5.1.3 Theoretical Calculations

Statics

To validate expected data from the cadaveric study, static calculations were performed to find theoretical joint reaction forces (JRF) within the elbow at different degrees of flexion. These calculations were performed so that they could later be compared to Tekscan data collected in

the biomechanical study. Static calculations were completed using anthropomorphic data and OpenSim software. This information collected from OpenSim and necessary general information regarding the specimens were compiled in an Excel sheet and was extracted for computation in MATLAB. Calculation of equations were performed in MATLAB.

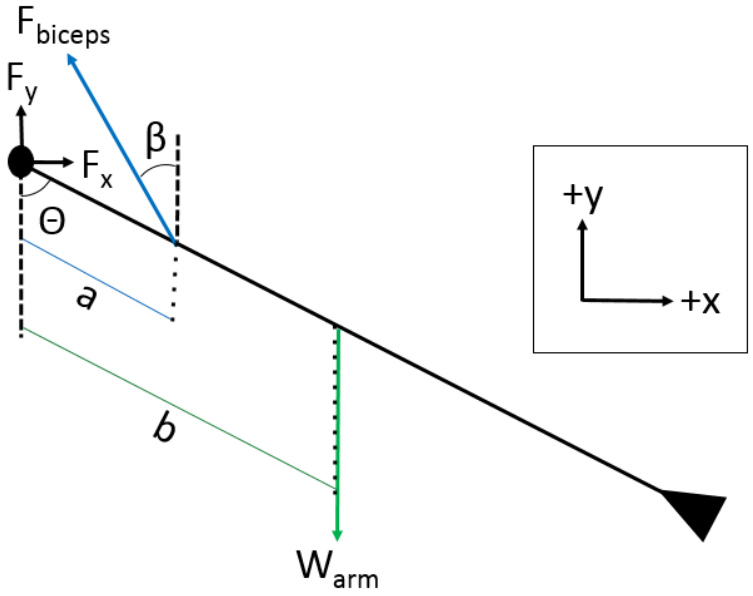

Figure 34: Free body diagram (left) and JRFs about the elbow (right)

$$\sum F_x = 0 \qquad \text{Eq. 3}$$

$$F_x - F_{biceps}\sin(\beta) = 0$$

$$\sum F_y = 0 \qquad \text{Eq. 4}$$

$$F_y - F_{biceps}\cos(\beta) - W_{arm} = 0$$

$$\circlearrowright \sum M_{elbow} = 0 \qquad \text{Eq. 5}$$

$$(-F_{biceps}\cos(\beta))(\text{acos}(\theta)) + (W_{arm})(bcos(\theta)) = 0$$

There were several known values before the calculations could be performed. The value for the distance from the elbow to the biceps insertion point (Labeled “a” in Figure **34** above) was found using anthropomorphic data from OpenSim and physical measurements taken from the cadaveric specimens. The OpenSim Arm 26 model was scaled to be the size of each cadaver ("OpenSim 3.2 [Open source software]," 2014). See section **5.1.1** for detailed explanation of this process. The value for the distance from the elbow to the where the force from the arm weight acts is the center of mass (COM) of the arm. The COM of each arm was found using the ratios given in *Biomechanics of Motor Control and Human Movement* by David A. Winter (Winter, 1990). For each cadaver, the COM ratio was multiplied by the forearm and hand length of each cadaver so that this value would be more accurate to each specimen. The forearm and hand length was found using ratios in Winter’s text and multiplying it by each cadaver’s height (Winter, 1990). The angle Θ shown in the equations 3-5 above is the angle of flexion. The angle β, shown in equation 3-5 above, was found using anthropomorphic data found in OpenSim. To find this, the Arm 26 model was scaled to be the size of each cadaver. From there, the forearm of each scaled model was flexed at 30°, 60°, and 90° where muscle origin and insertion points were collected using the same assumptions that were used in section **5.1.1**. See this section also for detailed information regarding which wrapping points were used for muscle insertion points. With this information, the vector between these two points was calculated and used to find the angle of the biceps brachii from vertical. With all of these known values, the force of the biceps could be found. With the force of the biceps, both the x and y joint reaction forces could be calculated. Because each of these values were specific to each cadaver, this allowed for the joint reaction and biceps brachii forces to be calculated for each cadaver. These values were then

compiled into a list where they were averaged. These averaged numbers are shown below in **Table 6**.

Flexion Angle	Average F_x	Average F_y	Average F_{biceps}
0°	0 N	0 N	0 N
30°	22.18 N	-32.07 N	53.10 N
60°	52.68 N	-32.07N	71.44 N
90°	160.24 N	-32.07 N	164.35 N

Table 6: Statics results at various degrees of flexion

The full scripts and corresponding Excel sheets used can be seen in **Appendix B**.

Inverse Dynamics

In addition to the statics calculations, inverse dynamics calculations were performed to take into account the rate at which the forearm would be moving. These equations can be seen below.

$$\sum F_x = I\alpha \qquad \text{Eq. 6}$$

$$F_x - F_{biceps}\sin(\beta) = I\alpha$$

$$\sum F_y = I\alpha \qquad \text{Eq. 7}$$

$$F_y - F_{biceps}\cos(\beta) - W_{arm} = I\alpha$$

$$\circlearrowright \sum M_{elbow} = I\alpha \qquad \text{Eq. 8}$$

$$(-F_{biceps}\cos(\beta))(\text{acos}(\theta)) + (W_{arm})(bcos(\theta)) = I\alpha$$

These calculations were performed at 30°, 60°, and 90° of forearm flexion. They were performed using the two rates used in design implementation, which were 5 mm/s and 10 mm/s. To find angular acceleration (labeled α in equations 6-8), the 5 mm/s rate was converted to angular

velocity and the time it took to complete the motion of flexion from 30° - 90° was approximately 4 seconds. The time to complete this range of flexion at the faster 10 mm/s velocity was approximately 2 seconds. This information was used to find the angular acceleration of the faster rate. These angular accelerations were used for the joint reaction force equations as well, instead of using *x* and y linear accelerations. This slight change had little impact on the validity of the calculations, however, because the motion was completed at a constant rate. This means that the acceleration is very small in magnitude and would, therefore, minimally affect the calculations anyways. The moment of inertia (labeled I in equations 6-8) was found using radius of gyration values given in Winter's text and the mass of the forearm and hand of each cadaver (Winter, 1990). Values for a, b, β, θ were found in the same way they were found for the statics calculations. Like with the static calculations, the information collected from OpenSim and necessary general information regarding the specimens were compiled in an Excel sheet ("OpenSim 3.2 [Open source software]," 2014). This data was extracted for computation in MATLAB. The averaged values from all cadavers can be seen below in **Table 7** and **Table 8**.

Flexion Angle	Average F_x	Average F_y	Average F_{biceps}
0°	0 N	0 N	0 N
30°	12.51 N	-11.54 N	30.33 N
60°	58.11 N	-37.34 N	79.01 N
90°	190.52 N	-41.39 N	199.13 N

Table 7: Inverse dynamics results at slow rate of 5 mm/s and various degrees of flexion

Flexion Angle	Average F_x	Average F_y	Average F_{biceps}
0°	0 N	0 N	0 N
30°	-18.59 N	54.59 N	-42.97 N
60°	69.42 N	-48.60 N	94.98 N
90°	266.23 N	-64.79 N	278.69 N

Table 8: Inverse dynamics results at fast rate of 10 mm/s and various degrees of flexion

The full scripts and corresponding Excel sheets used can be seen in **Appendix B.**

5.2 Setup Validation

Another major objective of this study was for the setup of the system to simulate dynamic flexion and extension of cadaveric elbow specimens. To validate that the conceptual design would create this motion properly, the team built a series of prototypes and used sawbones to mimic cadaver testing.

5.2.1 Cardboard Prototype

The first way in which the team tested the validity of the setup was by making the conceptual designs for the forearm guides and fixation plates out of cardboard. The setup included a PVC pipe with metal mounted pulleys attached to it. Nylon rope was attached to the sawbones with duct tape to mimic the insertion sites of the muscles and sutured tendons. A picture of this setup can be seen above in **Figure 26**.

This prototype was tested two ways: with the Instron in Goddard Hall and with the forearm guides. When attached to the Instron, the team was able to validate that the design was capable of simulating cycles of flexion and extension through the desired range of motion. When testing this setup with the Instron, the forearm guides were not included since they were made of

cardboard and therefore the dimensions of the slot were not accurate or precise. However, the concept was validated by manually moving the sawbones and forearm plates through the guides.

The first vise used to hold the PVC pipe was a suction vise. However, the setup was too heavy for the vise to support it and therefore another vise was used. The second vise had a clamp that allowed it to attach to the edge of a table. Although this vise held the PVC, the setup as a whole could not be tested since the vise had to be at the edge of a lab bench, which left no room for the rest of the setup (i.e. forearm guides). Because of this, a new vise, capable of being bolted to the table, was purchased. The bench vise bought was beneficial in two ways. First, it was strong enough to support the heavy specimen and PVC fixation device. Second, it doubled as a pipe vise, allowing for a better grip to the PVC.

We were able to learn quite a bit from the cardboard forearm guides. First, the slots in the guides were not made with precision because they were cut with a dull X-Acto knife. The lack of precision made it very difficult for the forearm to track smoothly in the forearm guides. While the slots in the forearm guides successfully prevented pronation, we learned that they need to be very precise in order to maintain functionality.

The cardboard forearm fixation plate was attached to the proximal end of the sawbones by drilling through the humerus and ulna while they were clamped down together. The team discovered that this method disrupted the joint space in the sawbones because the bones were clamped down too tightly in an unnatural position while being drilled. However, it was difficult to tell whether or not this would be an issue when testing with a cadaver specimen.

The setup was originally being designed for a pegboard table that was supporting the Instron in Gateway. This was advantageous because anything could be bolted to the table, providing an easy interface for the design setup. Therefore, the forearm guides and vise were going to be bolted to the table. Shortly after running tests with the prototype, however, the Instron was moved to a different room onto a different table with no pegboard surface. To remedy this, the team decided to brainstorm different types of bases to interface the vise and forearm guides with the Instron table. In the end, a raised wooden board heavily coated in lacquer was chosen as a platform for the new setup interface. Holes were drilled into the board to bolt the vise and forearm guides down.

5.2.2 Final Prototype

After making adjustments from the first setup validation testing conducted in Goddard Hall on WPI's main campus, the final designs for the forearm fixation plates and guides were machined out of clear acrylic sheets. Next, a wooden board was purchased and built for the base. Once all of the individual parts of the system were prepared, the team started assembling the final setup in the Gateway Lab located just off of WPI's campus. The board was raised off of the Instron table using 2x4's in order to allow each piece of the setup to be bolted down through the board and secured with nuts. Using bolts was more practical than screws because one forearm guide would need to be removed between experimental phases to allow access to the vise in order to load each specimen onto the setup. The bolts also make it possible to dissemble the setup for storage. After assembly, the wooden base was secured to the foot of the Instron by sliding a bolt through the tracks provided on the Instron and securing it with a nut. This allowed for a secure and stable setup.

Information gathered from OpenSim confirmed that the metal pulleys used on the previous model were too large to maintain the muscle lines of action. Smaller pulleys were researched and the correct sizes were unable to be ordered online. Therefore, custom-made pulleys were machined out of a circular nylon rod. The smallest diameter pulley that could be made had a 1 cm diameter measuring where the cable sits in the pulley. An image defining this diameter (d) can be seen below in **Figure 35**.

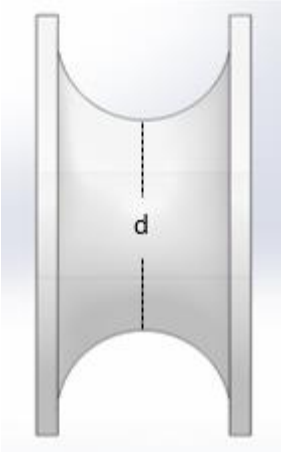

Figure 35: Pulley diameter (d)

The team determined that the PVC should be at least 5 cm away from the lateral humeral epicondyle and the cable on the pulleys needed to be at least 1 cm away from the humerus to leave room for elbow flexion and extension. This space also allowed us to account for variation of humerus diameter amongst cadavers. The muscle lines of action were calculated for the largest and smallest cadaver specimens using previously obtained measurements of forearm length. This yielded a range in which the pulleys could be placed along the PVC device. Within this range, using a distance of 7.5 cm away from the lateral humeral epicondyle as a constraint for the biceps brachii and brachialis pulley locations, the *distance x* of the cable from the humerus

was determined for both muscle groups. An image displaying these distances can be seen below in **Figure 36**.

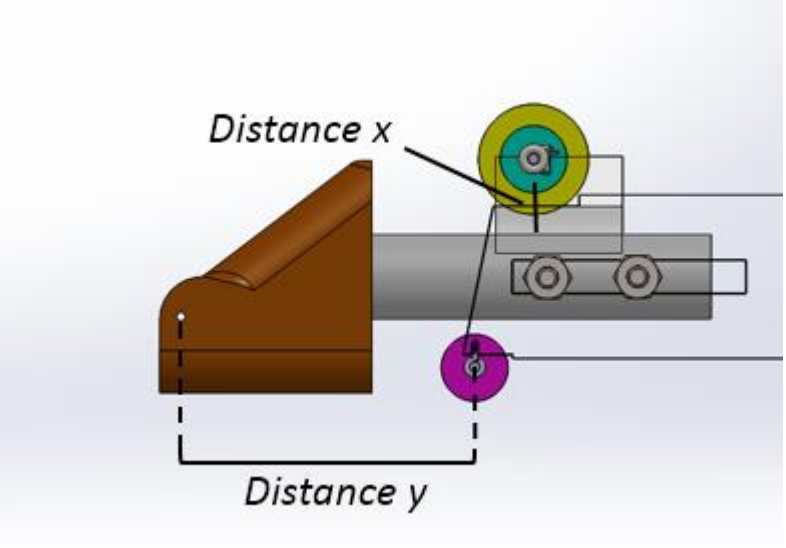

Figure 36: Distance y and Distance x

In order to fit both pulleys at the same distance away from the lateral humeral epicondyle, they needed to share an axle. To account for the difference in height needed for the biceps brachii in comparison to the brachialis, two different sized pulleys were machined. The biceps brachii pulley was the smaller pulley with a 1 cm diameter. The brachialis pulley was made larger with a diameter of 2.31 cm. The height of the pulley axle was determined to be 0.875 cm above the exterior of the PVC. The location of the pulley axle above the exterior of the PVC was determined by using the *x direction* away from the surface of the humerus minus the thickness of the PVC and the space between the surface of the humerus and the PVC. The detailed process used to calculate the pulley locations can be seen in the Pulley Locations results section above. Since the pulleys are custom made, the mounts were also customized. For the biceps brachii and brachialis, the mount was machined out of a PVC sheet and secured to the device with PVC

cement. Notches were cut out of the PVC under the bicep brachii, brachialis, and triceps brachii pulleys in order to mount them in their correct locations. A picture of the notch and the pulleys for the bicep and brachialis can be seen below in **Figure 37**Error! Reference source not found..

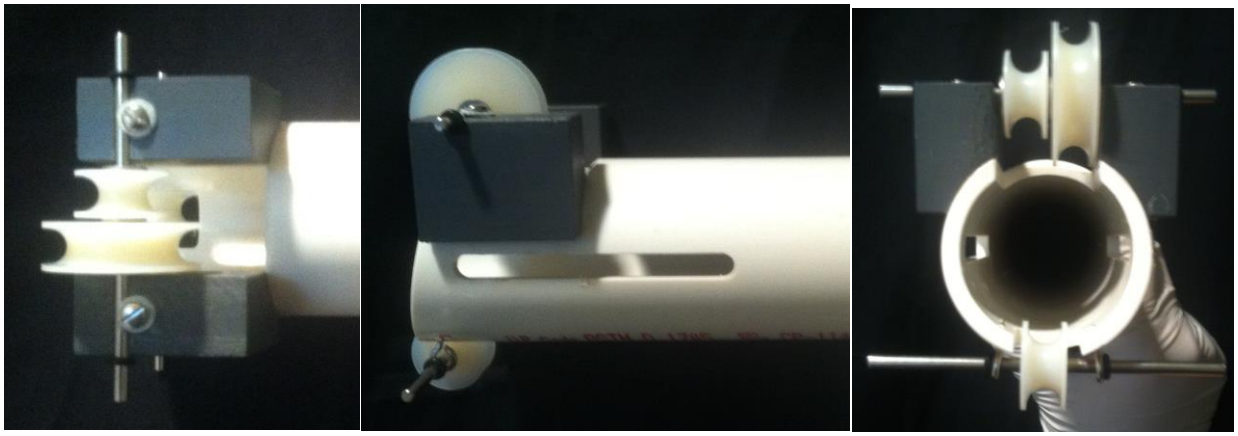

Figure 37: New Pulley Mount (from left to right: top, side, and front views)

The triceps brachii pulley needed to be located closer to the lateral humeral epicondyle than the other pulleys to maintain the muscle lines of action. In order to do so without restricting forearm flexion or extension, we shaved the front face of the PVC pipe at an angle. This made the bottom of the pipe, where the pulley would be placed, 1 cm longer than the top of the pipe, where the other two pulleys were placed. The triceps brachii pulley axle was placed 6.1 cm away from the lateral humeral epicondyle, taking care to stay within the previously calculated range. The pulley had a 1 cm diameter and was lowered approximately 0.21 cm below the PVC pipe. The axle was secured in the correct position using eye screws and O-rings prevented it from sliding side-to-side.

In order to suspend a free-hanging weight from the triceps brachii tendon, we had to create a pulley system to redirect the cable over the edge of the Instron table. The free-hanging weight was essential to the setup because it simulated co-contraction of relevant muscle groups and

forearm extension. The magnitude of this weight is dependent upon the forces applied to the biceps brachii and brachialis. During preliminary testing with a cadaver specimen, we applied approximately 44 N of force (10 lbs) to the triceps brachii when there was a force applied to the biceps brachii and brachialis which was in the range of 100 N to 200 N. The force applied to the triceps is over double the force applied to the flexor muscles because it has to overcome those forces in order to extend the forearm and create a controlled motion during flexion.

When it came time to assemble the forearm fixation components (forearm plates and guides), we discovered a couple of challenges. First, the forearm guides were too wide to fit close enough to the vise. This was easily remedied by trimming the edges closest to the vise by 2.7 cm. Next, when the setup was assembled we tested the tracks in the forearm guides using synthetic sawbones and found that the rod on the forearm plate did not move smoothly through the slot without hitting the acrylic. This is because the natural extension of the forearm occurs at a slight angle since the biceps brachii are a pronator muscles. This means the attachment sites of the biceps brachii are located on the radius and when contracted, it causes the radius to pronate over the ulna. To account for this, the slots were widened by 1/4 inch so the guides may support the forearm without restricting its motion. Additionally, to account for the natural angle of the human forearm when extending, the vise will be adjusted on its swivel to angle the humerus and allow the forearm to move in as straight a line as possible along the slots in the guides.

The design of the forearm fixation plates also needed adjustment. We tested the forearm plates by tightening them on a person's arm. By doing so, we found that the bolts were too short to secure the plates around the soft tissue on the proximal end of the forearm. This was easily fixed by purchasing longer bolts for this end of the forearm plate.

The initial Instron-cable interface simply consisted of tying the biceps brachii and brachialis cables tightly to the Instron. This interface, however, did not allow for the complete intended range of motion. To fix this, a pulley system was built to optimize the relation between angular displacement of the forearm and the linear displacement of the Instron.

After the rates were calculated with the Polhemus data, a BlueHill Instron test was configured to conduct cyclic testing using the validated rates. The rates were slightly higher than expected so the math and units were re-examined. The correct limits on the test needed to be set to ensure the Instron would not surpass the global limits and crash the software. The higher the rate, the farther the crosshead would move past the set limits in the test parameters.

5.2.3 Final Design

In the second round of final design setup validation conducted in the Gateway lab, the forearm fixation, pulley-Instron interface, test rates, and triceps brachii weight were validated to ensure the system was compatible with the Instron and capable of cyclic motion.

Forearm fixation

After the slots of the forearm guides were widened, they were tested again to make sure they did not inhibit the angle of the forearm during flexion and extension. The changes made significantly improved the interface between the forearm guides and the rod of the forearm plate. Also, applying a greater load to the triceps brachii decreased the angle of the forearm during flexion, resulting in a much smoother and more controlled movement.

Pulley-Instron Interface

One of our biggest challenges was perfecting the pulley-Instron interface component of the setup. First, the new pulley system was tested and we found that it allowed for the full range of

desired flexion. Next, we had to identify an appropriate cable to interface our setup with the Instron actuator. The first cable we used was a nylon rope (referred to as Yellow Yarn in graph below). This material, however, had a very low stiffness and allowed for too much slack in the system. It did not effectively simulate extension after flexion and we decided not to use it. Next, we tried a fishing line with a lead core surrounded by a polyester braid (referred to as Lead in graph below). While this material was strong enough to withstand the high loads applied to it, it had a comparatively high stiffness and did not give enough slack in the system. Therefore, this cable did not effectively simulate flexion because it did not transfer the loads from the actuator to the tendons to move the forearm. The next cable we tried was a 50 lbs traditional fishing line (referred to as Fishing Wire in graph below). Initially, this material seemed to work. After attempting several trials and applying high loads to the material, however, it stretched quite a bit and left too much slack within the system. This material was also difficult to tie to the sutures due to the differences in diameter and therefore we decided not to use it for the flexor muscles. However, the fishing line sufficiently supported the triceps brachii weight and we decided to use it for that part of the setup. Finally, a braided 65 lbs fishing line was tested and proved to allow a sufficient amount of slack within the system while maintaining its stiffness (referred to as braided fishing line in graph below). The desired cycles of unassisted flexion and extension were achieved using this cable. Mechanical testing was performed on all of the cable material options to test the load versus extension in order to observe their stiffness. A graph of these results can be seen below.

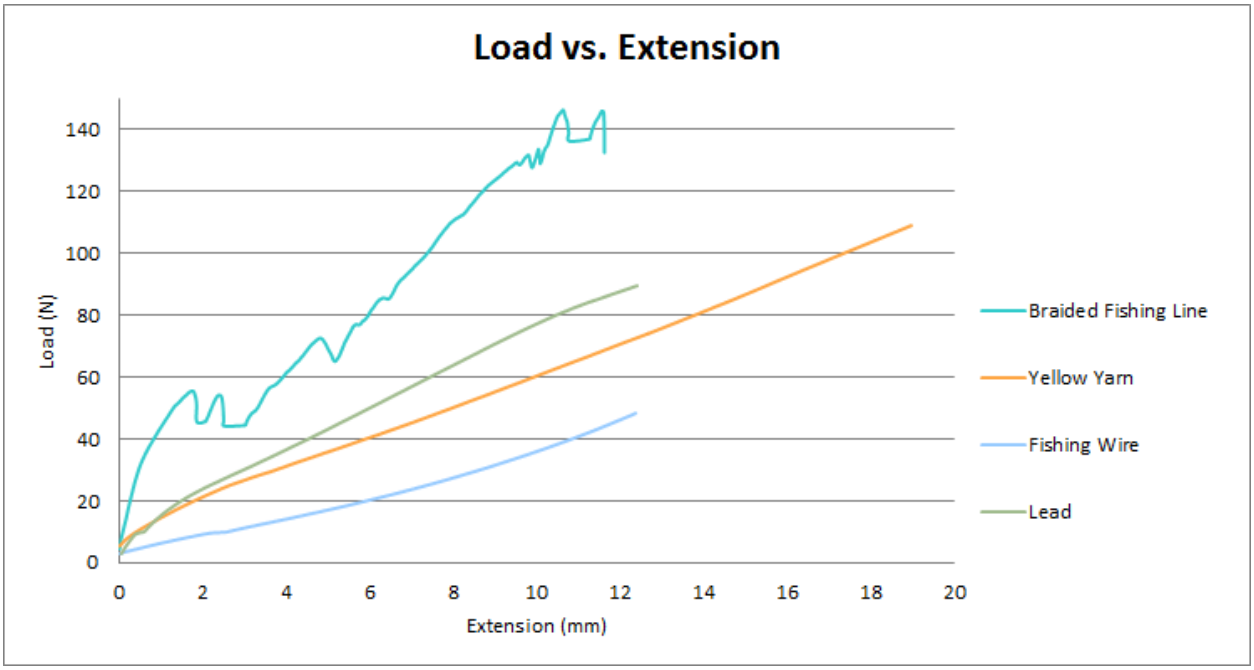

Figure 38. Load vs. Extension of Cables

The braided fishing line was tested multiple times on the Instron and the knots kept slipping. This could be due to a different person tying these knots. Even with the multiple slips, the braided fishing wire has the least amount of extension for the most amount of load. Also, the diameter of this cord was very small and easily fit through the pulleys. This cable was chosen for its ability to resist extension and its ability to easily move through the pulleys. With the system, a different person was able to tie the knots so that they did not slip.

Test Rates and Triceps Brachii Weight

The test rates and triceps brachii weight had to be validated together since they were dependent upon one another. We began by focusing on flexion using the different validated rates and arbitrary weights on the triceps brachii. These rates were too fast for the capacity of the Instron and, therefore, we had to use percentages of the lower validated rate. This validation was done simply via trial-and-error until we were able to create the desired motion. We successfully

simulated an unassisted range of flexion of 30° to 100° using a rate of 10 mm/s and applying a load of approximately 44 N onto the triceps brachii. Admittedly, this is not the full range of motion in which we intended to simulate, however, the UCL is the primary stabilizing ligament from 30° to 120° and simulating active flexion within this range sufficiently meets the project goals.

5.3 Design Implementation

After validating all of the separate system components and then testing the entire setup with a cadaver specimen, we were able to perform final design implementation in the form of a UCL biomechanical study. The study took place at Gateway Park on April 14th using the elbow simulator testing apparatus, validated setup, and ElectroPuls E1000 Instron actuator. Testing was conducted in three experimental phases: native UCL, transected UCL, and reconstructed UCL. The following sections outline the methods, data acquisition, analysis and results of this study.

5.3.1 Specimen Preparation

Specimen preparation was conducted prior to testing in order to make the process more efficient. The chosen specimen belonged to a 76-year-old Caucasian male donor. The forearm and humerus lengths were approximately 29.1 cm and 19.3 cm, respectively. The joint was in fairly good condition, but had severe signs of arthritis. The specimen was thawed approximately 24 hours prior to testing to ensure the soft tissues regained their mechanical properties. When completely thawed, the soft tissue around the humerus was dissected and it was predrilled with a drill press making two ¼ inch bolt clearance holes approximately 1 inch apart. Next, the soft tissues around the joint were dissected away to locate the tendons of the bicep brachii, brachialis, and triceps brachii. When the tendons were found, they were sutured using FiberWire suture

material. Saline solution was periodically sprayed onto the specimens during preparation (and testing) to prevent the tissues from becoming dehydrated. Next, the Tekscan sensor was inserted into the joint space using the “boat race” incision as previously described by (Duggan et al., 2011). Finally, the specimen was attached to the humeral fixation device by bolting the humerus to the PVC pipe using two ¼ inch bolts.

The lab and setup was also prepared prior to testing to increase efficiency. First, all personnel and appropriate surfaces were correctly prepared for a biohazardous experiment by donning all personal protective equipment (i.e. glasses, gloves, lab coat, etc.) and covering the lab bench with blue chuck. Next, we assembled as much of the testing setup as possible prior to conducting the experiment to allow for efficiency. Preliminary test setup included placing the baseboard onto the Instron table, bolting the inner forearm guide and vise to the board and fixing the board to the foot of the Instron via the secure bolt. Prior to setting up, the baseboard was thoroughly covered in plastic wrap to protect it from biohazardous substances. While this was being done, another member of the group started up the Instron and then the computer with the BlueHill software. Once the position and load limits were set using the Instron Console, BlueHill was opened and the previously configured test was located. We made sure to take careful note that the crosshead was at -27.00 mm and the console side bar stayed a constant green, which indicated that the Instron had full power. The crosshead position was placed at -27.00 mm which was close to the lower limit of -29.00 mm. This was to ensure that the stroke length of the Instron would be sufficient in creating the flexion/extension motion without surpassing the Instron position limits.

After specimen preparations were completed, we transferred the fixed specimen and PVC to the vise. Next, we ran the previously sutured tendons and respective cables through the appropriate pulleys and to the Instron and free-hanging weight for the flexor and extensor muscle groups, respectively. When tying the cable to the Instron actuator, we had to ensure there was no slack in the system and the specimen was at the zero position (30° of flexion). Then, we adjusted the Tekscan sensor to make sure it would not shift within the joint space during testing. Finally, we secured the remaining outside forearm guide to the wooden baseboard using the ¼ inch bolts.

5.3.2 Experimental Protocol

Each specimen was preconditioned prior to collecting experimental data in order to minimize the effects of the viscoelastic properties on the ligament biomechanics. Preconditioning protocols for this type of tissue include 25 cycles at a lower validated rate. Once preconditioned, the specimen was ready for testing. Each cadaver underwent three experimental phases: native UCL, transected UCL, and reconstructed UCL. For each phase, the specimen was tested at Rate #1 and Rate #2 for ten cycles per trial. Three trials were performed for each experimental phase. Next, UCL injury was simulated by transecting the ligament for Phase II testing, which followed the same protocol as Phase I. After Phase II testing was completed, the specimen was removed from the testing apparatus and brought to the designated surgical room where the collaborating surgeon, Dr. David Magit, performed a docking reconstruction of the UCL using the palmaris longus as a ligament graft. This reconstruction can be seen in **Figure 39** below. After the procedure was completed, Phase III testing was conducted to test the reconstructed UCL.

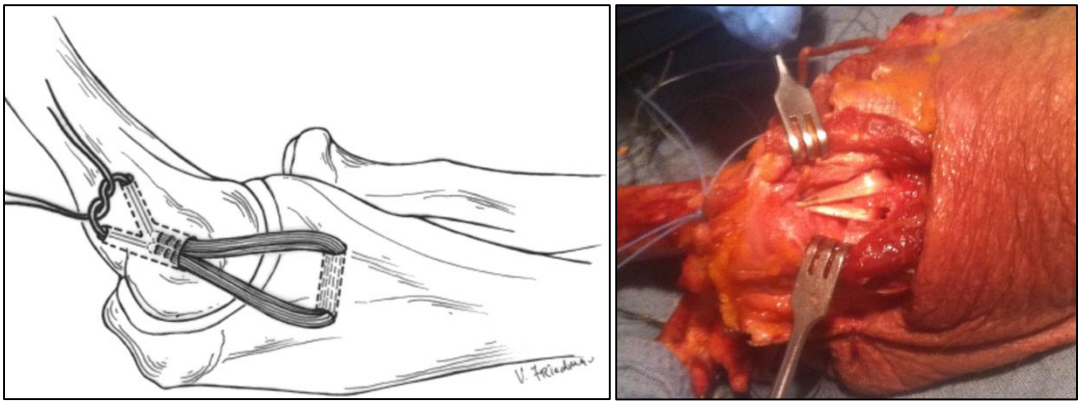

Figure 39: Diagram of Docking Reconstruction (left) (George A. Paletta et al., 2006); Dr. Magit's Docking Reconstruction (right)

5.3.3 Data Acquisition and Analysis

There was a 2 kN load cell attached to the Instron, which measured the force applied to the tendons. During cyclic testing, the Tekscan sensor remained within the joint space and collected the area and pressure distribution across the joint space for the duration of the experiment. The pre-calibrated sensor outputted data onto a computer software interface in which cells of various colors represented previously identified pressures.

5.3.4 Results

Data was collected from the Tekscan pressure sensor that was inserted into the joint in all three experimental phases. However, the data from experimental phase I (using the slow rate without weights) was the only set that was analyzed. This was because the Tekscan pressure sensor was damaged after this round of testing. The damage was evident because we could see pressure outputs from the sensor when no forces were being applied to it (while lying on the table). For this experimental phase I, the sensor was inserted posteriorly and also into both the ulnar and radial sides of the joint space. Inserting the sensor into the ulnar side of the joint was challenging because this side of the joint space was extremely tight in comparison to the radial side. The damage to the sensor that occurred after the first trial was from trying to forcefully reinsert the

sensor into the tight ulnar side of the joint space. The results from the other phases, as well as the experimental phase I fast rate, were not analyzed since the data had little integrity due to this damage. In future testing, we suggest that data be collected with a new sensor that is not damaged. If the sensor is damaged, however, a filter could be made to cancel out the pressures being sensed when no force is being applied. In future tests, we also suggest that the sensor be gently inserted into the radial side of the joint using passing sutures. Below is a diagram of the sensor orientation. The top of the sensor read the pressures exerted on the posterior side of the joint, while the bottom read the pressures exerted on the anterior side. The left and right sides of the sensor read the pressures exerted on the lateral and medial sides of the joint, respectively. The Tekscan sensor used in experimental phase I was only inserted into the joint space partially. This means that in all of the Tekscan images only the bottom of the image corresponds to the portion in the joint space.

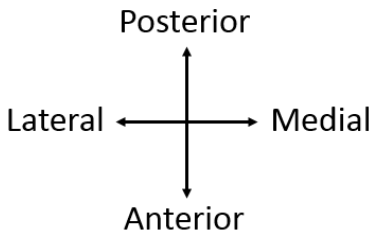

Figure 40: Orientation of Tekscan Sensor in Elbow

The following figures show the forearm at approximately 30° of flexion (**Figure 41**) and the associated Tekscan output (**Figure 42**). The Tekscan sensor output was isolated and matched to the correct degree of flexion using the appropriate video. The starting point was determined by the time in which the contact pressure started to change and this corresponded to 1 minute and 18 seconds into the video.

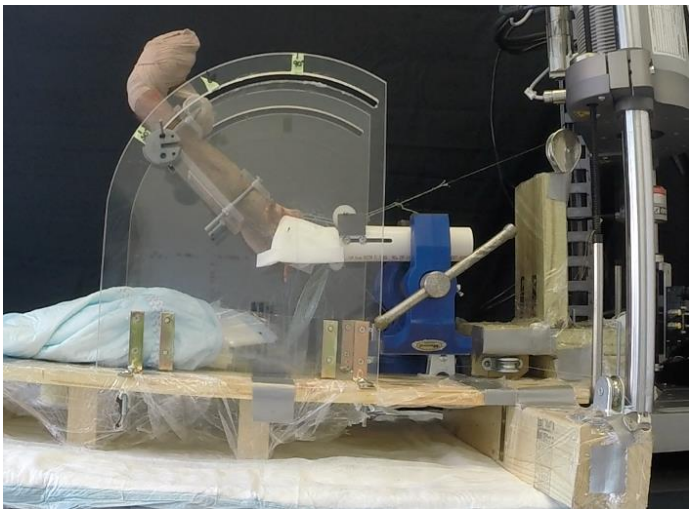

Figure 41: Phase I Slow Rate at approximately 30 degrees of flexion

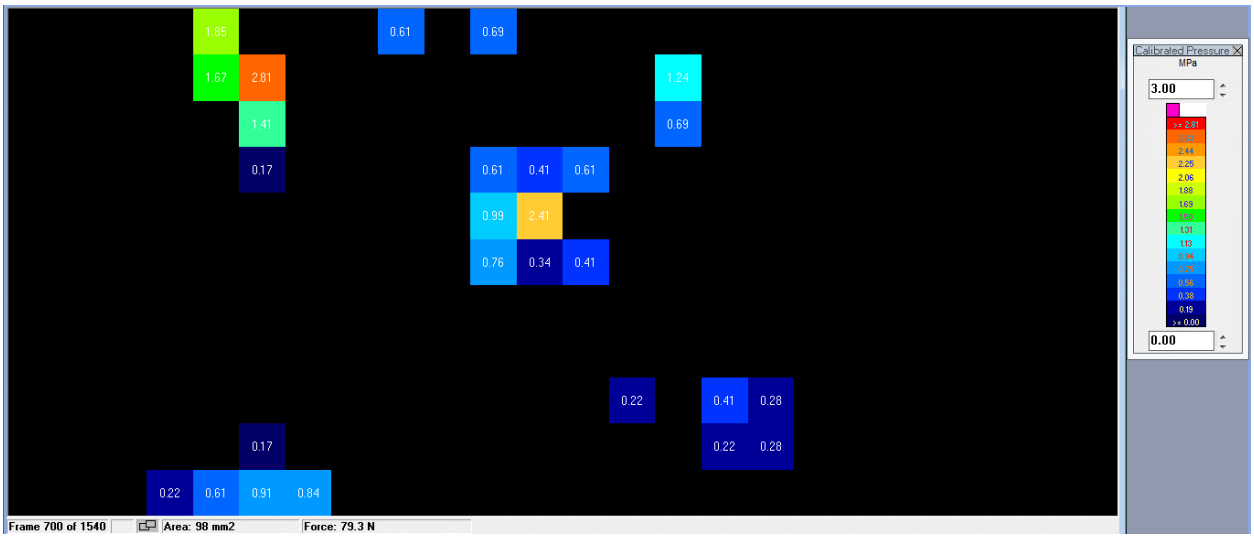

Figure 42: Tekscan at Phase I Slow Rate at approximately 30 degrees of flexion

In the above Tekscan image, you can see that the colors of the sensels began to change on the posterior side of the joint as the arm began to flex. This means that the pressure increased on the posterior side of the joint when the arm was at 30° of flexion.

The following figures are of the arm at approximately 60° of flexion (**Figure 43**) and the corresponding Tekscan output (**Figure 44**). This frame was isolated by counting the amount of seconds it took in the corresponding video to get from 30° to 60° of flexion, which was approximately 2 seconds and 20 Tekscan frames.

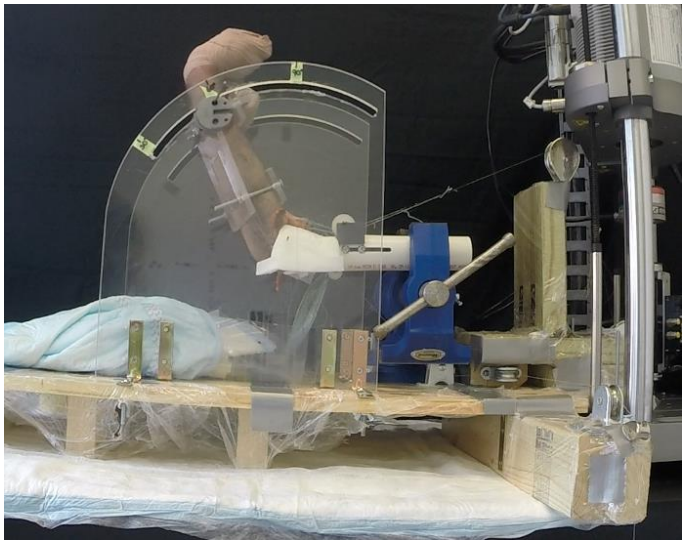

Figure 43: Phase I Slow Rate at approximately 60 degrees of flexion

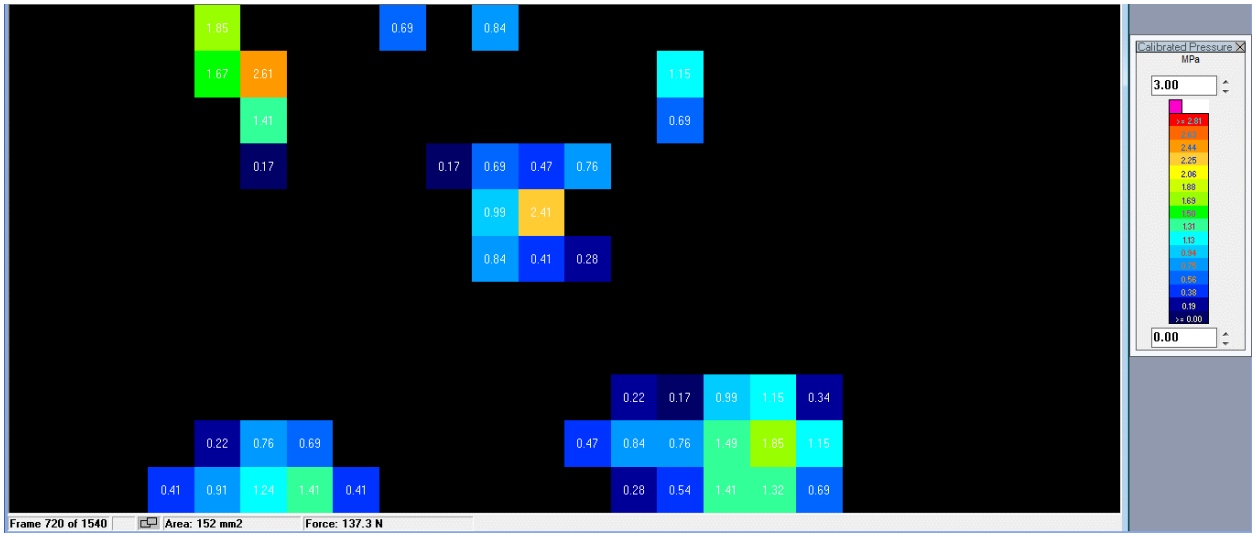

Figure 44: Tekscan at Phase I Slow Rate at approximately 60 degrees of flexion

In the above Tekscan frame, you can see the pressure has distributed across the joint space. This means that the contact area within the joint was greater at 60° than it was at 30° of flexion. There was also a moderate pressure increase in the regions of contact, which is shown by the green, yellow and orange sensels.

The following figures show the arm at approximately 90° of flexion (**Figure 45**) and the corresponding Tekscan output (**Figure 46**). This frame was isolated by counting the amount of

seconds it took in the corresponding video to get from 60° to 90° of flexion, which was approximately 3 seconds (30 Tekscan frames).

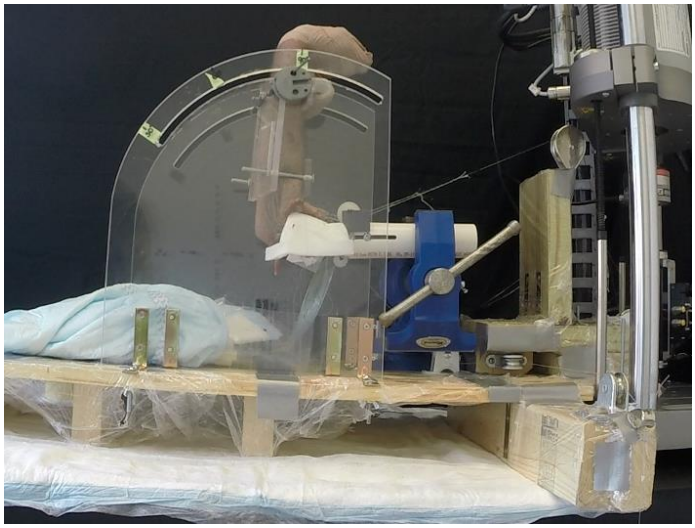

Figure 45: Phase I Slow Rate at approximately 90 degrees of flexion

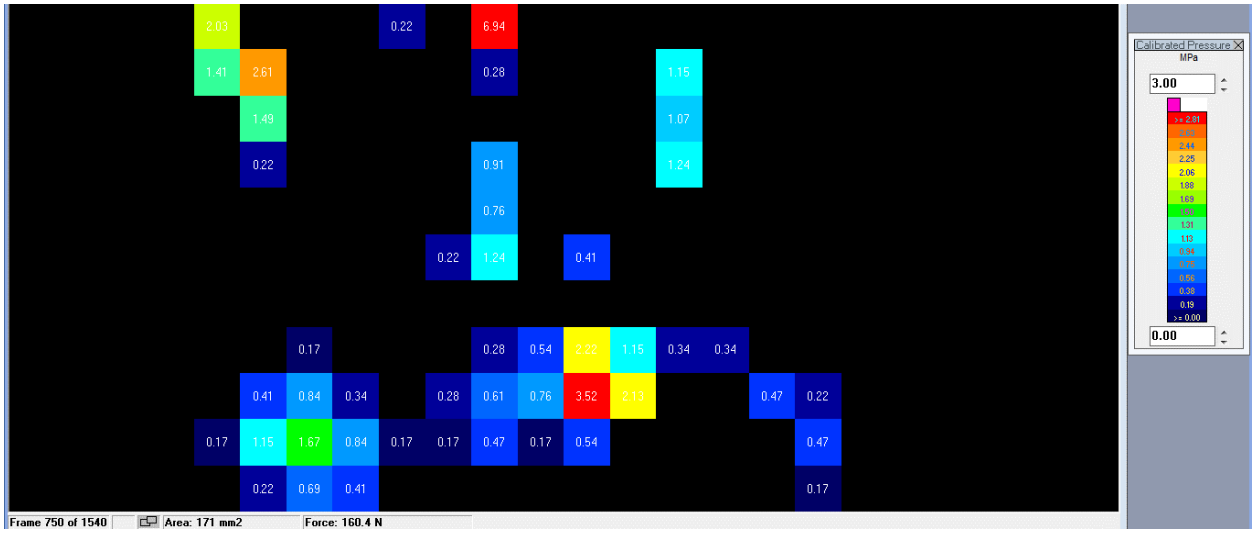

Figure 46: Tekscan at Phase I Slow Rate at approximately 90 degrees of flexion

In the above Tekscan frame, you can see there is a greater pressure distribution across the joint space at 90° of flexion than there was at 60° of flexion. This means the contact area has increased. There was also an increase in concentrated contact pressure. The regions of concentrated contact pressure are shown in yellow, orange and red.

The various parameters collected during design implementation testing included the articular contact area and overall force. The results obtained from the three different degrees of flexion from the first experimental phase can be seen in the chart below.

Degree of Flexion	Experimental		Theoretical
	Articular Contact Area $(mm)^2$	Overall Force (N)	Overall Force (N)
30°	98.0	79.3	12.9
60°	152.0	137.3	47.1
90°	171.0	160.4	132.5
Average	89.8	125.7	64.2

Table 9: Results Table of Tekscan Data from Phase 1 Slow Rate

From this chart, we can see that the articular contact area and overall force within the joint increased as the arm progressed to higher degrees of flexion. In future testing, data collected in the phase I (native UCL) will serve as a baseline to compare to data collected from phase II (transected UCL) and phase III (reconstructed UCL). Changes regarding changes in contact areas and shifts in concentrated contact pressures as well as the overall force within the joint will be observed to determine the degree to which UCL reconstruction alters the joint-contact mechanics.

Additionally, in this table are the theoretical inverse dynamics calculations for the slow rate. The theoretical forces in this table are calculated specifically for the one cadaver analyzed, rather than the averaged values for all the cadaver specimens. When these numbers are compared to the experimental values it can be seen that they are significantly lower in magnitude. This variation could be because there were forces recorded on the portion of the sensor that was outside of the joint.

6 Discussion

A description of the results obtained throughout the project is described in this chapter in order to better understand the meaning of the data. First, the significance of the design validation conclusions is discussed. Next, the results from the setup validation methods are analyzed. Then, the design implementation data and results are examined. The limitations and impact of the project are also outlined and discussed.

6.1 Design Validation

The purpose of conducting design validation was to ensure the system maintained as much physiological relevance as possible. This was done by strategically placing pulleys on the humeral fixation device to maintain muscle lines of action when applying loads to flexor muscle tendons. The locations of these pulleys were calculated using the Arm26 model in OpenSim. We also used validated rates to actuate the flexion motion, which were found by conducting a motion capture study. The calculations and results from OpenSim and the motion capture study are discussed in this section.

6.1.1 Pulley Locations

Calculations performed using information found in OpenSim allowed the team to validate the muscle lines of action. While this method provided a far more accurate method for determining muscle lines of action, several assumptions still needed to be made. The first major estimation made was using the OpenSim software itself, which was created based off of assumptions made of the human body. Within OpenSim, there were several more assumptions made, which are summarized here. For the biceps brachii, brachialis, and triceps brachii data, it was assumed that axis from which the measurements were collected from was situated at the surface of the

humerus. Next, for the biceps brachii and triceps brachii, wrapping points were used to represent muscle origin and insertion points because the muscle lines of action are not straight. Furthermore, for the triceps brachii, the muscle origin and second wrapping point were used. Because of this, it had to be assumed that the region in between these two points was straight even though there was one wrapping point between them. Lastly, for the biceps brachii and triceps brachii, which are muscle groups that contain several individual muscles, it was assumed that these muscle acted along the same line of action at the region close to the elbow. This allowed for one pulley to be used for each of these muscle groups. These assumptions reduced the accuracy of the calculations. Without them, however, it would have been impossible to estimate where the muscle lines of action were.

6.1.2 Polhemus Motion Capture

Utilizing the Polhemus G4 system for validating the rates at which the flexion/extension motion would be created allowed the team to choose common movements. Using these common movements made the testing more relevant to people with UCL injuries. However, assumptions were made in this process as well. It was assumed that the motion was only occurring in the y-z plane and it was also assumed that the motion being created was being done so in a uniform fashion.

6.2 Setup Validation

Setup validation was performed in order to ensure the separate components of the design properly functioned in a working system. Several series of mock testing were conducted prior to reaching the final working system. First, a cardboard prototype of the final conceptual design was built and tested. After numerous adjustments were made to this design, the first prototype was

built and tested using synthetic sawbones. When the issues with this setup design were identified and remedied, we tested the final product with a cadaver specimen. The results from each of these mock tests are discussed in this section.

6.2.1 Cardboard Prototype

The cardboard prototype aided in visualizing the design concept although the measurements were not accurate. During this round of mock testing, the team determined that applying active loads to the bicep brachii and brachialis tendons along with a applying a free hanging weight to the triceps brachii tendons would create a flexion/extension motion. It was also determined that the Instron in Goddard Hall could provide smooth actuation between a range of flexion of 30° and 120°. The vises used to hold the humeral fixation device (PVC pipe) were not compatible with the forearm guides. Additionally, the PVC pipe tended to slip and tilt in both vises that were tested. To avoid this problem, a pipe vise was purchased. The new pipe vise had bolt clearances allowing for it to be bolted to a table, which is compatible with the forearm guides. The pipe vise also griped the PVC pipe around the circumference, which provided greater stability.

The inaccurate slots of the cardboard forearm guides made the track nonfunctional and thus we learned that it was very important the arc of the slots be extremely smooth and precise. After talking to our machinist, Tom Partington, we decided that a slot could be drilled smoothly and accurately using a 3/8” acrylic sheet.

Creating the forearm fixation plates out of cardboard brought up a concern that the forearm fixation plates might disrupt the joint space. The team decided to continue with the design with the idea that bolting the bones while they were in their natural position would not disrupt the

joint as much and that the joint space would be less affected in a biological joint that has a joint space. This did not impact the design as it did not affect the joint space of the cadaveric specimen.

Next, we had to decide what kind of base to use for our setup in order to create a platform to bolt all of the assembly pieces down. Both wooden and metal bases were considered but a wooden base was constructed due to lack of time, machining skills, and available machinery to build with metal. The wooden base would be easily customizable because it could be drilled into and cut with tools that were available to the team.

6.2.2 Final Prototype

After mock testing with the cardboard setup and making all of the necessary changes, we brought the new prototype and setup to the Gateway Lab for testing. First, we quickly tested the setup with synthetic sawbones and then extensively with a cadaver specimen. During this round of mock testing, more issues were identified and addressed.

Using wood to build the base of the setup was a successful way to support the apparatus. The only improvement made during this phase of mock testing was to use wing nuts on the bolts that secure the forearm guide to the baseboard in order to facilitate quick and easy assembly.

Since the setup was placed on the same table as the Instron, we needed to redirect the cables for the triceps brachii in order to attach a free-hanging weight to the tendon. This free-hanging weight was a necessary component of the system in order to drive extension of the forearm and mimic co-contraction of the muscles. Without the free-hanging weight, the system would have been incapable of cyclic testing. Without co-contraction of the flexor and extensor muscles, the acceleration of the forearm would have been uncontrolled, which was not ideal. A series of

pulleys needed in order to successfully hang a weight off of the side of the Instron table. This component was added and tested in the final round of mock testing.

There were a couple adjustments that needed to be made to the forearm fixation component of the system. First, the bolts that were used to clamp the forearm plates around the forearm were too short on the proximal end due to the amount of soft tissue. This was easily remedied by purchasing longer bolts. The forearm guides also needed to be adjusted to account for the natural angle at which the forearm specimen was flexing. This angled flexion occurred since the biceps are pronator muscles, meaning when a load is applied to the tendons, it causes the radius to pronate over the ulna. This caused the rod on the forearm plate to come into contact with the side of the tracks, adding friction to the system. To account for this motion, we needed to widen the slots on the guides to give the rod a greater degree of freedom.

The Instron interface was originally very simple, consisting of cables fed through pulleys on the PVC device and directly attached to the Instron crosshead. This configuration, however, did not provide the full range of motion for the setup. We learned that we needed to add a series of additional pulleys in order to create the full desired range of motion. This new interface was built and tested in the final round of mock testing

The final adjustment that we made during this round of mock testing was associated with the rates of actuation. The rates of testing determined through analysis of Polhemus data proved to be too high for the limitations of the Instron. In order to choose rates that were still relevant to acts of daily living but would not exceed the global limits of the actuator, we needed to use

percentages of the lower validated rate. Validation of these experimental rates was conducted in the final round of mock testing.

6.2.3 Final Design

A final round of mock testing using a cadaver specimen was conducted in order to finalize the system as a whole. In this last round, the new forearm fixation adjustments were tested. Next, the new pulley system for the Instron-apparatus interface was tested. Then the pulleys used for redirection of the triceps weight and the magnitude of the weight on the triceps were validated. Finally, the Instron tests with associated experimental rates were validated using the whole system.

The forearm fixation needed to be tested again during this round of design validation. First, longer bolts were purchased to clamp the forearm plates around the specimen on the proximal end. These new bolts improved the functionality of the forearm plates. Next, to create a greater degree of freedom for the rod on the forearm plate, we widened the slots on the forearm guides by a ¼". This adjustment corrected the issues we were having in the previous round of mock testing, resulting in a smooth and frictionless motion.

Next, the Instron-apparatus interface needed to be improved in order to create the full desired range of motion. To do so, a pulley system was built and tested. With these new pulleys, we were able to displace the cable enough to create a range of flexion of 30° to 120°. However, the experimental range used was 30° to 100° since the apparatus could not easily simulate extension when the forearm flexed to 120°. This new range of flexion did not negatively impact the functionality of the apparatus since it is within the range of motion in which the UCL is the

primary stabilizing structure in the elbow. A picture of this new cable orientation can be seen below.

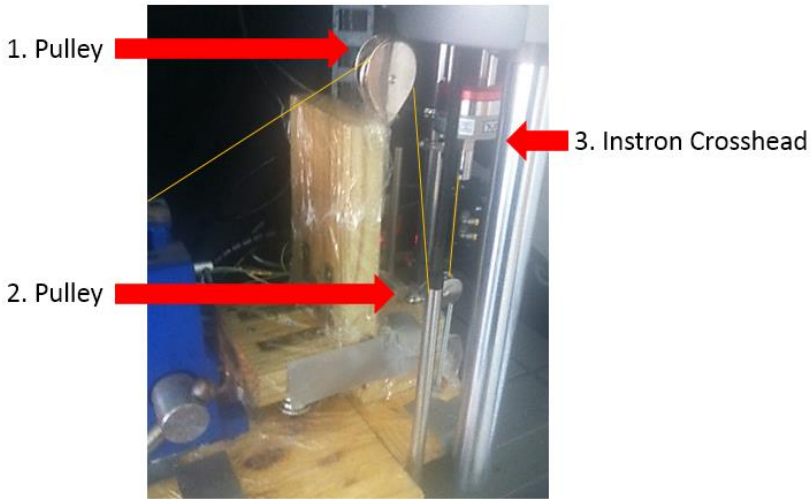

Figure 47: Cable-Instron Interface

The new pulley redirection system for the triceps brachii successfully provided enough clearance for the weight to be hung off of the edge of the table. Validation of the magnitude of the free-hanging weight was conducted on a trial-and-error basis. The rate of actuation and the magnitude of the weight on the triceps brachii were directly proportional. The rate of the Instron needed to increase as the magnitude of the weight did because the force applied to the flexor muscles needed to increase in order to overcome the added weight to the extensor muscles. This also simulated co-contraction of the muscles, which produced a controlled and accurate motion allowing for repeatability of the experiment.

Since using the rates that were validated from the motion capture study, conducted with Polhemus software, resulted in the system exceeding the global limits of the Instron, we used percentages of the slower rate for our experimental rates. The slower experimental rate (Rate 1) we chose to use was 5 mm/s and the faster rate (Rate 2) was 10 mm/s. This allowed for a safe

experiment while keeping the parameters of the motion in context with common ADLs. When using Rate 1 during testing, the validated magnitude of the triceps weight was 2 pounds. When using Rate 2 during testing, the validated magnitude of the triceps weight was 10 pounds. Validating these parameters lead to the development of Instron tests that were saved and used during design implementation. The experimental procedure can be found in **Appendix C.**

6.3 Design Implementation

Design implementation was conducted in order to verify the functionality of the custom apparatus and experimental setup. To validate that the dynamic elbow simulator met all of the design objectives, we used the apparatus to test a cadaveric specimen at various efficiencies of the elbow UCL. The custom apparatus will be used in a biomechanical study conducted by the Troy lab in the future. The objective of the study will be to observe any changes in joint contact biomechanics of the elbow joint after UCL reconstruction. Although the study had not been conducted at the time of this project, the team tested one cadaveric specimen. We used the left arm of a 76 year old male donor who was 5’ 8” and 129 lbs. With this specimen, we were able to measure the articular contact area and overall force at 30°, 60°, and 90° of flexion of the intact specimen. Data from this experimental phase showed an increase in articular contact area and total force as the forearm increased in degrees of flexion. The data from the transected and reconstructed UCL phases were not analyzed due to the Tekscan sensor being damaged during phase I. A different method of Tekscan insertion has been suggested in hopes to prevent damage to the sensor and secure it in place better. This new method involves inserting the Tekscan anteriorly while using passing sutures from the posterior.

6.4 Limitations

Like any project, ours had different limitations that are important to recognize when analyzing results. The several kinds of limitations associated with the validation methods used, the design of our apparatus and the experiment conducted during design implementation are discussed in this section.

6.4.1 OpenSim Limitations

As previously discussed, the major limitation of the OpenSim software was that it required many assumptions to be made in order to complete the calculations. Also, human error when taking measurements of the cadaver specimens may have affected the OpenSim results.

6.4.2 Polhemus Limitations

Several limitations of the Polhemus system may have affected the results of the motion capture study. Human error was one of the main limitations of this system. This included that the marker on the elbow was not exactly at the center of rotation of the elbow which affects the accuracy of the data. Also, while the motion in which the subject performed was slightly constricted, not all unwanted movement could be prevented which could have skewed results. Also, any presence of metal can distort the ability of the system to work accurately. The location of the setup of the Polhemus system was intentionally placed away from metal and, therefore, this limitation had little to no impact on the study.

6.4.3 Design Limitations

One limitation of the design was that we only had one actuator to apply loads to the muscles. Because of this, the triceps brachii were statically loaded with a free-hanging weight while the biceps brachii and brachialis were loaded via active actuation with the same Instron. Also, the system was incapable of simulating unassisted extension when the forearm was flexed to 120°,

therefore, we limited the range of flexion to 100°. This resulted in a smooth and unassisted motion.

6.4.4 Experimental Limitations

There were experimental limitations that affected the biomechanical study conducted to implement the design. Some minor limitations of the study included the surgeon's schedule and preferred reconstruction technique as well as the Instron rate capabilities. A major limitation was the small sample of cadaver specimens that we were able to test. Due to time constraints, we were only able to test one forearm cadaver specimen for the design implementation process. The other limitations of the study were associated with the use of a cadaver model. Cadavers can only withstand 3-5 freeze/thaw cycles before the mechanical properties degrade (Crandall et al., 2011). Another limitation of cadaveric specimens is that approximately 10% of people do not have the palmaris longus which may limit the usability of some cadavers for this particular study (Andrews et al., 2012). A detailed description of the limitations of cadaver studies was discussed previously in Chapter 1.

6.5 Impact of Design

While designing and fabricating the testing apparatus and planning the biomechanical study, the impact of this project was considered.

6.5.1 Ethics

The first aspect that was considered was the ethical impact of our design and study. When using cadaveric specimens, one must understand that these people have died and donated their body to science. Due to that agreement, the testing done with them must work towards the

betterment of science and be conducted respectfully. To ensure the cadaveric specimens are used efficiently, the setup was validated with sawbones before using the cadaveric specimens.

Another ethical aspect of our study was that it will improve the ability of surgeons to validate new surgery techniques without having to test them on a patient. This would make implementing the new surgery technique more beneficial since the surgeon would have a better idea of how the surgery would affect joint health. Knowing how a surgery affects the joint longevity could lead to technical improvements. As surgery techniques improve, the quality of life of patients improve as well.

6.5.2 Economy

The next concern the team had was the study's potential impact on the economy. Once our advisor has completed the biomechanical study, the data collected will be used to validate a computer model of the elbow joint and associated tissues. Such a model will allow surgeons to simulate effects of new reconstruction techniques in order to understand how the joint will be affected by the procedure prior to clinical trials. This will reduce the time and money that is spent validating surgeries as well as additional patient care after reconstruction. This will help improve the healthcare system and the economy.

6.5.3 Health and Safety

The next concern the team had regarded health and safety issues. While working with cadavers, the health and safety of the team was important to consider. Proper safety precautions were taken to decrease the risk of any pathogens transferring from the specimens to team members. All of the proper lab safety and equipment training was conducted prior to participation. Proper lab procedures were followed to reduce the risk of pathogens from contaminating the lab. To

protect ourselves, lab coats and rubber gloves were worn while handling the specimens. Proper disposal of biohazardous waste was also exercised.

Our design could eventually improve the health of patients since the surgical effects on the joint contact mechanics could be understood prior to performing surgery on a patient. This could reduce the risk of developing complications as a result of an ineffective reconstruction.

6.5.4 Environmental

The design and cadaveric experiment does not have any substantial environmental impact that is not found in other cadaveric experiments. The one main environmental impact of cadaveric experiments is the amount of biohazardous waste that is produced. This is nearly unavoidable and is necessary to ensure the safety of the lab workers. Biohazardous waste is autoclaved to destroy any organisms in it and sterilize the waste. This could have detrimental effects on the environment if the autoclave is not working properly as it will increase the amount of living organisms that could be passed on to the environment.

6.5.5 Social Influence

The team considered the social influence of this design and experiment. The only social influence that might play a part is the increased support or reluctance of surgeons and patients to perform or receive a surgery depending on the experimental results of that surgery. The team believes this informed decision on both the surgeons' and patients' sides will help improve the healthcare system.

6.5.6 Political

The team considered the political ramifications of this design and experiment but believed there are none.

6.5.7 Manufacturability

It is important to examine the impact of the manufacturability of a design. For this project, however, the device was not intended to be manufactured. It was created and assembled specifically for the Troy lab located in Worcester Polytechnic Institute's Gateway Park and, therefore, it is not necessary to examine the manufacturability impact.

6.5.8 Sustainability

The team considered the sustainability of this design and believes that the device could have been made with more sustainable products although the use of the setup is sustainable.

7 Final Design and Validation

The goal of this project was to design and fabricate a dynamic elbow flexion simulator for cadaveric specimens to be used in a biomechanical study in the Troy lab. The objective of this study was to determine whether or not UCL reconstruction alters the joint contact mechanics of the elbow. Additionally, the study aimed to understand the long term implications of such a procedure. In order to achieve these goals, the team had to complete the following objectives:

1. Design and fabricate a testing fixture for cadaveric specimens to simulate physiologically relevant elbow flexion and extension.

2. Implement the design by testing with a cadaveric specimen under various UCL efficiencies.

7.1 Objective 1

The first objective of this project was to design and fabricate a dynamic testing apparatus. Instead of designing the fixture as one device, we categorized it into three major components that

interface with one another to create a working system. These components were humeral fixation, forearm fixation, and actuation.

The first component of the system was humeral fixation. The function of this component was to safely secure the cadaver specimen to the apparatus and to the lab table. This was achieved by fixing the humerus in a horizontal position using the custom made humeral fixation device. First, the soft tissue was removed from the distal end of the humerus in order to expose the bone. A custom-made PVC pipe was then placed around the exposed humerus and secured using two ¼ inch bolts running through a horizontal slot on the side of the PVC pipe, through the bone and out through an identical horizontal slot on the opposite side of the PVC pipe. The device and secured specimen were then placed in a pipe-vise that was bolted to the wooden base of the setup using four ½ inch bolts. The identical horizontal slots on either side of the PVC pipe allowed for adjustability based on the humerus length of each specimen. An image of the humeral fixation device of the apparatus is shown below in **Figure 48**.

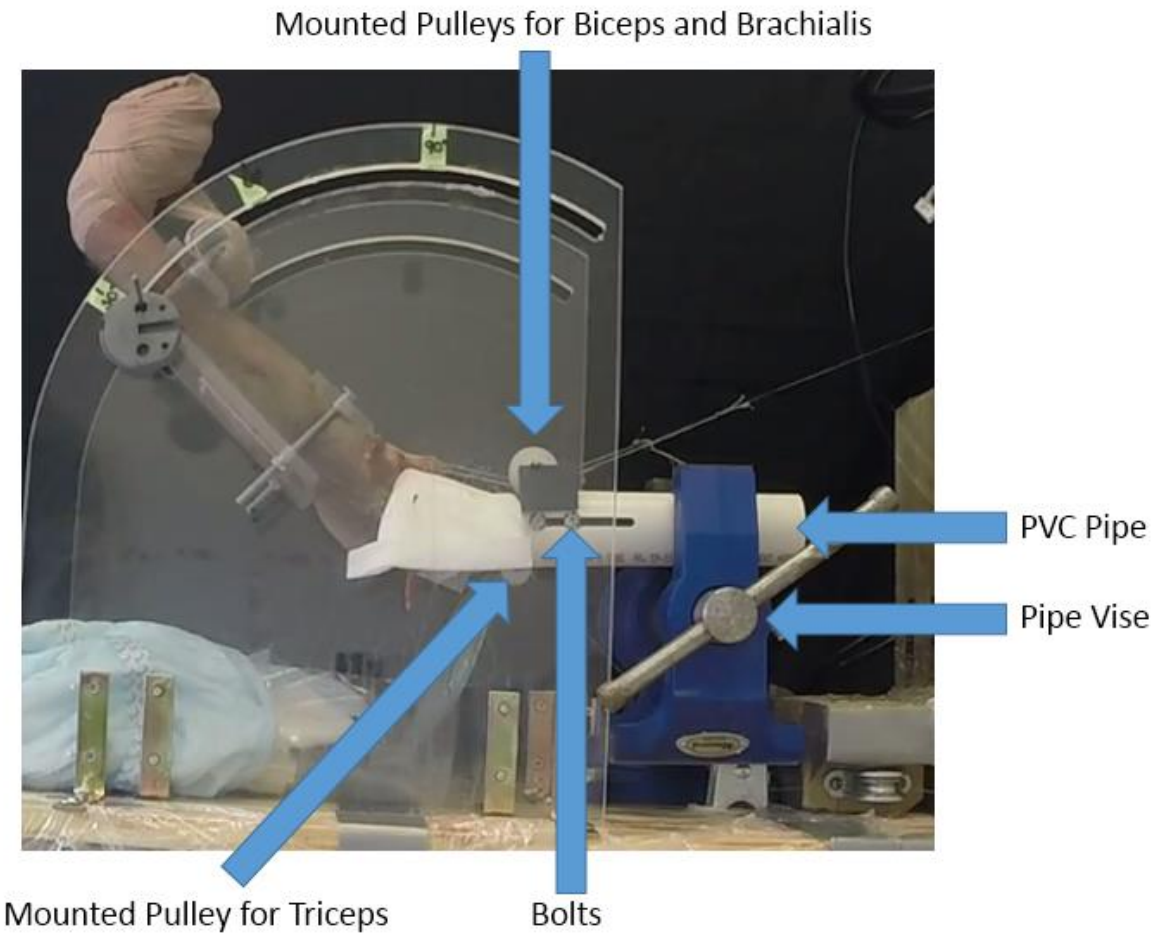

Figure 48: Humeral Fixation with Labels

The second major component of the apparatus was forearm fixation. In order to successfully simulate and analyze a series of controlled flexion/extension cycles, it was necessary to prohibit unwanted movement of the forearm during flexion. Unwanted movements include pronation or supination and side-to-side movement of the forearm while testing. Restricting the kinematics of the forearm allowed for the generation of precise and reproducible data. To prevent pronation or supination of the forearm, two acrylic fixation plates were designed and created in order to clamp the forearm in a neutral, supinated position. The larger of these plates was secured lengthwise along the posterior side of the forearm and had a metal rod extending perpendicular

to the wrist along the distal end of the plate. The two smaller plates were bolted to the larger plate on the anterior side of the forearm in order to clamp the forearm of the specimen in place. To prevent any side-to-side movement of the forearm, two acrylic forearm guides were designed. Each of these guides had an arc cut out at the top of the acrylic sheet and a slot cut just below the arc. These forearm guides were positioned and bolted to the wooden base of the setup on either side of the vise and secured specimen. The slots in each guide served as a track, which allowed the metal rod secured to the large forearm fixation plate to slide through. The interface of the plate and guides restricted the kinematics of the forearm to moving along the track. A picture of this component of the apparatus is shown below in **Figure 49** and **Figure 50**.

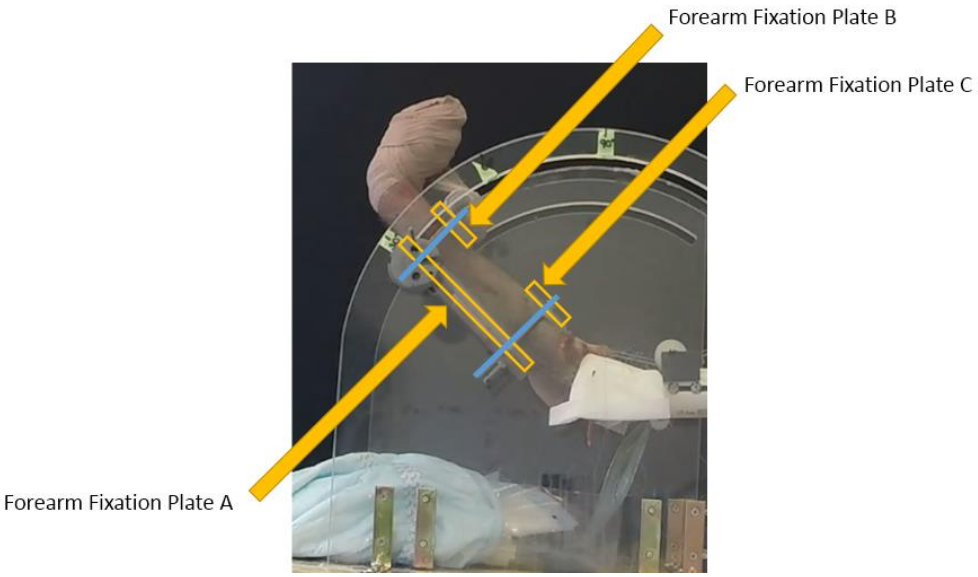

Figure 49: Forearm Fixation Plates

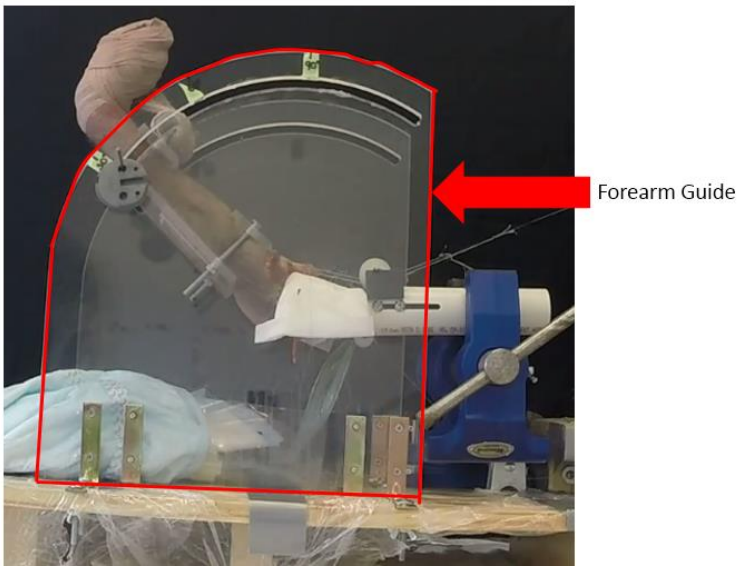

Figure 50: Forearm Guide

The final major component of the apparatus was actuation. The purpose of this component was to drive the movement needed to simulate cycles of flexion and extension. Since it was readily available, the team chose to use the ElectroPuls E1000 Instron machine located at Gateway Park as an actuator to create active flexion. Active flexion allows for the generation of precise and repeatable data since it is automated and uses controlled, known values to actuate the motion.

A major component of the design objective was to simulate a physiologically relevant motion. To preserve the physiological relevance as much as possible, the movement was created by applying controlled loads to muscle tendons of the specimen. Cables were attached to the biceps brachii and brachialis muscle tendons, run through a series of pulleys and attached to the Instron crosshead. The crosshead moved up at a controlled rate, which drove flexion of the arm. A free-hanging weight was attached to the triceps brachii muscle tendon in order to create co-contraction of the muscles and drive forearm extension when the actuator slowly returned to the zero position, releasing the load on the flexor tendons. To preserve the muscle lines of action,

the pulleys for each muscle group were mounted to the PVC pipe at locations carefully calculated from OpenSim. Calculations for the pulley placement can be reviewed in Chapter 5. An image of the actuation component of the design can be seen below.

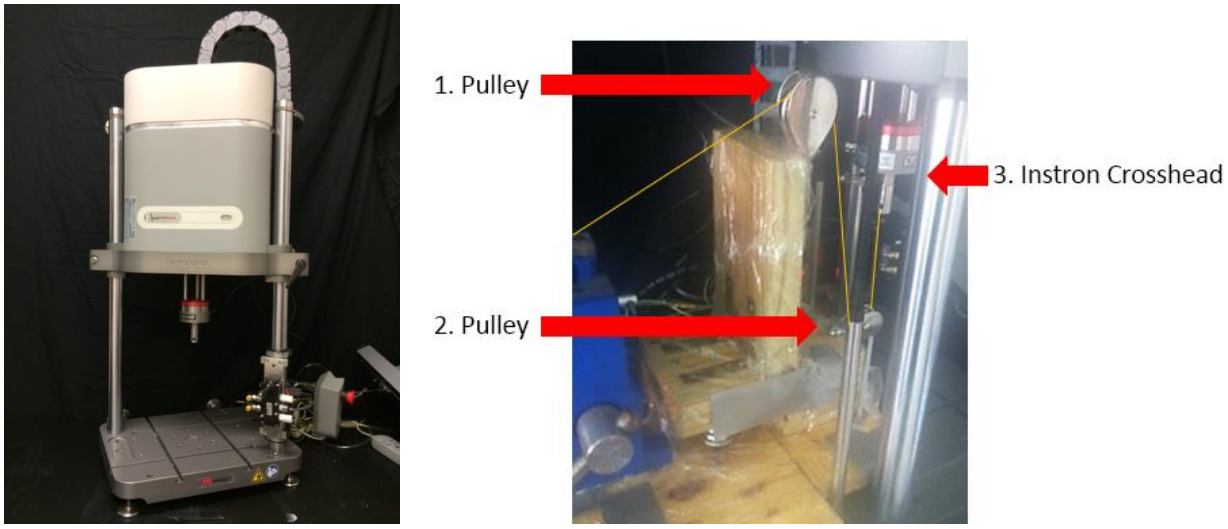

Figure 51: Instron (left) and Cable-Instron Interface (right)

7.2 Objective 2

The second objective of this project was design implementation. This was achieved by testing the apparatus with a cadaver specimen at various levels of UCL efficiency. Testing of the specimen involved simulating cycles of elbow flexion and extension with the use of our custom-made apparatus. A Tekscan pressure sensor was inserted into the elbow joint of the specimen prior to testing in order to measure the contact pressures across the joint-space during dynamic motion. Unfortunately, the sensor was damaged while testing the native ligament of the specimen and the data was not useful during the design implementation phase. However, the objective was to validate that the design of our apparatus successfully simulates physiologically relevant cycles of flexion and extension and the design implementation allowed us to do so.

Testing occurred in three phases using the native UCL, transected UCL and reconstructed UCL. During the first phase, the specimen's native, or healthy, UCL was tested in order to create a baseline of data for later comparison. After the first phase, the UCL was transected by our collaborating surgeon in order to simulate injury, and then tested in this state. Results from this phase show how the joint contact mechanics of the elbow are altered due to UCL injury. Finally, in the third phase, the transected UCL was reconstructed by the surgeon using a docking technique. After reconstruction, the specimen was then tested once again. In the biomechanical study conducted by the Troy lab, the results from these phases were compared in order to understand to what degree the reconstructed ligament alters the joint-contact mechanics of the elbow. The full protocol used in the testing of the cadaver specimens is detailed in **Appendix C**.

8 Conclusions

There were several design specifications outlined in the client statement given at the start of the project. The first was to design and fabricate a dynamic elbow flexion simulator for cadaveric testing. We were able to meet this objective by designing a system composed of three separate components. The first of these components was humeral fixation. This component functioned to secure the humerus of the specimen in a horizontal position in order to manipulate the forearm to create the desired motion. We chose to fix the humerus by bolting the humerus to a custom-made PVC device. The PVC device was clamped to the baseboard of the setup using a pipe vise. The second component was forearm fixation. This component functioned to prevent pronation/supination and varus/valgus, or side-to-side, motion of the forearm to create a controlled and repeatable motion. We fixed the forearm in a supinated position by clamping the acrylic forearm plates around the forearm and used the acrylic guides to lead the forearm

through cycles of flexion and extension. The third component was actuation. We chose to use a combination of active actuation and a free-hanging weight to drive the flexion and extension, respectively.

The next design specification given in the client statement was to simulate physiologically relevant cycles of flexion and extension. The first step taken to achieve this goal was to apply loads to the appropriate muscle tendons in order to actuate flexion and extension. The biceps brachii and brachialis muscle tendons were used to actuate flexion. Cables were sutured to these tendons, pulled through a series of pulleys and attached to the crosshead of the ElectroPuls E1000 Instron. The crosshead of the Instron moved at a controlled rate, which applied known loads to the tendons and drove flexion of the forearm. The free-hanging weight was attached to a separate cable that was sutured to the tendon of the triceps brachii. This weight functioned to drive extension of the forearm when the Instron crosshead returned to the zero position. The muscle lines of action of all three muscle groups were maintained in order to provide more physiological relevance to the system. The way we did so was by carefully calculating the PVC pulley locations using OpenSim software. The range of flexion that we chose to simulate was 30° to 120° since this is the range in which the UCL is the primary stabilizing structure within the elbow. However, during testing, added gravity created an uncontrolled motion after 100° of flexion and therefore we chose to stop flexion at this point. Since this is within the relevant range of motion, this change had no impact on the success of the design. Finally, we conducted a motion capture study to validate rates of common activities of daily living to use for experimental rates in order to create a physiologically relevant motion. However, the validated rates were too

fast to use with the Instron and, therefore, we used approximately 5% and 10% of the lower rate found in the study.

The final design specification outlined in the client statement was to use the custom-made apparatus to test a cadaver specimen at various UCL efficiencies. First, we tested the native, or healthy, state of the ligament. Next we simulated injury to the UCL and tested this transected state. A collaborating surgeon performed the transection of the UCL. In the third and final experimental phase, the surgeon performed a docking reconstruction of the ligament using the palmaris longus autograft from the specimen. After the reconstruction, the specimen was tested once more. In order to measure the joint-contact mechanics of the elbow at each experimental phase, a Tekscan pressure sensor was inserted into the joint space prior to testing. This sensor outputs an array of colors that correspond to previously calibrated pressures.

In conclusion, we were able to meet the project objectives and design specifications that were given in the client statement. We successfully designed and fabricated a dynamic elbow flexion simulator that was used to create physiologically relevant cycles of flexion and extension. This apparatus was used to test a cadaveric specimen at various levels of UCL efficiency in order to observe changes in joint-contact mechanics within the elbow joint after UCL reconstruction.

8.1 Recommendations

There were several recommendations we have in order to create a more accurate and efficient process. First, while testing the first specimen, we had been zeroing the load cell on the Instron between trials. This seemed logical because with this method the preload in the Instron test would consistently need to be equal to the free-hanging triceps brachii weight. However, by disregarding the initial force applied to the biceps brachii and brachialis tendons, it was

impossible to calculate the correct loads applied to those tendons. In future testing, we recommend the load cell not be zeroed between trials and the specimen be manually preloaded until it is ready to begin to flex.

Our next recommendation is to carefully insert the Tekscan sensor into the radial side of the joint. Since the ulnar side of the joint is much tighter than the radial side, the sensor was damaged when we tried inserting it into both sides of the joint. In the future, we recommend to simply insert it into the radial side of the joint using passing sutures and then suture it to the tissue of the specimen to keep it from shifting during testing.

Our third recommendation is to use an adjustable cable system with cables that have been pre-stretched prior to testing. The 65 lbs braided fishing line successfully allowed for flexion of the forearm when it was preloaded and stretched prior to testing. Each time the system needed adjusting, however, the cable needed to be cut from the Instron crosshead since it was impossible to untie without fraying the cable. Then a new section of cable was tied to the original, but since it was not pre-stretched, a trial-and-error approach had to be taken to remove slack from the system. We recommend pre-stretching several yards of cable prior to testing so that if the cable needs to be retied, the pre-stretched cable could be used. Additionally, creating an adjustable cable system would be beneficial. This could be achieved with the use fishing clip, winch or similar ratcheting system.

Finally, in order to create an efficient testing protocol, multiple specimens should be tested at one experimental phase before moving to the next experimental phase. This would increase

efficiency as our collaborating surgeon could transect or reconstruct multiple UCLs without having to wait for testing of a single cadaver to be completed.

References

639 Musculoskeletal Problems. (2014). from http://quizlet.com/13101273/639-musculoskeletal-problems-flash-cards/

(UK), N. C. C. f. C. C. (2008). *Osteoarthritis: National Clinical Guideline for Care and Management in Adults.* (Vol. 59): Royal College of Physicians (UK).

Anderson, D. D., Chubinskaya, S., Guilak, F., Martin, J. A., Oegema, T. R., Olson, S. A., & Buckwalter, J. A. (2011). Post‐traumatic osteoarthritis: Improved understanding and opportunities for early intervention. *Journal of Orthopaedic Research, 29*(6), 802-809. doi: 10.1002/jor.21359

Anderson, D. D., Marsh, J. L., & Brown, T. D. (2011). The pathomechanical etiology of post-traumatic osteoarthritis following intraarticular fractures. *The Iowa orthopaedic journal, 31*, 1-20.

Andrews, J. R., Jost, P. W., & Cain, E. L. (2012). The Ulnar Collateral Ligament Procedure Revisited: The Procedure We Use *Sports Health* (Vol. 4, pp. 438-441).

Azar, F. M., Andrews, J. R., Wilk, K. E., & Groh, D. (2000). Operative Treatment of Ulnar Collateral Ligament Injuries of the Elbow in Athletes. *American Orthopaedic Society for Sports Medicine, 28*(1), 16-23.

Bhandari, M. (2011). *Evidence-Based Medicine : Evidence-based Orthopedics*. Hoboken, NJ, USA: Wiley-Blackwell.

Bruce, J. R., & Andrews, J. R. (2014). Ulnar collateral ligament injuries in the throwing athlete. *Journal of the American Academy of Orthopaedic Surgeons, 22*, 315+.

Buckwalter, J. (2006). Osteoarthritis. *58*(2), 150–167.

Buckwalter, J. A. (2003). Sports, Joint Injury, and Posttraumatic Osteoarthriris. *Journal of Orthopaedic & Sports Physical Therapy, 33*(10), 578-588.

Caine, D. J., & Golightly, Y. M. (2011). Osteoarthritis as an outcome of paediatric sport: an epidemiological perspective. *Br J Sports Med, 45*, 298-303.

Caine, D. J., & Maffulli, N. (2005). *Epidemiology of Pediatric Sports Injuries Individual Sports*

Chammas, M. (2014). Post-traumatic osteoarthritis of the elbow. *Orthopaedics & traumatology, surgery & research : OTSR U6 - ctx_ver=Z39.88-2004&ctx_enc=info%3Aofi%2Fenc%3AUTF-8&rfr_id=info:sid/summon.serialssolutions.com&rft_val_fmt=info:ofi/fmt:kev:mtx:journal&rft.genre=article&rft.atitle=Post-traumatic+osteoarthritis+of+the+elbow&rft.jtitle=Orthopaedics+%26+traumatology%2C+surgery+%26+research+%3A+OTSR&rft.au=Chammas%2C+M&rft.date=2014-02-01&rft.eissn=1877-0568&rft.volume=100&rft.issue=1 Suppl&rft.spage=S15&rft_id=info:pmid/24461231&rft.externalDocID=24461231&paramdict=en-US U7 - Journal Article U8 - FETCH-LOGICAL-e842-7090c162bd6194a050fd6d2930ab343ddd5e0d2e741926698858f9b356ceaf431, 100*(1 Suppl), S15.

Crandall, J. R., Bose, D., Forman, J., Untaroiu, C. D., Arregui‐Dalmases, C., Shaw, C. G., & Kerrigan, J. R. (2011). Human surrogates for injury biomechanics research. *Clinical Anatomy, 24*(3), 362-371. doi: 10.1002/ca.21152

Creamer, P., & Hochberg, M. C. (1997). Osteoarthritis. *The Lancet, 350*(9076), 503-509.

Docking technique to repair torn elbow ligament yields favorable results in teen baseball players. (Apr. 7, 2013). 32.

Dugas, J. R., Bilotta, J., Watts, C. D., Crum, J. A., Fleisig, G. S., McMichael, C. S., . . . Andrews, J. R. (2012). Ulnar Collateral Ligament Reconstruction With Gracilis Tendon in Athletes With Intraligamentous Bony Excision. *American Orthopaedic Society for Sports Medicine*. doi: 10.1177/0363546512446927

Duggan, J. P., Osadebe, U. C., Alexander, J. W., Noble, P. C., & Lintner, D. M. (2011). The impact of ulnar collateral ligament tear and reconstruction on contact pressures in the lateral compartment of the elbow. *Journal of Shoulder and Elbow Surgery, 20*(2), 226-233. doi: 10.1016/j.jse.2010.09.011

Duggan Jr, J. P., Osadebe, U. C., Alexander, J. W., Noble, P. C., & Lintner, D. M. (2011). The impact of ulnar collateral ligament tear and reconstruction on contact pressures in the lateral compartment of the elbow. *Journal of Shoulder and Elbow Surgery, 20*(2), 226-233. doi: http://dx.doi.org/10.1016/j.jse.2010.09.011

Dunning, C. E., Duck, T. R., King, G. J. W., & Johnson, J. A. (2001). Simulated active control produces repeatable motion pathways of the elbow in an in vitro testing system. *Journal of Biomechanics, 34*(8), 1039-1048. doi: http://dx.doi.org/10.1016/S0021-9290(01)00065-3

Dunning, C. E., Gordon, K. D., King, G. J. W., & Johnson, J. A. (2003). Development of a motion-controlled in vitro elbow testing system. *Journal of Orthopaedic Research, 21*(3), 405-411. doi: http://dx.doi.org/10.1016/S0736-0266(02)00233-4

EngArc - L - Tensile Test. (2014). from http://www.engineeringarchives.com/les_mom_tensiletest.html

Franchi, M., Ottani, V., Stagni, R., & Ruggeri, A. (2010). Tendon and ligament fibrillar crimps give rise to left-handed helices of collagen fibrils in both planar and helical crimps. *J Anat, 216*(3), 301-309. doi: 10.1111/j.1469-7580.2009.01188.x

George A. Paletta, J., Klepps, S. J., Difelice, G. S., Allen, T., Brodt, M. D., Burns, M. E., . . . Wright, R. W. (2006). Biomechanical Evaluation of 2 Techniques for Ulnar Collateral Ligament Reconstruction of the Elbow. doi: 10.1177/0363546506289340

Goldring, M. B., Laboratory for Cartilage Biology, R. D., The Hospital for Special Surgery, Weill College of Medicine of Cornell University, New York, Hospital for Special Surgery, C. R. B., Room 528, 535 East 70th Street, New York, NY 10021., Goldring, S. R., & Laboratory for Cartilage Biology, R. D., The Hospital for Special Surgery, Weill College of Medicine of Cornell University, New York. (2014). Osteoarthritis. *Journal of Cellular Physiology, 213*(3), 626-634. doi: 10.1002/jcp.21258

Institute, T. B. F. (2014). BFI | Sight & Sound | Festen (1998).

Instron : Materials Testing Machines for Tensile, Fatigue, Impact & Hardness Testing. (2014). from http://www.instron.us/wa/home/default_en.aspx?ref=https://www.google.com/

Iverson, C. (2014).

Jobe, F. W., Stark, H., & Lombardo, S. J. (1986). Reconstruction of the ulnar collateral ligament in athletes. *J Bone Joint Surg Am, 68*(8), 1158-1163.

Johns Hopkins Sports Medicine Patient Guide to UCL Injuries of the Elbow (Ulnar Collateral Ligament). (2014). from http://www.hopkinsortho.org/ucl.html

Johnson, J. A., Rath, D. A., Dunning, C. E., Roth, S. E., & King, G. J. W. (2000). Simulation of elbow and forearm motion in vitro using a load controlled testing apparatus. *Journal of Biomechanics, 33*(5), 635-639. doi: 10.1016/S0021-9290(99)00204-3

Langer, P., Fadale, P., & Hulstyn, M. (2006). Evolution of the treatment options of ulnar collateral ligament injuries of the elbow. *Br J Sports Med, 40*(6), 499-506. doi: 10.1136/bjsm.2005.025072

Lerner, K. L. (2007). Elbow: Anatomy and Physiology (pp. 214-216): Thomson Gale.

Lynch, J. L., Maerz, T., Kurdziel, M. D., Davidson, A. A., Baker, K. C., & Anderson, K. (2013). Biomechanical evaluation of the TightRope versus traditional docking ulnar collateral ligament reconstruction technique: kinematic and failure testing. *The American Journal of Sports Medicine, 41*(5), 1165-1173.

Maffulli, N., Longo, U. G., Gougoulias, N., Loppini, M., & Denaro, V. (2010). Long-term health outcomes of youth sports injuries. *British Journal of Sports Medicine, 44*(1).

. OpenSim 3.2 [Open source software]. (2014). Retrieved from https://simtk.org/project/xml/downloads.xml?group_id=91

P. Langer, P. F. a. M. H. (2006). Evolution of the treatment options of ulnar collateral ligament injuries of the elbow. *Br J. Sports Med., 40*(6), 499-506.

Patel, R. M., Lynch, T. S., Amin, N. H., Calabrese, G., Gryzlo, S. M., & Schickendantz, M. S. (2014). The Thrower's Elbow. *Orthopedic Clinics of North America, 45*(3), 355-376.

Prescale Sheet Type | Fujifilm Global. (2014). from http://www.fujifilm.com/products/prescale/prescale_sheettype/ - features

Pressure Sensors in Various Sizes and Resolutions. (2014). from http://www.tekscan.com/pressureSensors

Qu, X. (1992). Morphological Effects of Mechanical Forces on the Human Humerus. *British Journal of Sports Medicine, 26*, 51-53.

Rogers, M. R., Bergfield, T. G., & Aulicino, P. L. (1991). The failed ulnar nerve transposition. Etiology and treatment. *Clin Orthop Relat Res*(269), 193-200.

Rohrbough, J. T., Altchek, D. W., Hyman, J., Williams, R. J., 3rd, & Botts, J. D. (2002). Medial collateral ligament reconstruction of the elbow using the docking technique. *Am J Sports Med, 30*(4), 541-548.

Scott, C. W., Nicole, L. G., Sue, L. H., & James, E. S. (2011). Conditioning of the Achilles tendon via ankle exercise improves correlations between sonographic measures of tendon thickness and body anthropometry. *Journal of Applied Physiology, 110*(5), 1384-1389. doi: 10.1152/japplphysiol.00075.2011

Seiber, K., Gupta, R., McGarry, M. H., Safran, M. R., & Lee, T. Q. (2009). The role of the elbow musculature, forearm rotation, and elbow flexion in elbow stability: An in vitro study. *Journal of Shoulder and Elbow Surgery, 18*(2), 260-268. doi: http://dx.doi.org/10.1016/j.jse.2008.08.004

. shutterstock119687548copy. (2013). Shutterfly.com.

Tan, J. S., & Uppuganti, S. (2012). Cumulative multiple freeze-thaw cycles and testing does not affect subsequent within-day variation in intervertebral flexibility of human cadaveric lumbosacral spine. *Spine, 37*(20), 1238-1242.

Teramoto, A., & Luo, Z.-P. (2008). Temporary tendon strengthening by preconditioning. *Clinical Biomechanics, 23*(5), 619-622. doi: http://dx.doi.org/10.1016/j.clinbiomech.2007.12.001

Testers & Stands | Chatillon Force Measurement. (2014). from http://www.chatillon.com/products/testers-and-stands/index.aspx

Thompson, W. H., Jobe, F. W., Yocum, L. M., & Pink, M. M. (2001). Ulnar collateral ligament reconstruction in athletes: Muscle-splitting approach without transposition of the ulnar nerve. *Journal of Shoulder and Elbow Surgery, 10*(2), 152–157.

Tochigi, Y., Rudert, M. J., Saltzman, C. L., Amendola, A., & Brown, T. D. (2006). Contribution of articular surface geometry to ankle stabilization. *The Journal of Bone & Joint Surgery, 88*(12), 2704-2713.

Troy, K. (2014).

. UCL Reconstruction (Tommy John Surgery). (2014).

Vitale, M. A., & Ahmad, C. S. (2008). The Outcome of Elbow Ulnar Collateral Ligament Reconstruction in Overhead Athletes. *The American Journal of Sports Medicine*. doi: 10.1177/0363546508319053

Watson, J. N., McQueen, P., & Hutchinson, M. R. (2013). A Systematic Review of Ulnar Collateral Ligament Reconstruction Techniques. *American Journal of Sports Medicine*.

Wikipedia. (2014). Biceps Muscle.

Winter, D. A. (1990). *Biomechanics and Motor Control of Human Movement* (4th ed.). Hoboken, New Jersey: John Wiley & Sons, Inc.

Zellner, B., & May, M. M. (2013). Elbow Injuries in the Young Athlete-an Orthopedic Perspective. *Pediatric Radiology*.

Appendix A: Polhemus Motion Capture Analysis

```
clear all; clc;
filename = 'Rate1Trail1.xlsx';
A = xlsread(filename);
Time = A(:,5);

YDirection = A(:,8);

ZDirection = A(:,9);
```

Sensor 2: Y-Direction vs. Time plot

```
S2_location = find(A(:,1) == 2);

S2_time = zeros(length(S2_location),1);

S2_YDirection = zeros(length(S2_location),1);

for i = 1: length(S2_location)
    j = S2_location(i);
    S2_time(i)= Time(j);
    S2_YDirection(i) = YDirection(j);
    S2_ZDirection(i) = ZDirection(j);
    S2_ZDirection = S2_ZDirection';
end
```

Sensor 3: Y-Direction vs. Time plot

```
S3_location = find(A(:,1) == 3);

S3_time = zeros(length(S3_location),1);

S3_YDirection = zeros(length(S3_location),1);

for i = 1: length(S3_location)
    j = S3_location(i);
    S3_time(i)= Time(j);
    S3_YDirection(i) = YDirection(j);
    S3_ZDirection(i) = ZDirection(j);
    S3_ZDirection = S3_ZDirection';
end
state = 0;

ii = 1;
```

```
n = 1;

Threshold_locations = [];

while ii<length(S3_YDirection);
    if state == 0
       if S3_YDirection(ii) > 5;
           Threshold_locations(n,:) = [ii, S3_YDirection(ii), S3_ZDirection(ii),
S3_time(ii)];
           n = n+1;
           state = 1;
       end
       ii = ii+1;
    end
    if state == 1;
       if S3_YDirection(ii) > 8;
           Threshold_locations(n,:) = [ii, S3_YDirection(ii), S3_ZDirection(ii),
S3_time(ii)];
           n = n+1;
           state = 2;
       end
       ii = ii+1;
    end
    if state == 2;
       if S3_YDirection(ii) < 4;
           state = 0;
       end
       ii = ii+1;
    end
end

Ang_velocities = [];
Radius_list = [];
pt1_ind = 1;
pt2_ind = 2;
for iii = 1:length(Threshold_locations)/2;
    pt_location1 = Threshold_locations(pt1_ind,1);
    pt_location2 = Threshold_locations(pt2_ind,1);
    PT1a = S2_YDirection(pt_location1+1);
    PT1b = S2_ZDirection(pt_location1+1);
    PT2a = S3_YDirection(pt_location1);
    PT2b = S3_ZDirection(pt_location1);
    Vector1 = [(PT2a-PT1a),(PT2b-PT1b)];
    V1_squ = Vector1.*Vector1;
    PT3a = S2_YDirection(pt_location2+1);
    PT3b = S2_ZDirection(pt_location2+1);
    PT4a = S3_YDirection(pt_location2);
    PT4b = S3_ZDirection(pt_location2);
    Vector2 = [(PT4a-PT3a),(PT4b-PT3b)];
    V2_squ = Vector2.*Vector2;
```

```
    vector_dot = dot(Vector1,Vector2);
    vector_mag = (sqrt(sum(V1_squ))*(sqrt(sum(V1_squ))));
    cos_theta = vector_dot/vector_mag;
    theta = acos(cos_theta);
    Time_region = abs(Threshold_locations(pt1_ind,4)-Threshold_locations(pt2_ind,4));
    pt1_ind = pt1_ind+2;
    pt2_ind = pt2_ind+2;
    Ang_velocities(iii,:) = theta/Time_region;
    Angular_velocity = mean(Ang_velocities);
    Radius = 1.8194600673228;
    Linear_velocity = (Angular_velocity)*(Radius);
end
```

Appendix B: Theoretical Calculations

For all tables from excel that were used for the theoretical calculations, the orientation of the biceps brachii muscle origin and insertion points is such that *X* is directed anteriorly from elbow joint center of rotation. The *Y* component of the origin and insertion points is directed superiorly from the elbow joint center of rotation. Refer to **Figure 29** for a picture of the axis position and orientation. The biceps brachii muscle origin point is located on the ulna. The biceps brachii muscle insertion point used for these calculations was not a true insertion point, but was instead a muscle wrapping point. For details regarding what assumptions were made in order to take these origin and insertion points can be seen in section **5.1.1**.

Statics

Statics Calculations at 30° of flexion

From Excel:

Donor #	Biceps Muscle Origin Point		Biceps Muscle Insertion Point		Weight (lbs)	Weight (N)	Height (in)	Height (m)
	X (m)	Y (m)	X (m)	Y (m)				
1404245R	0.007	-0.042	0.063	0.08	149	662.7848	63	1.6002
1404238R	0.007	-0.043	0.064	0.081	160	711.7152	66	1.6764
1403970R	0.008	-0.05	0.074	0.095	216	960.8155	74	1.8796
1403965R	0.007	-0.045	0.066	0.085	129	573.8204	63	1.6002
1403959R	0.007	-0.045	0.067	0.086	121	538.2346	68	1.7272
1403102R	0.007	-0.044	0.066	0.084	203	902.9887	60	1.524
1403092R	0.008	-0.052	0.077	0.098	129	573.8204	68	1.7272
1402922R	0.007	-0.043	0.064	0.081	152	676.1294	65	1.651
1402921R	0.006	-0.04	0.06	0.076	190	845.1618	66	1.6764
1402893R	0.007	-0.046	0.068	0.087	245	1089.814	67	1.7018
1401717R	0.007	-0.047	0.07	0.089	146	649.4401	70	1.778
1401664R	0.008	-0.05	0.074	0.094	139	618.3026	72	1.8288
1401653R	0.007	-0.047	0.07	0.089	140	622.7508	65	1.651
1311388R	0.008	-0.052	0.077	0.098	195	867.4029	73	1.8542

From MATLAB:

```
clear all; clc;
filename = 'Statics30Degrees.xlsx';
A = xlsread(filename);
JRForces = [];
n = 1;
for i = 1: length (A(:,1));
    PT1a = A(i,1);
    PT1b = A(i,2);
    PT2a = A(i,3);
    PT2b = A(i,4);
    Vector1 = [(PT2a-PT1a),(PT2b-PT1b)];
    arg = (Vector1(1,1))/(Vector1(1,2));
    theta = atan(arg);
    W_a = 0.022 * (A(i,6));
    a = abs(A(i,2));
    b = (0.253*(A(i,8)))*0.318;
    F_b = (W_a*b)/(a*cos(theta));
    F_x = F_b*(sin(theta));
    F_y = W_a - F_b*(cos(theta));
    JRForces (n,:) = [F_x, F_y, F_b];
    n = n+1;
end
AvgF_x = mean(JRForces(:,1));
StDevF_x = std(JRForces(:,1));
AvgF_y = mean(JRForces(:,2));
StDevF_y = std(JRForces(:,2));
AvgF_b = mean(JRForces(:,3));
StDevF_b = std(JRForces(:,3));
ALL = [AvgF_x, StDevF_x, AvgF_y, StDevF_y, AvgF_b, StDevF_b];
```

Statics Calculations at 60° of flexion

From Excel:

Donor #	Biceps Muscle Origin Point		Biceps Muscle Insertion Point		Weight (lbs)	Weight (N)	Height (in)	Height (m)
	X (m)	Y (m)	X (m)	Y (m)				
1404245R	0.007	-0.042	0.095	0.038	149	662.7848	63	1.6002
1404238R	0.007	-0.043	0.096	0.039	160	711.7152	66	1.6764
1403970R	0.008	-0.05	0.112	0.045	216	960.8155	74	1.8796
1403965R	0.007	-0.045	0.1	0.04	129	573.8204	63	1.6002
1403959R	0.007	-0.045	0.101	0.041	121	538.2346	68	1.7272
1403102R	0.007	-0.044	0.099	0.04	203	902.9887	60	1.524
1403092R	0.008	-0.052	0.116	0.047	129	573.8204	68	1.7272
1402922R	0.007	-0.043	0.096	0.039	152	676.1294	65	1.651
1402921R	0.006	-0.04	0.09	0.036	190	845.1618	66	1.6764
1402893R	0.007	-0.046	0.102	0.041	245	1089.814	67	1.7018
1401717R	0.007	-0.047	0.105	0.042	146	649.4401	70	1.778
1401664R	0.008	-0.05	0.11	0.045	139	618.3026	72	1.8288
1401653R	0.007	-0.047	0.105	0.043	140	622.7508	65	1.651
1311388R	0.008	-0.052	0.115	0.047	195	867.4029	73	1.8542

From MATLAB:

```
clear all; clc;
filename = 'Statics60Degrees.xlsx';
A = xlsread(filename);
JRForces = [];
n = 1;
for i = 1: length (A(:,1));
    PT1a = A(i,1);
    PT1b = A(i,2);
    PT2a = A(i,3);
    PT2b = A(i,4);
    Vector1 = [(PT2a-PT1a),(PT2b-PT1b)];
    arg = (Vector1(1,1))/(Vector1(1,2));
    theta = atan(arg);
    W_a = 0.022 * (A(i,6));
    a = abs(A(i,2));
    b = (0.253*(A(i,8)))*0.318;
    F_b = (W_a*b)/(a*cos(theta));
    F_x = F_b*(sin(theta));
```

```
    F_y = W_a - F_b*(cos(theta));
    JRForces (n,:) = [F_x, F_y, F_b];
    n = n+1;
end
AvgF_x = mean(JRForces(:,1));
StDevF_x = std(JRForces(:,1));
AvgF_y = mean(JRForces(:,2));
StDevF_y = std(JRForces(:,2));
AvgF_b = mean(JRForces(:,3));
StDevF_b = std(JRForces(:,3));
ALL = [AvgF_x, StDevF_x, AvgF_y, StDevF_y, AvgF_b, StDevF_b];
```

Statics Calculations at 90° of flexion

From Excel:

Donor #	Biceps Muscle Origin Point		Biceps Muscle Insertion Point		Weight (lbs)	Weight (N)	Height (in)	Height (m)
	X (m)	Y (m)	X (m)	Y (m)				
1404245R	0.007	-0.042	0.101	-0.014	149	662.7848	63	1.6002
1404238R	0.007	-0.043	0.102	-0.014	160	711.7152	66	1.6764
1403970R	0.008	-0.05	0.119	-0.017	216	960.8155	74	1.8796
1403965R	0.007	-0.045	0.107	-0.015	129	573.8204	63	1.6002
1403959R	0.007	-0.045	0.108	-0.015	121	538.2346	68	1.7272
1403102R	0.007	-0.044	0.106	-0.015	203	902.9887	60	1.524
1403092R	0.008	-0.052	0.123	-0.017	129	573.8204	68	1.7272
1402922R	0.007	-0.043	0.102	-0.014	152	676.1294	65	1.651
1402921R	0.006	-0.04	0.096	-0.013	190	845.1618	66	1.6764
1402893R	0.007	-0.046	0.109	-0.015	245	1089.814	67	1.7018
1401717R	0.007	-0.047	0.112	-0.015	146	649.4401	70	1.778
1401664R	0.008	-0.05	0.118	-0.016	139	618.3026	72	1.8288
1401653R	0.007	-0.047	0.112	-0.016	140	622.7508	65	1.651
1311388R	0.008	-0.052	0.123	-0.017	195	867.4029	73	1.8542

From MATLAB:

```
clear all; clc;
filename = 'Statics90Degrees.xlsx';
A = xlsread(filename);
JRForces = [];
n = 1;
```

```
for i = 1: length (A(:,1));
    PT1a = A(i,1);
    PT1b = A(i,2);
    PT2a = A(i,3);
    PT2b = A(i,4);
    Vector1 = [(PT2a-PT1a),(PT2b-PT1b)];
    arg = (Vector1(1,1))/(Vector1(1,2));
    theta = atan(arg);
    W_a = 0.022 * (A(i,6));
    a = abs(A(i,2));
    b = (0.253*(A(i,8)))*0.318;
    F_b = (W_a*b)/(a*cos(theta));
    F_x = F_b*(sin(theta));
    F_y = W_a - F_b*(cos(theta));
    JRForces (n,:) = [F_x, F_y, F_b];
    n = n+1;
end
AvgF_x = mean(JRForces(:,1));
StDevF_x = std(JRForces(:,1));
AvgF_y = mean(JRForces(:,2));
StDevF_y = std(JRForces(:,2));
AvgF_b = mean(JRForces(:,3));
StDevF_b = std(JRForces(:,3));
ALL = [AvgF_x, StDevF_x, AvgF_y, StDevF_y, AvgF_b, StDevF_b];
```

Inverse Dynamics

Inverse Dynamics Calculations at 30° of flexion

From Excel:

Donor #	Biceps Muscle Origin Point		Biceps Muscle Insertion Point		Weight (lbs)	Weight (N)	Height (in)	Height (m)
	X (m)	Y (m)	X (m)	Y (m)				
1404245R	0.007	-0.042	0.063	0.08	149	662.7848	63	1.6002
1404238R	0.007	-0.043	0.064	0.081	160	711.7152	66	1.6764
1403970R	0.008	-0.05	0.074	0.095	216	960.8155	74	1.8796
1403965R	0.007	-0.045	0.066	0.085	129	573.8204	63	1.6002
1403959R	0.007	-0.045	0.067	0.086	121	538.2346	68	1.7272
1403102R	0.007	-0.044	0.066	0.084	203	902.9887	60	1.524
1403092R	0.008	-0.052	0.077	0.098	129	573.8204	68	1.7272
1402922R	0.007	-0.043	0.064	0.081	152	676.1294	65	1.651
1402921R	0.006	-0.04	0.06	0.076	190	845.1618	66	1.6764
1402893R	0.007	-0.046	0.068	0.087	245	1089.814	67	1.7018
1401717R	0.007	-0.047	0.07	0.089	146	649.4401	70	1.778
1401664R	0.008	-0.05	0.074	0.094	139	618.3026	72	1.8288
1401653R	0.007	-0.047	0.07	0.089	140	622.7508	65	1.651
1311388R	0.008	-0.052	0.077	0.098	195	867.4029	73	1.8542

From MATLAB:

```
clear all; clc;
filename = 'Statics30Degrees.xlsx';
A = xlsread(filename);
JRForces = [];
n = 1;
for i = 1: length (A(:,1));
    PT1a = A(i,1);
    PT1b = A(i,2);
    PT2a = A(i,3);
    PT2b = A(i,4);
    Vector1 = [(PT2a-PT1a),(PT2b-PT1b)];
    arg = (Vector1(1,1))/(Vector1(1,2));
    theta = atan(arg);
    W_a = 0.022 * (A(i,6));
    a = abs(A(i,2));
    b = (0.253*(A(i,8)))*0.328;
    omega = 0.01/(a);
    fast = 2;
    alpha = omega/fast;
    rho = 0.827*(0.253*(A(i,8)));
    I = rho*W_a;
```

```
    F_b = ((W_a*(b*cos(30)))-I*alpha)/(a*cos(theta)*cos(30));
    F_x = F_b*(sin(theta))-I*alpha;
    F_y = W_a - F_b*(cos(theta))-I*alpha;
    JRForces (n,:) = [F_x, F_y, F_b];
    n = n+1;
end
AvgF_x = mean(JRForces(:,1));
StDevF_x = std(JRForces(:,1));
AvgF_y = mean(JRForces(:,2));
StDevF_y = std(JRForces(:,2));
AvgF_b = mean(JRForces(:,3));
StDevF_b = std(JRForces(:,3));
ALL = [AvgF_x, StDevF_x, AvgF_y, StDevF_y, AvgF_b, StDevF_b];
```

Inverse Dynamics Calculations at 60° of flexion

From Excel:

Donor #	Biceps Muscle Origin Point		Biceps Muscle Insertion Point		Weight (lbs)	Weight (N)	Height (in)	Height (m)
	X (m)	Y (m)	X (m)	Y (m)				
1404245R	0.007	-0.042	0.095	0.038	149	662.7848	63	1.6002
1404238R	0.007	-0.043	0.096	0.039	160	711.7152	66	1.6764
1403970R	0.008	-0.05	0.112	0.045	216	960.8155	74	1.8796
1403965R	0.007	-0.045	0.1	0.04	129	573.8204	63	1.6002
1403959R	0.007	-0.045	0.101	0.041	121	538.2346	68	1.7272
1403102R	0.007	-0.044	0.099	0.04	203	902.9887	60	1.524
1403092R	0.008	-0.052	0.116	0.047	129	573.8204	68	1.7272
1402922R	0.007	-0.043	0.096	0.039	152	676.1294	65	1.651
1402921R	0.006	-0.04	0.09	0.036	190	845.1618	66	1.6764
1402893R	0.007	-0.046	0.102	0.041	245	1089.814	67	1.7018
1401717R	0.007	-0.047	0.105	0.042	146	649.4401	70	1.778
1401664R	0.008	-0.05	0.11	0.045	139	618.3026	72	1.8288
1401653R	0.007	-0.047	0.105	0.043	140	622.7508	65	1.651
1311388R	0.008	-0.052	0.115	0.047	195	867.4029	73	1.8542

From MATLAB:

```
clear all; clc;
filename = 'Statics60Degrees.xlsx';
A = xlsread(filename);
JRForces = [];
n = 1;
for i = 1: length (A(:,1));
    PT1a = A(i,1);
```

```
    PT1b = A(i,2);
    PT2a = A(i,3);
    PT2b = A(i,4);
    Vector1 = [(PT2a-PT1a),(PT2b-PT1b)];
    arg = (Vector1(1,1))/(Vector1(1,2));
    theta = atan(arg);
    W_a = 0.022 * (A(i,6));
    a = abs(A(i,2));
    b = (0.253*(A(i,8)))*0.328;
    omega = 0.005/(a);
    slow = 4;
    alpha = omega/slow;
    rho = 0.827*(0.253*(A(i,8)));
    I = rho*W_a;
    F_b = ((W_a*(b*cos(60)))-I*alpha)/(a*cos(theta)*cos(60));
    F_x = F_b*(sin(theta))-I*alpha;
    F_y = W_a - F_b*(cos(theta))-I*alpha;
    JRForces (n,:) = [F_x, F_y, F_b];
    n = n+1;
end
AvgF_x = mean(JRForces(:,1));
StDevF_x = std(JRForces(:,1));
AvgF_y = mean(JRForces(:,2));
StDevF_y = std(JRForces(:,2));
AvgF_b = mean(JRForces(:,3));
StDevF_b = std(JRForces(:,3));
ALL = [AvgF_x, StDevF_x, AvgF_y, StDevF_y, AvgF_b, StDevF_b];
```

Inverse Dynamics Calculations at 90° of flexion

From Excel:

Donor #	Biceps Muscle Origin Point		Biceps Muscle Insertion Point		Weight (lbs)	Weight (N)	Height (in)	Height (m)
	X (m)	Y (m)	X (m)	Y (m)				
1404245R	0.007	-0.042	0.101	-0.014	149	662.7848	63	1.6002
1404238R	0.007	-0.043	0.102	-0.014	160	711.7152	66	1.6764
1403970R	0.008	-0.05	0.119	-0.017	216	960.8155	74	1.8796
1403965R	0.007	-0.045	0.107	-0.015	129	573.8204	63	1.6002
1403959R	0.007	-0.045	0.108	-0.015	121	538.2346	68	1.7272
1403102R	0.007	-0.044	0.106	-0.015	203	902.9887	60	1.524
1403092R	0.008	-0.052	0.123	-0.017	129	573.8204	68	1.7272
1402922R	0.007	-0.043	0.102	-0.014	152	676.1294	65	1.651
1402921R	0.006	-0.04	0.096	-0.013	190	845.1618	66	1.6764
1402893R	0.007	-0.046	0.109	-0.015	245	1089.814	67	1.7018
1401717R	0.007	-0.047	0.112	-0.015	146	649.4401	70	1.778
1401664R	0.008	-0.05	0.118	-0.016	139	618.3026	72	1.8288
1401653R	0.007	-0.047	0.112	-0.016	140	622.7508	65	1.651
1311388R	0.008	-0.052	0.123	-0.017	195	867.4029	73	1.8542

From MATLAB:

```
clear all; clc;
filename = 'Statics90Degrees.xlsx';
A = xlsread(filename);
JRForces = [];
n = 1;
for i = 1: length (A(:,1));
    PT1a = A(i,1);
    PT1b = A(i,2);
    PT2a = A(i,3);
    PT2b = A(i,4);
    Vector1 = [(PT2a-PT1a),(PT2b-PT1b)];
    arg = (Vector1(1,1))/(Vector1(1,2));
    theta = atan(arg);
    W_a = 0.022 * (A(i,6));
    a = abs(A(i,2));
    b = (0.253*(A(i,8)))*0.328;
    omega = 0.01/(a);
    fast = 2;
    alpha = omega/fast;

    rho = 0.827*(0.253*(A(i,8)));

    I = rho*W_a;
    F_b = ((W_a*(b*cos(90)))-I*alpha)/(a*cos(theta)*cos(90));
    F_x = F_b*(sin(theta))-I*alpha;
    F_y = W_a - F_b*(cos(theta))-I*alpha;
```

```
    JRForces (n,:) = [F_x, F_y, F_b];
    n = n+1;
end
AvgF_x = mean(JRForces(:,1));
StDevF_x = std(JRForces(:,1));
AvgF_y = mean(JRForces(:,2));
StDevF_y = std(JRForces(:,2));
AvgF_b = mean(JRForces(:,3));
StDevF_b = std(JRForces(:,3));
ALL = [AvgF_x, StDevF_x, AvgF_y, StDevF_y, AvgF_b, StDevF_b];
```

Appendix C: Experimental Protocol

Materials:

Test setup

Humerus Fixation

PVC device with mounted pulleys
Pipe vise
¼" bolts and nuts (2 per setup) for humerus fixation
½" bolts and nuts (x4) for vise

Forearm Guide

Forearm guide (x2)
16 ¼" bolts and wing nuts

Forearm Fixation

Forearm fixation plates
- 1 Big
- 2 Small

4 ¼" bolts and nuts

Other

10 lbs free hanging weight for triceps
Tools for tightening
Vaseline for coating the track
65 lbs braided fishing line
50 lbs fishing line
Instron
Baseboard of setup with pulley systems

Specimen setup

14 Cadaveric specimens amputated mid-humerus
Spray bottle of saline solution
- 5.85 g of salt per 650mL

Scalpel
Forceps
Scissors
Drill press
¼" Drill bit
Suture kits

Data Analysis

Tekscan system
Tekscan sensors
Tekscan calibration jig
Goniometer

Safety

Nitrile gloves
Disposable lab gowns
Safety glasses
10% Bleach solution
Lysol spray
Clorox spray
Blue absorbent pads
Plastic wrap

Specimen Preparation:

Thaw cadaver specimen(s) overnight or approximately 12 hours prior to testing in the fridge in the specimen preparation room. If cadaver needs to be thawed quickly, place the cadaver into a warm water bath in the specimen preparation room.

1. Bring thawed specimen to the specimen preparation room, which should be cleaned and set up with the necessary biohazard precautions (i.e. blue absorbent pads, plastic wrap, etc.).
2. Be sure to periodically spray the specimen with a saline solution to prevent the soft tissue from drying out.
3. Dissect away soft tissue to make the incision for the Tekscan pressure sensor insertion, suturing of the muscle tendons, and drilling into the humerus.
4. Suture to the biceps brachii and brachialis tendons and the triceps brachii upper neurosis using the strong FiberWire sutures.
5. Drill a hole into the humerus of the specimen with a ¼" drill bit and the drill press approximately 8.5 cm away from the radial epicondyle. Drill a second hole approximately 2.5 cm away from the first hole, leaving at least 2.5cm of space away from the end of the humerus.
6. When the specimen has been completely prepped, secure the specimen to the PVC humerus fixation device using two ¼" x 3" bolts.
7. Attach (loosely) the forearm fixation plates to the forearm using ¼" bolts, making sure to orient the specimen in a supinated position. Ensure that the joint space is not being disrupted.
8. Cut 2 approximately 7 foot long lengths of 65 lbs braided fishing line. Wrap the fishing line around a secure object and pull on it for preconditioning.
9. Tie one of the preconditioned fishing lines to the biceps tendon suture and the other to the brachialis tendon suture using one square knot and two half hitches.
10. Cut one approximately 8 feet length of 50 lbs fishing line. Tie to the triceps brachii upper neurosis suture using one square knot and two half hitches.

Setup Preparation:

1. Cover the entire setup with plastic wrap and the Instron table with blue absorbent pads.
2. Bolt the vise and inner forearm guide to the appropriate pre-drilled holes.
3. While the specimen is being prepped for the experiment, another member of the group should turn on the Instron. After the Instron has gone through its startup cycle, turn on the computer.
4. Login and start the Instron console. Turn on limits.
5. Move the Instron to -27.00 mm position.
6. Start up the BlueHill software and open the previously configured preconditioning test.
7. Place the baseboard onto the Instron table with the vise closest to the Instron.
8. Bolt the baseboard to the Instron.
9. Bring the prepared cadaveric specimen to the Instron room in a plastic tub with a blue chuck lining the inside of the tub.
10. Insert the previously calibrated Tekscan sensor into the joint space using the "boat race" incision and passing suture method as previously described in Duggan et. al and carefully clamp the edge(s) to create stable guidelines for data analysis.
11. Place the PVC humerus fixation component and fixed specimen into the vise, making sure to align the specimen's lateral epicondyle with the labeled "origin" on the inner forearm guide and the rod of the forearm fixation plate is in the inner forearm guide.
12. Run the sutured cables from the biceps brachii and brachialis tendons through their respective pulleys.
13. Tie cables to the Instron using one square knot and two half hitches making sure that there is no slack in the system and the arm rests at 30° of flexion.
14. Run the sutured cable from the triceps tendon through the pulley system and attach the 10 lbs free-hanging weight.
15. Secure the remaining outside forearm guide to the table using ¼" bolts making sure to lock the rods on the forearm plate into the tracks so that controlled flexion of the specimen can be achieved.

Test:

Rate #1 = 5 mm/s
Rate #2 = 10 mm/s

Native UCL State

1. 25 cycles of preconditioning
2. Test at rate #1 for 10 cycles
3. Test at rate #2 for 10 cycles

Transected UCL State

1. Remove the outside forearm guide
2. Have collaborating surgeon transect the UCL
3. Put the outside forearm guide back into place and secure with wing nuts

4. Test at rate #1 for 10 cycles
5. Test at rate #2 for 10 cycles

Reconstructed UCL

1. Unload specimen from the jig and take to specimen preparation room for surgical reconstruction
2. When complete, re-load the specimen onto the jig
3. Test at rate #1 for 10 cycles
4. Test at rate #2 for 10 cycles